Energy and AI 15 (2024) 100317

Contents lists available at ScienceDirect

Energy and AI

journal homepage: www.sciencedirect.com/journal/energy-and-ai

AI-enabled materials discovery for advanced ceramic electrochemical cells

Idris Temitope Bello [a], Ridwan Taiwo [a], Oladapo Christopher Esan [b], Adesola Habeeb Adegoke [c], Ahmed Olanrewaju Ijaola [d], Zheng Li [a], Siyuan Zhao [a], Chen Wang [a], Zongping Shao [e], Meng Ni [a,*]

[a] Department of Building and Real Estate, Research Institute for Sustainable Urban Development (RISUD) & Research Institute for Smart Energy (RISE), The Hong Kong Polytechnic University, Hung Hom, Kowloon, Hong Kong, China
[b] Department of Mechanical Engineering, The Hong Kong Polytechnic University, Hung Hom, Kowloon, Hong Kong, China
[c] Department of Civil Engineering, University of Johannesburg, South Africa
[d] Department of Mechanical Engineering, Wichita State University, Kansas, USA
[e] WA School of Mines: Minerals, Energy and Chemical Engineering, Curtin University, Perth, Western Australia, 6845, Australia

HIGHLIGHTS

- AI for materials design in CECs reviewed.
- Materials descriptors, algorithms, cases, challenges, and future directions discussed.
- Materials exploration, discovery, and structure-property insights emphasized.
- Recommendations to advance materials science and AI for clean energy provided.

GRAPHICAL ABSTRACT

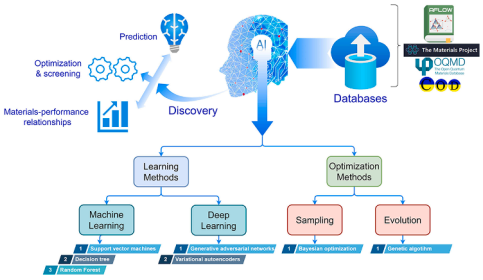

ARTICLE INFO

Keywords:
Ceramic electrochemical cells
Artificial intelligence
Materials design
Materials optimization
Materials performance
Machine learning

ABSTRACT

Ceramic electrochemical cells (CECs) are promising devices for clean and efficient energy conversion and storage due to their high energy efficiency, more extended system durability, and less expensive materials. However, the search for suitable materials with desired properties, including high ionic and electronic conductivity, thermal stability, and chemical compatibility, presents ongoing challenges that impede widespread adoption and further advancement in the field. Artificial intelligence (AI) has emerged as a versatile tool capable of enhancing and expediting the materials discovery cycle in CECs through data-driven modeling, simulation, and optimization techniques. Herein, we comprehensively review the state-of-the-art AI applications for materials design and optimization for CECs, covering various material aspects, database construction, data pre-processing, and AI methods. We also present some representative case studies of AI-predicted and synthesized materials for CECs and provide insightful highlights about their approaches. We emphasize the main implications and contributions of the AI approach for advancing the CEC technology, such as reducing the trial-and-error experiments, exploring the vast materials space, discovering novel and optimal materials, and enhancing the understanding of the materials-performance relationships. We also discuss the AI approach's main limitations and future directions for CECs, such as addressing the data and model challenges, improving and extending the AI models and methods,

* Corresponding author.
E-mail address: meng.ni@polyu.edu.hk (M. Ni).

https://doi.org/10.1016/j.egyai.2023.100317

Available online 9 November 2023

and integrating with other computational and experimental techniques. We conclude by suggesting some potential applications and collaborations for AI in materials design for CECs.

1. Introduction

Energy is essential for human civilization and development [1]. However, the current energy systems rely heavily on fossil fuels, such as coal, oil, and gas, which cannot meet the rapidly increasing global energy demand driven by population growth, economic development, and urbanization [2]. Ensuring a sustainable and secure energy supply has become an immense challenge [1]. Furthermore, the combustion of fossil fuels depletes the limited natural resources and emits greenhouse gases that cause global warming and climate change [2]. The average global ground surface temperature has risen by about 1.2 °C since the pre-industrial era, posing severe threats to the environment, human health, and social stability [1]. Therefore, there is an urgent need for clean, renewable, sustainable, and efficient alternative energy sources. Ceramic electrochemical cells (CECs) emerge as one of the promising candidates capable of utilizing ceramic electrolytes to convert chemical energy into electrical energy and vice versa [2,3]. These cells can operate in various modes depending on the direction of ion flow, including fuel cell mode, electrolysis mode, and reversible mode [4–6]. CECs offer numerous advantages over conventional energy conversion devices, including high efficiency, minimal emissions, fuel flexibility, and potential for cogeneration [7–9].

Despite the advantages of CECs, several challenges must be overcome to realize the commercialization of this technology. One of the primary challenges involves developing stable and efficient electrolyte materials capable of maintaining high ionic conductivity while minimizing electronic conductivity under varying operating conditions [4,10,11]. These electrolyte materials must also exhibit good chemical compatibility with the electrode materials and possess low thermal expansion mismatch with other cell components [4,10,11]. Another significant challenge lies in designing and optimizing electrode materials and structures that facilitate electrochemical reactions at the interfaces and minimize polarization losses [7,8,12–15]. The electrode materials should possess high catalytic activity, excellent electronic and ionic conductivity, suitable porosity and gas permeability, and long-term stability under desired ambient testing conditions [16–18].

Moreover, the fabrication and integration of CECs into practical systems also pose technical difficulties, such as achieving uniform and dense electrolyte layers, preventing gas leakage and interdiffusion, and ensuring reliable sealing and interconnection [19–22]. Further research and innovation are necessary to address these challenges and improve the performance and durability of CECs for various applications. Incorporating artificial intelligence (AI) in materials discovery, design, optimization, and characterization can significantly accelerate progress in overcoming these obstacles. Exploring the current state-of-the-art of AI and its prospects in materials development for CECs is, therefore, crucial to fully realizing the potential of this technology in the energy industry.

AI is a branch of computer science dedicated to developing machines or systems capable of performing tasks that typically require human intelligence, such as learning, reasoning, decision-making, and problem-solving [23]. AI methods have been extensively applied for material discovery in various materials-related domains, including catalysis, photovoltaics, quantum materials, ion-selective membranes, thermoelectrics, mechanical materials, and energy-efficient materials [24–33]. However, AI's specific use and potential for CECs have been relatively underexplored and underreported [34–36]. Therefore, a comprehensive and critical review is needed to examine how AI can facilitate the development of novel materials with superior performance and stability in the context of CECs. AI has the potential to significantly accelerate the materials discovery cycle for CECs by enabling data-driven modeling, simulation, and optimization of material properties and performance [28,29,37]. The materials discovery cycle typically comprises four stages: design, synthesis, characterization, and testing [25,37] At each stage, AI can generate faster and more accurate predictions, explore larger and more complex materials spaces, discover novel and optimal materials, and enhance our understanding of materials-performance relationships [24–33]. However, no existing review article specifically and extensively focused on the application of AI for materials discovery and development in CECs.

In this review article, we aim to bridge the current research gap by comprehensively surveying state-of-the-art AI applications for materials design and optimization in the context of CECs. We begin by extensively covering various material aspects relevant to CECs, exploring database construction, data pre-processing, and the range of AI methods that can be employed in materials design and optimization for CECs. We also present some case studies showcasing AI-predicted and synthesized materials for CECs, offering valuable insights into their respective approaches. Furthermore, we emphasize the significant implications and contributions of the AI approach to the advancement of CEC technology. We also identify the critical research gaps and opportunities for leveraging AI in materials design for CECs. In line with this, we propose future directions and recommendations to facilitate the integration of AI in materials design for CECs. These recommendations include the development of new performance metrics and evaluation methods, fostering interdisciplinary and cross-sectoral partnerships, and exploring new applications and collaborations for AI in materials design within the scope of CECs. The structure and content of the article are organized as follows: Section 2 reviews the material aspects crucial for CECs, highlighting the key challenges and opportunities for material design and optimization. Section 3 elaborates on the significance of database construction, relevant CEC material descriptors, data preprocessing, and feature engineering. Section 4 explores the main AI methods relevant to materials design and optimization specifically tailored for CECs. Section 5 showcases a selection of representative case studies that demonstrate the application of AI in predicting and synthesizing materials for CECs. Section 6 elucidates the primary implications and contributions of the AI approach in advancing CEC technology. Section 7 discusses the main limitations of the AI approach when applied to CECs. Moving forward, in Section 7, we provide recommendations and propose future directions for applying AI approaches in materials design and development for CECs. Finally, Section 8 concludes the article by summarizing the main findings and insights gleaned from our review.

2. Materials aspects of CECs

CECs are devices that directly convert chemical energy into electrical energy (fuel cells) or vice versa (electrolysis cells) by using solid ceramic materials as electrolytes and electrodes [38–40]. Fig. 1 illustrates the working mechanism of CECs. CECs can be classified into two types based on the nature of ion transport in the electrolyte: solid oxide cells (SOCs), which mainly conduct oxide ions, and protonic ceramic cells (PCCs), which dominantly conduct protons [39,41,42]. The latter type has some advantages over the former, such as lower activation energy and non-dilution of the fuel at the anode (fuel cell mode) [12]. Furthermore, CECs can operate in different modes, depending on the type and direction of ion flow: fuel cell mode, where hydrogen or other fuels are oxidized at the anode and oxygen is reduced at the cathode to produce electricity (Fig. 1**a & b**); electrolysis mode, where electricity is employed to split water into hydrogen and oxygen (Fig. 1**c & d**); and co-electrolysis mode, where electricity is used to convert water and

carbon dioxide into syngas or other hydrocarbons [43–45]. The performance and efficiency of CECs depend largely on the key material aspects, such as composition, structure, and microstructure, which affect the transport and reaction of ions, electrons, and gases in the cells [46–49]. Therefore, materials design and optimization for CECs require a comprehensive understanding of these aspects and their interplay with the electrochemical processes [50–56].

To provide an overview of the current state-of-the-art electrolyte and electrode materials for CECs, we have compiled a table that summarizes the typical electrolyte and electrode materials used for CECs, along with their composition, structure, and limitations, as shown in Table 1.

Table 1 shows that different materials have different advantages and disadvantages for CECs, depending on their performance, stability, compatibility, and cost. For example, YSZ has high oxygen ion conductivity and good chemical stability but also low proton conductivity and high operating temperature [60,61]. SDC has high oxygen ion conductivity and lower activation energy, but it also has low chemical stability and relatively higher electronic conductivity [62,63]. LSGM has high oxygen ion conductivity and good chemical stability, but it also has high cost, complex synthesis, and low mechanical strength [64,65].

Similarly, different electrodes have different strengths and weaknesses for CECs, depending on their catalytic activity, durability, and thermal expansion. For example, BCFZ and BCFZY electrode materials have good catalytic activity but have low chemical stability, high electronic conductivity, and phase transition at high temperatures [68,69]. Ni-YSZ cermet has high electronic conductivity and good catalytic activity, but it also has poor mechanical strength and low durability under redox cycling [71,93]. LSM cathode has high electronic conductivity and good thermal expansion match with YSZ, but it also has low catalytic activity and poor compatibility with proton-conducting electrolytes [71,72]. LSCF has high electronic conductivity and oxygen surface exchange coefficient but also poor redox stability and degradation in CO_2 and H_2O atmospheres [81,82]. BSCF has high mixed ionic-electronic conductivity, excellent oxygen surface exchange coefficient but poor redox stability, and a detrimental high TEC [70].

Therefore, the selection of suitable materials for CECs is a challenging task that requires a comprehensive understanding of the material properties and their interactions with each other. AI can provide a powerful tool to assist in this task by predicting the optimal material combinations and configurations for CECs based on various criteria and constraints.

2.1. Materials composition

One of the most critical material aspects of CECs is the composition of the electrolyte and electrode materials, which determines their intrinsic properties such as conductivity, stability, compatibility, and catalytic activity [95–100]. For example, the electrolyte should have high ionic and negligible to zero electronic conductivity to minimize ohmic losses and internal short-circuiting [101]. PCFCs and PCECs use

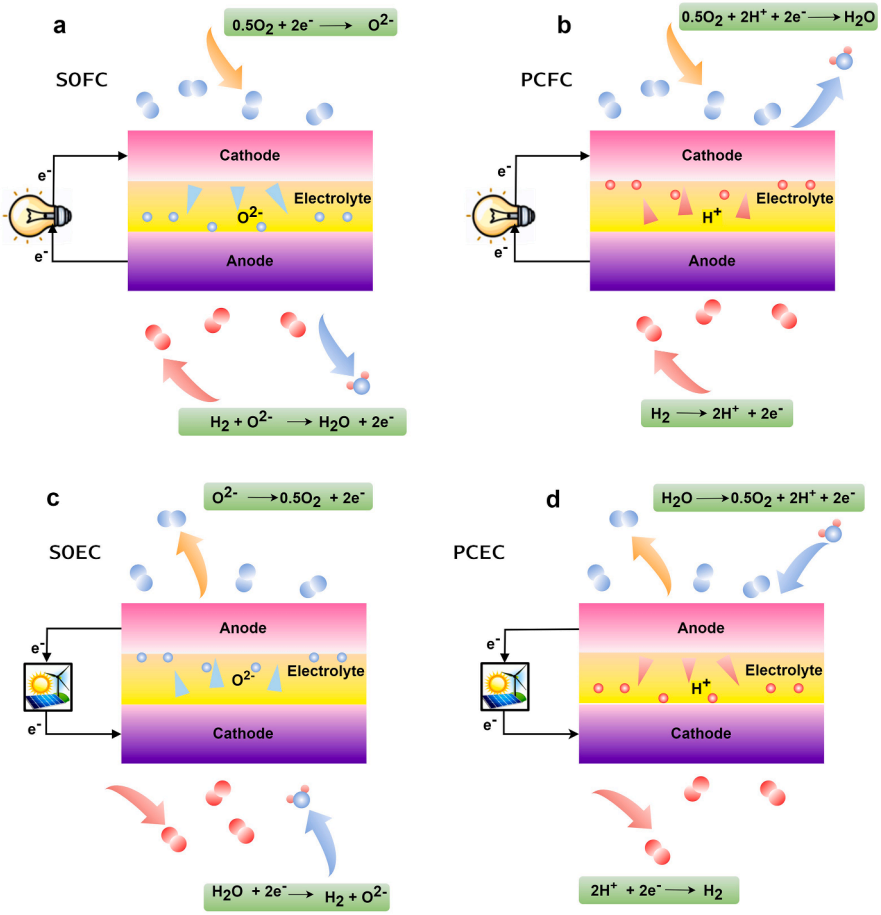

Fig. 1. Comparison of different types of CECs and their operating principles: (a) In the solid oxide fuel cell (SOFC), the oxidation half-reaction occurs at the anode: $H_2 + O^{2-} \rightarrow H_2O + 2e^-$. The reduction half-reaction occurs at the cathode: $0.5O_2 + 2e^- \rightarrow O^{2-}$. Oxide ions ($O^{2-}$) transport through the electrolyte. (b) In the protonic ceramic fuel cell (PCFC), the oxidation half-reaction at the anode is $H_2 \rightarrow 2H^+ + 2e^-$. The reduction half-reaction at the cathode is $0.5O_2 + 2e^- + 2H^+ \rightarrow H_2O$. Protons ($H^+$) transport through the electrolyte [57,58]. (c) In the solid oxide electrolysis cell (SOEC), a voltage is applied, reversing the direction of oxide ion flow, causing steam at the cathode to split into hydrogen and oxygen via reverse reactions. (d) A similar reversal of proton flow in the protonic ceramic electrolysis cell (PCEC) causes water to split into hydrogen and oxygen at the anode [59].

Table 1
A summary of notable electrolyte and electrode materials for CECs.

Material	Composition	Structure	Limitations	Ref.
Electrolyte	$Zr_{0.84}Y_{0.16}O_{1.92}$	Cubic fluorite	Low proton conductivity, high operating temperature	[60,61]
Electrolyte	$Ce_{0.8}Sm_{0.2}O_{2-\delta}$	Cubic fluorite	Low chemical stability, relatively higher electronic conductivity	[62,63]
Electrolyte	$La_{0.8}Sr_{0.2}Ga_{0.8}Mg_{0.2}O_{3-\delta}$	Perovskite	High cost, complex synthesis, low mechanical strength	[64,65]
Electrode	$BaCo_{0.4}Fe_{0.4}Zr_{0.2}O_{3-\delta}$	Perovskite	Low chemical stability, high electronic conductivity, phase transition at high temperature	[66,67]
Electrode	$BaCo_{0.4}Fe_{0.4}Zr_{0.1}Y_{0.1}O_{3-\delta}$	Perovskite	Low chemical stability, high electronic conductivity, phase transition at high temperature	[68,69]
Electrode	$Ba_{0.5}Sr_{0.5}Co_{0.8}Fe_{0.2}O_{3-\delta}$	Perovskite	Poor redox stability, high thermal expansion coefficient, degradation in CO_2 and H_2O environments	[70]
Electrode	$La_{0.8}Sr_{0.2}MnO_{3-\delta}$	Perovskite	Low catalytic activity, poor compatibility with proton-conducting electrolytes, high polarization resistance	[71,72]
Electrode	$PrBa_{0.5}Sr_{0.5}Co_{1.5}Fe_{0.5}O_{5+\delta}$	Perovskite	Poor redox stability, high thermal expansion coefficient, degradation in CO_2 and H_2O environments	[73,74]
Electrode	Ni- $BaZr_{0.1}Ce_{0.7}Y_{0.1}Yb_{0.1}O_{3-\delta}$	Composite of Ni and BZCYYb7111 (perovskite)	Susceptible to carbon deposition and sintering, poor mechanical strength, low durability under redox cycling	[75,76]
Electrolyte	$BaZr_{0.1}Ce_{0.7}Y_{0.2}O_{3-d}$	Perovskite	Low chemical stability, high electronic conductivity, phase transition at high temperature	[77,78]
Electrolyte	$BaZr_{0.1}Ce_{0.7}Y_{0.1}Yb_{0.1}O_{3-\delta}$	Perovskite	Low chemical stability, high electronic conductivity, phase transition at high temperature	[79,80]
Electrode	$La_{0.6}Sr_{0.4}Co_{0.2}Fe_{0.8}O_{3-\delta}$	Perovskite	Poor redox stability, high thermal expansion coefficient, degradation in CO_2 and H_2O environments	[81,82]
Electrode	$La_{0.6}Sr_{0.4}FeO_{3-\delta}$	Perovskite	Low catalytic activity, poor compatibility with proton-conducting electrolytes, high polarization resistance	[83,84]
Electrode	$NdBa_{0.5}Sr_{0.5}Co_{1.5}Fe_{0.5}O_{5+\delta}$	Perovskite	Poor redox stability, high thermal expansion coefficient, degradation in CO_2 and H_2O environments	[85]
Electrode	Ni-$BaZr_{0.4}Ce_{0.4}Y_{0.1}Yb_{0.1}O_{3-\delta}$	Composite of Ni and BCZYYb4411 (perovskite)	Susceptible to carbon deposition and sintering, poor mechanical strength, low durability under redox cycling	[5]
Electrode	Ni- $BaZr_{0.1}Ce_{0.7}Y_{0.2}O_{3-d}$	Composite of Ni and BCZY20 (perovskite)	Susceptible to carbon deposition and sintering, poor mechanical strength, low durability under redox cycling	[86,87]
Electrode	Ni- $BaCe_{0.85}Y_{0.15}O_{3-\delta}$	Composite of Ni and BCY15 (perovskite)	Susceptible to carbon deposition and sintering, poor mechanical strength, low durability under redox cycling	[88–90]
Electrode	Ni-SDC	Composite of Ni and SDC20 (cubic fluorite)	Susceptible to carbon deposition and sintering, poor mechanical strength, low durability under redox cycling	[63,91,92]
Electrode	Ni-YSZ	Composite of Ni and YSZ10 (cubic fluorite)	Susceptible to carbon deposition and sintering, poor mechanical strength, low durability under redox cycling	[71,93]
Electrode	BCFZY-NiO-BCZYYb4411-NiO-BCFZY (BNBNB) 5-layered composite electrode	Composite of BCFZY (perovskite), NiO (cubic), BCZYYb4411 (perovskite), NiO (cubic), BCFZY (perovskite) 5-layered structure	Complex fabrication process, high cost, possible interfacial reactions	[94]

proton-conducting ABO_3 perovskite oxides as electrolytes, which can be doped with various cations to increase their proton transport and hydration ability by creating oxygen vacancies, modifying the bond strength and length of A-O and B-O bonds, and enhancing the ionic character of dopant-oxygen bonds [11,102–107]. For instance, doping $BaCeO_3$-based perovskites with Y, Sc, Ga, In, Gd, or Er can increase their hydration and proton mobility by lowering the energy barriers for water dissociation and proton migration [108]. In $BaZrO_3$-based perovskites, doping the B-site with Yb can improve grain growth and reduce the reactivity with Ni electrodes, resulting in higher proton conductivity and stability [108]. As for $CaTiO_3$-based perovskites, doping with Mg and Al can create oxygen vacancies that facilitate water dissociation and proton incorporation, leading to high proton conductivity at low temperatures [106]. Fig. 2 illustrates the concept of material composition, showing different elements in the periodic table and the potential site they may occupy in a perovskite oxide lattice.

The electrode should have optimal ionic-electronic conductivity and efficient catalytic activity to facilitate optimal gas diffusion, charge transfer, bulk and surface exchange kinetics at the electrode-electrolyte interface [17,119,120]. The electrolyte and electrode materials should also be chemically stable and mechanically compatible with each other to avoid degradation and delamination during operation [121–125]. Moreover, the composition of the materials can be tailored by doping, exsolution, infiltration, or mechanical mixing to enhance their properties or introduce new functionalities [81,126–145]. For instance, Shao and Haile improved the performance and stability of the $SrCo_{0.8}Fe_{0.2}O_{3-\delta}$ (SCF) air electrode material for intermediate temperature SOFCs by partially doping the A-site of SCF with 50 % Ba, resulting in the widely

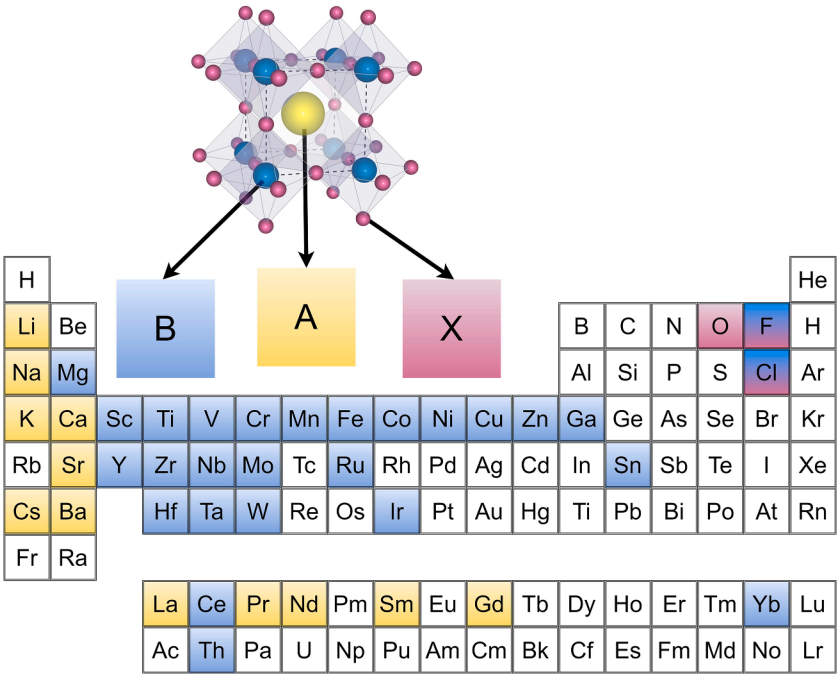

Fig. 2. A perovskite unit cell demonstrating occupiable positions by A, B, or X site cations in the map of elements based on common experimentally characterized perovskite oxides in the literature for CECs [109–118].

used $Ba_{0.5}Sr_{0.5}Co_{0.8}Fe_{0.2}O_{3-\delta}$ (BSCF) with enhanced oxygen reduction reaction (ORR) [8]. Similarly, Duan et al. [146,147] co-doped Zr and Y into $BaCo_{0.4}Fe_{0.4}Zr_{0.1}Y_{0.1}O_{3-\delta}$ (BCFZY) to boost its ORR and achieved peak power densities (PPDs) of 0.97 and 0.46 W cm^{-2} at 500 °C for SOFCs and PCFCs, respectively, using H_2 fuel. Kwon et al. [148] reviewed exsolution mechanisms in perovskite oxide materials for CECs, which has been promising in improving the materials' composition by designing metal nanoparticles for electrocatalysis. They further discussed the driving forces of exsolution, and classified perovskite structures based on their exsolution behaviors [148]. Kim et al. [149] proposed a diffusion model based on classical nucleation and diffusion to explain the particle growth process in perovskite materials for CECs, using $(La,Ca)_{1-\alpha}(Ni,Ti)O_3$ (TF-LCNT, α: A-site-deficiency). They showed that exsolution involved Ni diffusion and reduction, leading to Ni-rich nanoparticles on the surface and Ni-poor matrix in bulk. They also showed that Ni diffusion was hindered by the perovskite lattice, resulting in a steep Ni concentration gradient at the nanoparticle-matrix interface. This suggested that particle growth was limited by the perovskite structure and that exsolved Ni nanoparticles were mainly located on the surface and near-surface regions of the perovskite matrix [149].

Similarly, layered nickelates ($Ln_2NiO_{4+\delta}$) are promising electrode materials for PCFCs and PCECs, which can be modified by changing the lanthanide element (Ln) or adding other oxides to improve their oxygen transport and electrocatalysis [101,108]. Hence, the composition of electrolyte and electrode materials plays a crucial role in determining the intrinsic properties of CECs, including conductivity, stability, compatibility, and catalytic activity. Researchers have enhanced their performance and stability by doping and tailoring the materials' composition. Therefore, understanding the mechanisms and behaviors associated with material composition, as evidenced by exsolution studies and diffusion models, provides valuable insights for future material design and development in CECs.

2.1.1. *Key challenges and opportunities for materials composition design and optimization*

One of the main challenges for materials composition in CECs is finding the optimal doping level and stoichiometric or mixing ratio that can maximize the materials' conductivity, stability, compatibility, and catalytic activity [40,150–154]. Another challenge is to avoid undesirable side effects such as phase segregation or degradation caused by doping, infiltration, exsolution, or mixing [155–162]. Therefore, one of the main opportunities for materials' composition is to explore new combinations of elements or compounds that can create novel and superior materials with enhanced properties for the electrolyte and electrode materials. AI can help address these challenges and opportunities by predicting the optimal composition for a given property or performance target and discovering new materials with desirable features.

2.2. *Materials structure*

Another necessary material aspect of CECs is the structure of the electrolyte and electrode materials, which mainly refers to their crystallographic arrangement and defect configuration [163–165]. The structure of the materials affects their transport properties by influencing the formation and migration of charge carriers such as ions and electrons [166–168]. For example, oxygen-ion conducting electrolytes such as doped-zirconia (YSZ) or doped-ceria (SDC or GDC) have cubic or fluorite cubic structures with oxygen vacancies as the primary defects that enable oxygen-ion transport [169]. Proton-conducting electrolytes such as barium zirconate ($BaZrO_3$) or caesium dihydrogen phosphate (CsH_2PO_4) have perovskite or layered structures with protonic defects that enable proton transport [170–172]. The structure of the materials can also affect their stability and compatibility by influencing their thermal expansion and phase transition behaviors [4,154]. For example, some proton-conducting electrolytes, such as CsH_2PO_4 undergo dehydration or decomposition at high temperatures or low humidities, which limits their operational range [170,171]. Some electrode materials, such as perovskites or nickelates, undergo structural changes or phase separation under reducing or oxidizing conditions, which affect their electrochemical performance [108,173]. The phase diagrams in Fig. 3 illustrate how NiO–$LaO_{1.5}$ oxide systems can undergo structural changes or phase separation under reducing or oxidizing conditions, which affect their electrochemical performance [173]. The structure of the materials can be controlled by adjusting their composition, synthesis method, or processing conditions.

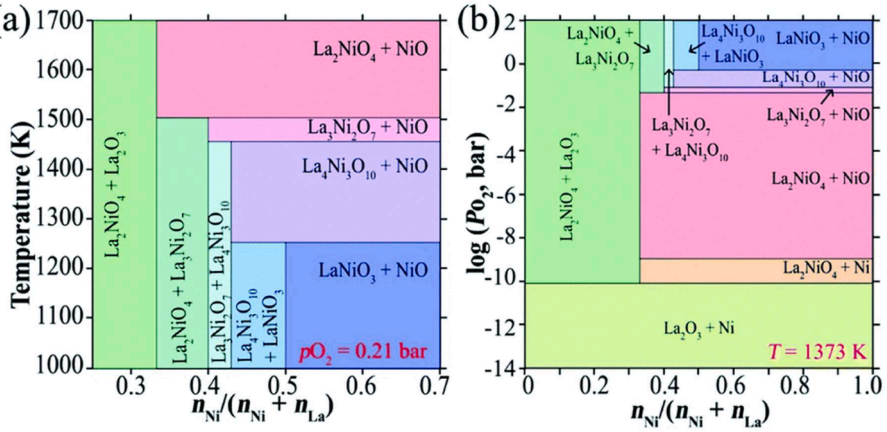

Fig. 3. The phase stability of NiO–$LaO_{1.5}$ oxide systems under different temperature (T) and oxygen partial pressure (pO_2) conditions. (a) The T-based phase diagram shows the regions of single-phase and two-phase mixtures of NiO and $LaO_{1.5}$ as a function of the Ni content. (b) The pO_2-based phase diagram shows the regions of single-phase and two-phase mixtures of NiO and LaO1.5 as a function of the pO2. Copyright 2021, Royal Society of Chemistry [173].

Lee et al. [106] proposed strategy for enhancing proton conductivity in $CaTiO_3$ by replacing lattice oxygens with hydroxide groups using a solvothermal process. The resulting material, $Ca_{0.92}TiO_{2.84}(OH)_{0.16}$, shows one order of magnitude higher bulk conductivity (10^{-4} Scm^{-1}at 200 °C) than hydrated $CaTiO_3$ prepared by traditional solid-state synthesis due to the higher concentration of protonic defects and variation in the crystal structure. Fig. 4 shows the results of neutron diffraction analysis of two samples of calcium titanate (CTO), one prepared by solid-state synthesis (CTO(SS)) and the other prepared by solvothermal synthesis (CTO(ST)). One interesting finding from the study is that CTO (ST) has a shorter O—O distances than CTO(SS), which facilitates intra-proton transfer along the edges of octahedra. Another interesting finding is that Ni^{2+} ions can be substituted for Ca^{2+} ions in CTO(ST), leading to the exsolution of Ni nanoparticles on the perovskite surfaces upon reduction. These findings suggest new ways of enhancing proton conductivity and catalytic activity of CTO for energy applications based on material structural modification [106].

Tailoring the oxygen electrode material structure is critical to the performance and stability of CECs since it determines the electrode's catalytic, ionic, and electronic conductivity. For instance, the oxygen

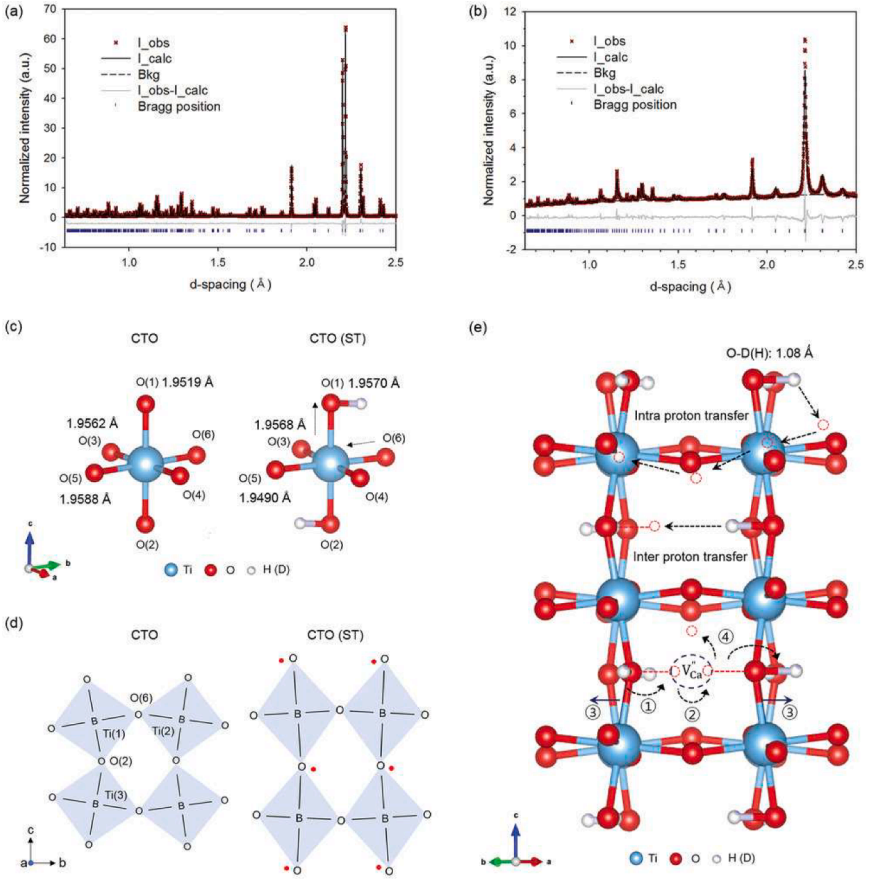

Fig. 4. (a,b) High-resolution powder diffraction analysis of deuterated CTO(SS) and CTO(ST) (c) Comparison of the Ti-O bond lengths in CTO(ST) and CTO(SS). (d-e) Schematic illustration of the unit cells (CTO(SS) and CTO(ST)) and proton transfer mechanism in CTO(ST). Copyright 2021, Wiley [106].

electrode of PCECs should have triple conductivity, comprising protonic defects, oxygen vacancy, and electrons to facilitate water oxidation and ORR at reduced temperatures. Ding et al. [79] described $PrNi_{0.5}Co_{0.5}O_{3-\delta}$ (PNC) as a triple conducting oxide (TCO) electrode for PCECs with superior performance and self-sustainable reversible operation. The structural defect of PNC is correlated with its performance by showing that Ni doping can reduce the oxygen vacancy formation energy and the proton migration energy, thus enhancing proton conduction and electrocatalytic activity. Hence, the structure of materials comprising various descriptors, such as ionic radius, bond length and angle, coordination number, tolerance factor, defect characteristics, and more, influence the performance and stability of CEC materials.

2.2.1. Key challenges and opportunities for materials structural design and optimization

Controlling the defect formation and migration that enable charge transport in the materials has been identified as one of the major challenges of material structure [163–165]. Furthermore, preventing the structural changes or phase transitions that affect the stability and compatibility of the material remains a challenge [174–177]. To mitigate this challenge, an opportunity exists to manipulate the materials' crystallographic arrangement and defect configuration to tune their transport and catalytic properties [178–182]. AI can help address these challenges and offers opportunities by modeling the defect chemistry and thermodynamics of the materials and designing new structures with improved performance and stability.

2.3. Materials microstructure

The third vital material aspect of CECs is the microstructure of the electrolyte and electrode layers, which refers to their morphology, porosity, grain size, and grain boundary. The microstructure of the materials affects their transport properties by influencing the effective pathways for charge carriers and gases [138,183]. For instance, the electrolyte layer should have a dense microstructure to prevent gas leakage and electronic conduction [108,184]. The electrode layer should have a porous microstructure to facilitate gas diffusion and reaction sites [185,186]. Moreover, the grain size and boundary of the materials can affect their conductivity and catalytic activity by controlling the defect concentration and mobility [187,188]. Therefore, by tailoring the grain size and boundaries of electrode and electrolyte materials used in CECs with mixed ionic-electronic conductivity, it is possible to minimize the electronic leakage, enhance the ionic conductivity, suppress the degradation, promote triple conductivity in the oxygen electrode, and improve the efficiency of the cells under various operating conditions [189,190]. The microstructure of the materials can be engineered by optimizing their fabrication method, sintering temperature, and sintering time [191–193]. Kim et al. [194] demonstrate a simple co-impregnation method to construct active heterointerfaces in the air electrode of CECs and shows that the microstructure tailoring can enhance the electrochemical activity and stability of the electrode (Fig. 5).

Hence, one way to improve the electrode microstructure for PCECs is to create a self-architectured mesh-like electrode with high porosity and

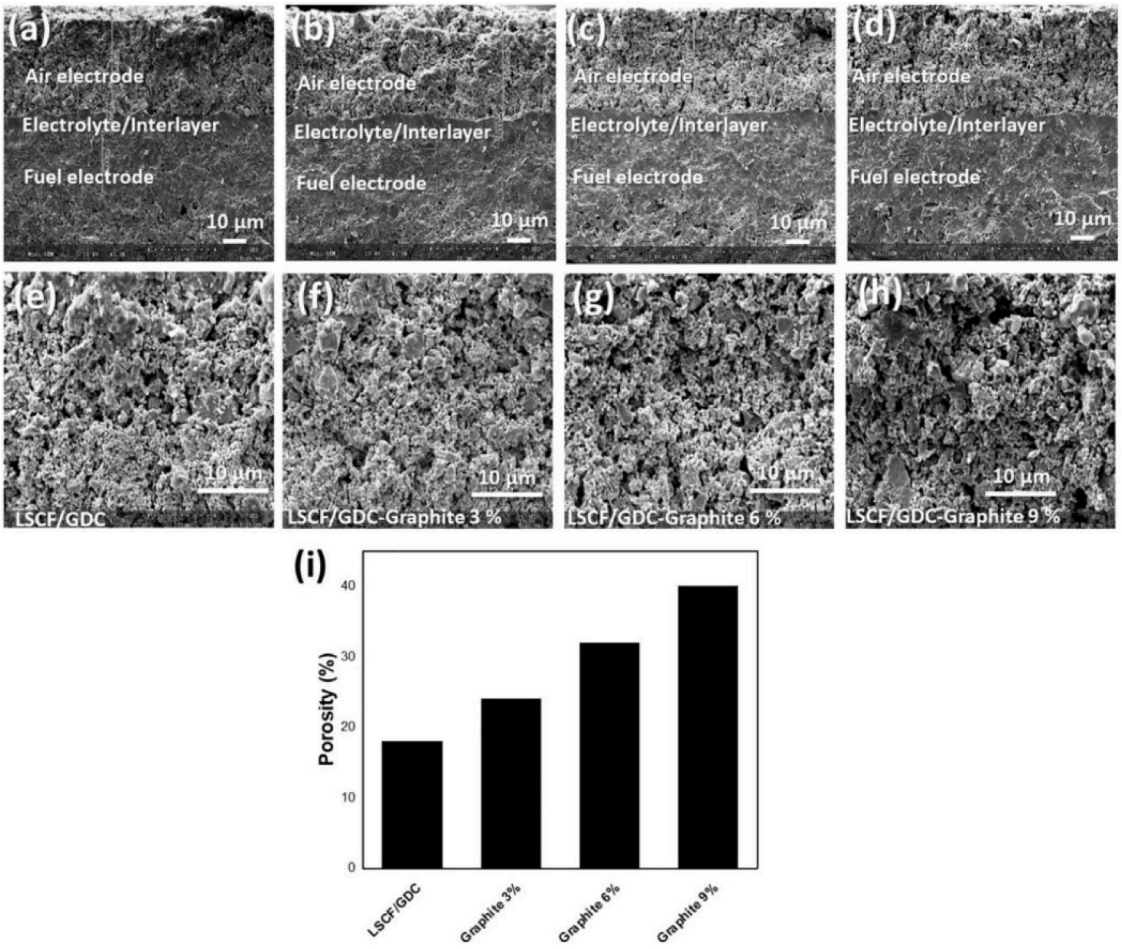

Fig. 5. A schematic illustration of the co-impregnation method and the cross-sectional SEM images of the air electrodes with different amounts of graphite pore former. The co-impregnation method can create active heterointerfaces between LSCF and GDC, enhancing the ORR activity and stability of the air electrode. Copyright 2021, Elsevier [194].

nanostructure, as shown in Fig. 6. The figure displays scanning and transmission electron microscopy images of the $PrNi_{0.5}Co_{0.5}O_{3-\delta}$ (PNC) oxide electrode, which consists of hollow-fiber-like strings that form a mesh structure [79]. Each string is composed of nanoparticles with a size of about 50 nm [79]. The mesh-like electrode can enhance the mass transport and gas diffusion throughout the electrode, leading to improved electrochemical performance of PCECs.

2.3.1. *Key challenges and opportunities for materials microstructural design and optimization*

Optimizing the microstructural parameters of materials is a challenging task that requires engineering the morphology, porosity, grain size, and grain boundary to enhance their transport and reaction properties while ensuring their mechanical integrity and durability under thermal and electrochemical stress [150,188,195]. However, this challenge also presents an opportunity to create novel and effective microstructures with tailored properties by engineering the shape, size, orientation, and distribution of the grains and pores. This opportunity can be actualized by leveraging AI to simulate the fabrication and sintering processes of the materials and by optimizing the microstructure parameters for a given performance target. The various materials aspects relevant to the application of AI for materials development in CECs are summarized in Table 2.

3. Database construction and data pre-processing

3.1. *Database construction*

Data gathering is essential for AI-based materials design, optimization, and discovery for CECs. Usually, extensive data is organized and structured in a database to facilitate easy storage, management, and retrieval. The data on CECs materials and systems are generated from various sources and methods, such as material simulations, measurements, experiments, and general inorganic material databases. It is noteworthy that there is no database dedicated explicitly to CECs, but such a database can be established by employing suitable material descriptors that account for the unique features and challenges of CECs, such as the electrochemical reactions, the stability and compatibility of materials, and the fabrication and integration of cells. Hence, database construction is designing and executing a database system to meet the requirements and specifications of materials aspects of CECs [196,197]. The data quality in the database system determines the accuracy of the

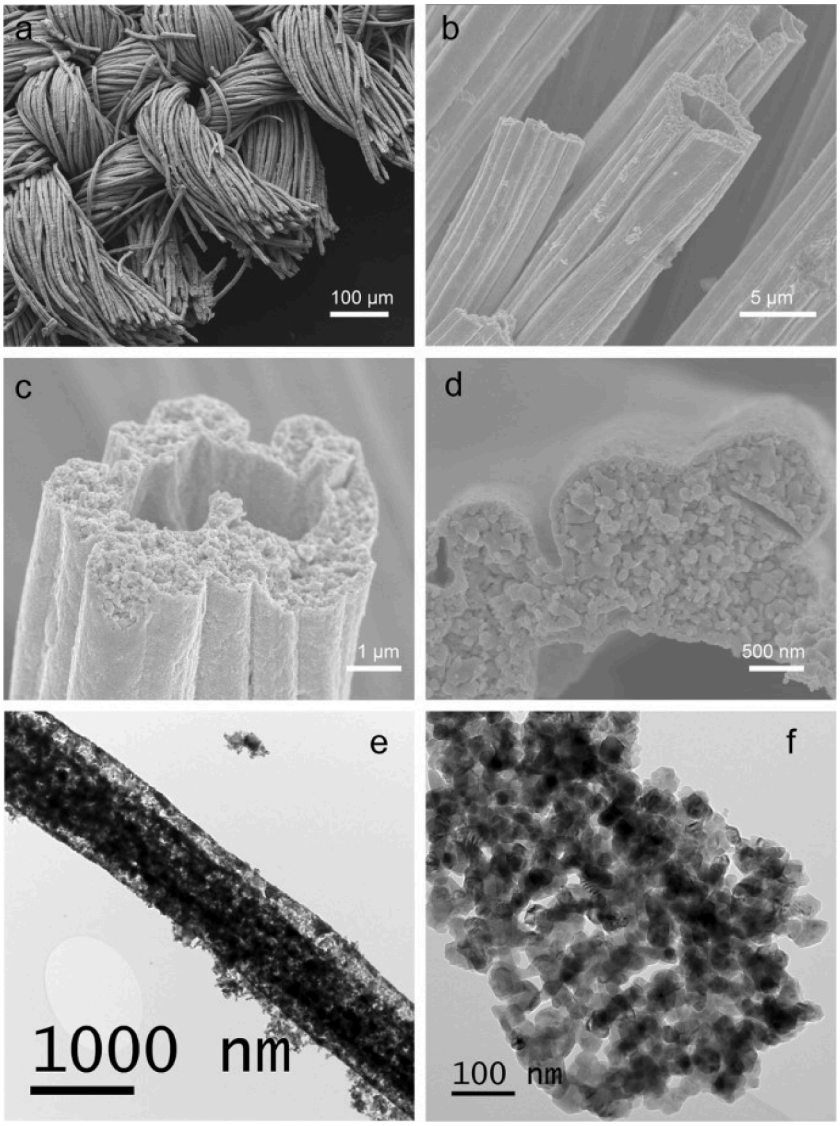

Fig. 6. A self-architectured mesh-like PNC electrode with high porosity and nanostructure. (a–d) SEM images of the electrode mesh with different magnifications depict a hollow-fiber-like string self-architecture to form a mesh structure. (e,f) TEM images of a single nanofiber composed of ~50 nm particles. Copyright 2020, Nature [79].

Table 2
Summary of the key points relevant to materials development for CECs.

Materials aspect	Definition	Effect on CECs	Challenges and opportunities	AI applications
Composition	The chemical composition of the electrolyte and electrode materials	Determines their intrinsic properties such as conductivity, stability, compatibility, and catalytic activity	Finding the optimal doping level or mixing ratio; avoiding undesirable side effects; exploring new combinations of elements or compounds	Predicting the optimal composition for a given property or performance target; discovering new materials with desirable features
Structure	The crystallographic arrangement and defect configuration of the electrolyte and electrode materials	Affects their transport properties by influencing the formation and migration of charge carriers; affects their stability and compatibility by influencing their thermal expansion and phase transition behaviors	Controlling the defect formation and migration; preventing structural changes or phase transitions; manipulating the crystallographic arrangement and defect configuration	Modeling the defect chemistry and thermodynamics of the materials; designing new structures with improved functionality
Microstructure	The morphology, porosity, grain size, grain boundary, etc. of the electrolyte and electrode layers	Affects their transport properties by influencing the effective pathways and barriers for charge carriers and gasses; affects their catalytic activity by influencing the defect concentration and mobility	Optimizing the morphology, porosity, grain size, and grain boundary of the materials; ensuring the mechanical integrity and durability of the materials	Simulating the fabrication and sintering processes of the materials; optimizing the microstructural parameters for a given property or performance target

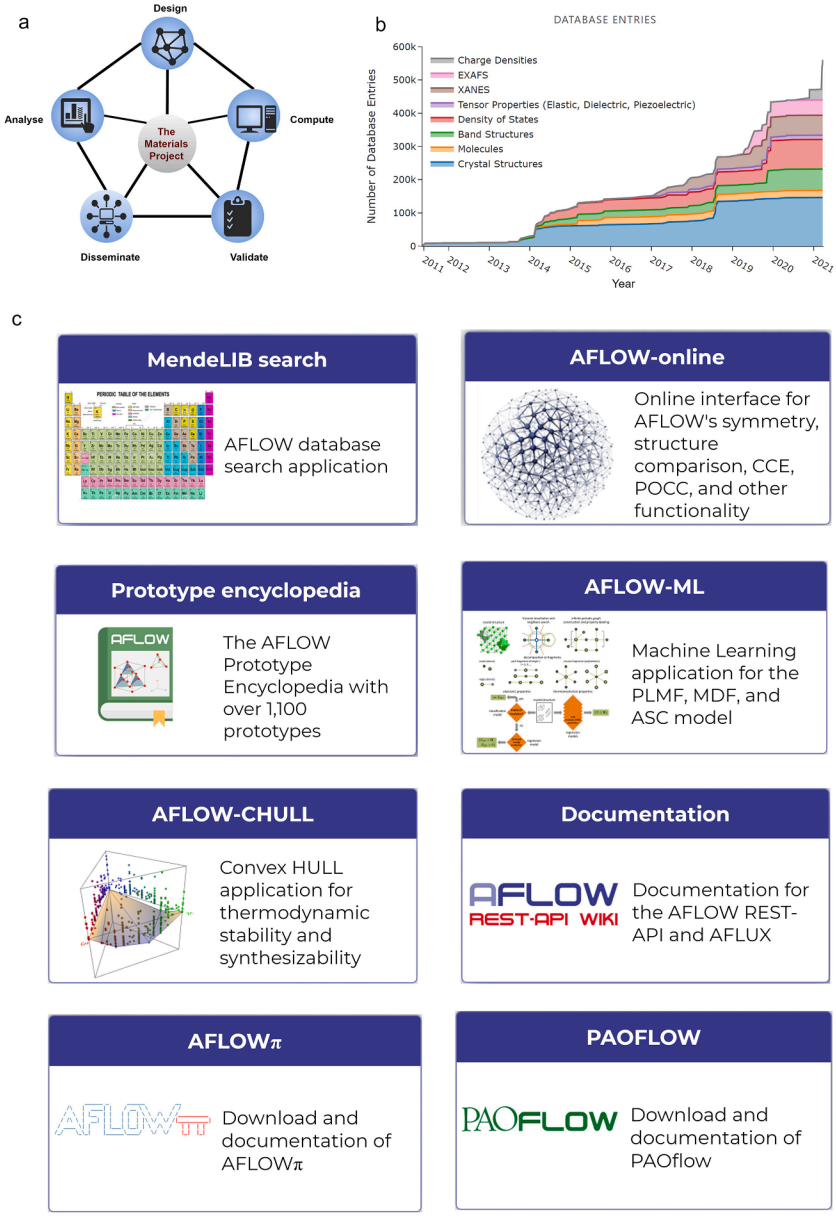

Fig. 7. Some relevant opensource inorganic material databases (a) Representation of the thrust of materials project database [199] (b) Content of materials project database [200] (c) Overview of AFLOW database applications [201].

AI learning and optimization models [198].

The past two decades have experienced an increase and improvement in materials database systems. Several open-source databases offer valuable resources for developing novel materials. For instance, the Materials Project is a globally accessible database that employs high-throughput theoretical simulations using density functional theory (DFT) to investigate inorganic materials [199,200]. Fig. 7**a** indicates the framework of the materials project, which is to design and compute materials-related data, validate, and distribute the data for the broader scientific community. Fig. 7**b** summarizes the nature and number of the database content over the years. AFLOWLIB is another database that facilitates DFT calculations for various material properties, including electronic structure, thermodynamics, and more, to achieve improved energy materials for. It contains over 3.5 million materials, and the calculated properties are over 730 million, making it an encyclopedia of crystallographic prototypes [201]. Fig. 7**c** depicts the available AFLOW applications and documentation from the website.

The Open Quantum Materials Database (OQMD) is another instance that specializes in inorganic crystal structures, leveraging DFT calculations and boasting a collection of approximately 1000,000 hypothetical materials properties [202,203]. Another important database is the Crystallography Open Database (COD), an open-access collection of crystal structures. The COD contains over 502,849 entries as of June 2023 [204,205]. Researchers in CECs can utilize the COD to access a wide range of crystallographic information for AI predictions and modeling [206]. The Material Genome Engineering Databases (MGED) integrate seven functional modules, such as materials database, materials design tools, data processing software, text mining system, high-throughput computational engine, inter-atomic potentials database, and materials data mining system, to provide comprehensive tools and data for material genome engineering research [207]. These databases serve as valuable input data repositories for AI-based methods, enabling the prediction and optimization of materials that could be tailored for CEC applications.

Table 3 summarizes some of the key open-source inorganic materials databases that could provide useful data for AI-enabled materials discovery and optimization for CECs. The databases offer extensive data on the properties of inorganic compounds and materials that could inform the design of suitable electrolytes, electrodes, and other components for CECs. However, none of the databases have CEC-specific data and have varying degrees of relevance and limitations with respect to direct application to CECs. When utilizing these databases, care must be taken to validate data quality and reliability. These resources serve as a good starting point and supplemental data source for constructing machine learning models and informing materials selections for advanced CECs.

3.2. Descriptors for materials design in CECs

Descriptors for materials design play a crucial role in CECs by capturing different mechanisms, organizing independent variables, and revealing relationships between hidden data and relevant features [208]. These descriptors cover the different aspects of materials in CECs, including composition, structure, and microstructure. The material composition descriptors, which are usually controllable, encompass molecular formula, stoichiometric ratio, atomic percent, mass fraction, mole fraction, volume fraction, and element, which are correlated with various intrinsic material property functions such as thermal expansion coefficient, ionic conductivity, triple ionic and electronic conductivity, valence state, and oxygen vacancy concentration [108,209–211].

The material structure descriptors include bond length, bond angle, coordination number, tolerance factor, defect characteristics, and ionic radius. These descriptors contribute to material property functions such as surface structure, phase stability, crystal structure, charge transfer, symmetry, and triple ionic and electronic conductivity [212–216].

Regarding material microstructure, descriptors such as morphology, pore size, shape, orientation, crystallite size, grain boundary, and grain size, shape, and orientation play a crucial role. These descriptors can be associated with material transport property functions such as triple ionic

Table 3
Summary of relevant materials databases for CECs.

Database	Main Features	Relevance to CECs	Limitations for CECs	URL
NOMAD CoE	Materials informatics and machine learning	Highly relevant for CEC materials design	No specific CEC data; relies on computations	[https://www.nomad-coe.eu/]
NREL materials database	Renewable energy materials data	Moderately relevant data could apply to CECs	No CEC-specific data; depends on data quality	[https://materials.nrel.gov/]
Citrine informatics	Materials data analytics and machine learning	Moderately relevant to optimize CEC materials	No CEC-specific data; requires login	[https://citrine.io/]
OQMD	Thermodynamic data from DFT	Moderately relevant for CEC material stability	No CEC-specific data; relies on computations	[http://oqmd.org/]
Materials project	High-throughput computational data	Moderately relevant data for CEC materials	No CEC-specific data; relies on computations	[https://legacy.materialsproject.org/]
CompMatRepo	Computational examples	Slightly relevant computational studies for CECs	No CEC-specific data; requires programming	[https://cmr.fysik.dtu.dk/]
SUNCAT	Catalytic interface studies	Slightly relevant to improve CEC materials	No CEC-specific data; requires collaboration	[http://suncat.stanford.edu/]
ChemSpider	Chemical properties data	Slightly relevant to find CEC materials	No CEC-specific data; variable data quality	[https://chemspider.com/]
Crystallography open database	Crystal structure data	Slightly relevant for potential CEC materials	No CEC performance data	[http://www.crystallography.net/cod/]
American mineralogist crystal structure DB	Crystal structure data	Slightly relevant for potential CEC materials	No CEC performance data	[https://www.geo.arizona.edu/AMS/amcsd.php]
MPDS	Experimental materials data	Slightly relevant data could apply to CECs	No CEC-specific data; requires login	[https://mpds.io/#start]
AFLOW	High-throughput material computations	Slightly relevant to inform CEC material design	No CEC-specific data; relies on computations	[http://aflowlib.org/]
MatNavi	Ceramic materials data	Slightly relevant data could apply to CECs	No CEC-specific data; requires login	[https://mits.nims.go.jp/en/]
NIST materials data repository	Materials data sharing platform	Not relevant	No CEC-specific data; requires login	[https://materialsdata.nist.gov/]
NCCR MARVEL	Materials informatics for energy	Not relevant	No CEC-specific data; requires login	[https://www.nccr-marvel.ch/]
Materials cloud	Computational materials platform	Not relevant	No CEC-specific data; relies on computations	[https://www.materialscloud.org/]

and electronic conductivity, gas diffusion, reaction sites, and surface area [209,217–219]. Table 4 summarizes some cogent descriptors and property functions that could support the AI methods in CECs in making predictions, optimizations, and revealing material-property relationships.

Some more descriptors have been proposed, which could aid in designing electrode materials for CECs [198,220–227]. The valence state and surface structure have been underscored as crucial factors in optimizing the ORR of manganese-based oxides, leading to enhanced ORR performance [227]. Calle–Vallejo et al. [226] suggested that the outer electrons of transition metal-containing oxides can be a unique descriptor for predicting adsorption energies and scaling relationships. The A-site ionic electronegativity descriptor has also been explored as a reliable parameter for designing effective electrocatalysts [225]. Jacobs et al. [224] also found that the oxygen p-band center is an essential descriptor of the surface exchange coefficient, which correlates with the ORR activity of cathode materials for CECs. Hong et al. [223] demonstrated that reducing the solid-state charge-transfer energy of perovskites can alter the mechanisms of the OER from electron-transfer-limited to proton–electron-coupled to proton-transfer-limited reactions in CECs. This concept is vital for comprehending the interplay between catalytic mechanisms and interfacial charge-transfer kinetics, ultimately leading to the discovery of electrode materials with superior performance. In addition, bulk thermochemistry of transition metal oxides (TMOs) has also been identified as a valuable descriptor for electrocatalytic activity in CECs, as it is influenced by outer electron configuration [222,226]. This knowledge can guide the design of efficient materials for CECs. Lee et al. [220] highlighted the significance of the oxygen p-band center and the energy associated with oxygen vacancy formation, derived from first-principles calculations, as crucial descriptors for catalytic ORR in CECs. These descriptors provide insights into the underlying principles governing catalytic activity. Suntivich et al. [221] identified eg-filling of surface transition-metal ions as a primary descriptor for the ORR activity of perovskite oxides. This descriptor has predictive power and provides valuable insights into the role of electronic structure in controlling the catalytic activity of oxides. Understanding these descriptors can aid researchers in gaining a deeper understanding of the basic principles influencing the catalytic activity of oxygen and air electrodes in CECs, enhancing the smooth discovery and design of more efficient materials.

Based on the evaluation of descriptors for CEC materials design, we can classify them into several broad categories based on their characteristics for simplification purposes. These classifications include controllable versus uncontrollable descriptors, elemental versus structural descriptors, and numerical versus categorical descriptors. the

a **Controllable versus uncontrollable descriptors:** The descriptors that can be chosen before synthesizing a material or preparing a mixture, such as elements, their stoichiometric ratio, atomic percent, mass fraction, mole fraction, volume fraction, and other external conditions are called controllable descriptors [108,209,210]. In contrast, descriptors such as crystal structure, surface charge, grain and crystallite sizes, defects configuration, and more that depend on the actual synthesis or material processing are called uncontrollable descriptors. Hence, we can infer that all structural and microstructural properties are uncontrollable descriptors since they are not external conditions [209,217–219].

b **Elemental versus structural descriptors:** Descriptors, such as atomic number, electronegativity, or oxidation states, that describe the chemical composition of the material are called elemental descriptors. On the other hand, descriptors, including bond length, bond angle, or coordination number, that describe the geometric arrangement of atoms or molecules in a material can be tagged as structural descriptors [225,228,229].

c **Numerical and categorical descriptors:** The descriptors with a continuous range of values, such as band gap, atomic coordinates, conductivity, and density of states, are called numerical descriptors [230–232]. In contrast, categorical descriptors have a discrete set of values, such as space group, oxidation state, or crystal system. For instance, extensive research has proven that cubic phase materials with a pm3m space group have good oxygen vacancy concentration, which is necessary for efficient air or oxygen electrode catalytic activity [233–235].

Elemental descriptors are related to the chemical composition and stoichiometry of a material, which affect the intrinsic properties of CEC materials such as conductivity, stability, oxygen vacancy concentration, and catalytic activity [220]. For example, the choice of elements determines the valence state and surface structure of CEC materials, which are crucial for catalytic activity [236]. The stoichiometric ratio affects the charge balance and oxygen vacancy formation of CEC materials, which influence the conductivity and stability [237,238]. Some studies have used elemental descriptors such as electronegativity, oxidation state, and atomic number to predict the OER activity of perovskite oxides and to screen for optimal compositions of CEC materials [223,225,229,239].

Structural descriptors are related to the geometric arrangement and defect configuration of atoms or molecules in a material, which affect the phase stability, symmetry, charge transfer, and ionic/electronic conductivity of CEC materials [163,164,166]. For example, the bond length and bond angle affect the crystal structure and phase transition of

Table 4
Some relevant descriptors and material property functions for AI learning and optimization methods in CECs.

Materials aspects	Important descriptors	Material property function	Ref.
Material composition	• Molecular formula • Stoichiometric ratio • Atomic percent • Mass fraction • Mole fraction • Volume fraction • Element	• Thermal expansion coefficient • Ionic conductivity • Triple ionic and electronic conductivity • Chemical stability • Catalytic activity	[108,154,209,210]
Material structure	• Bond length • Bond angle • Coordination number • Tolerance factor • Defect characteristics • Ionic radius	• Surface structure • Phase stability • Crystal structure • Charge transfer • Symmetry • Triple ionic and electronic conductivity • Oxygen vacancy concentration	[212–215]
Material microstructure	• Morphology • Pores size, shape, and orientation • Crystallite size • Grain boundary • Grain size, shape, and orientation	• Triple ionic and electronic conductivity • Gas diffusion • Reaction sites • Surface area	[209,217–219]

CEC materials, which influence the symmetry and transport properties [212–216]. The coordination number and tolerance factor affect the formation and migration of charge carriers and gases in CEC materials, which influence the conductivity and catalytic activity. The defect characteristics and ionic radius affect the oxygen vacancy concentration and electronic structure of CEC materials, which influence the stability and conductivity. Some studies have used structural descriptors such as bond valence sum, defect energy, and lattice parameter to predict the stability and conductivity of CEC materials and to optimize the structural design of CEC materials [212–215].

Nevertheless, the various descriptor types have pros and cons in the context of AI methods for CECs. The uncontrollable descriptors, for instance, are challenging to manipulate and optimize compared with the controllable descriptors [209,217–219]. Hence, controllable descriptors are more reliable in directly influencing the performance and stability of CEC materials, but they cannot capture all the salient information about a material. In addition, the elemental descriptors are more straightforward and general than the structural descriptors; however, they do not reflect a vivid picture of the diversity and complexity of a material [225, 229]. The numerical descriptors are more precise and quantitative than the categorical descriptors but may require more data and complex computation than categorical descriptors [202,204]. A good understanding of these categories and their pros and cons can aid researchers in selecting the appropriate descriptors for AI methods in materials design and development for CECs.

Table 5 provides a comparison of different materials descriptors that can be utilized in AI methods for discovering and designing novel materials for CECs. Six descriptor types are analyzed: controllable, uncontrollable, elemental, structural, numerical, and categorical. For each descriptor type, the table outlines the definition, advantages, disadvantages, examples relevant to CECs, and the specific relevance to modeling and optimizing CEC material properties.

3.3. Data pre-processing and feature engineering

After collecting high volumes of data relevant to the materials aspects of CECs, it is essential to carry out adequate data pre-processing and feature engineering [240,241]. These steps are crucial before applying AI methods to the data generated from various materials aspects of CECs. Data pre-processing entails preparing and cleaning raw data by handling missing values, encoding categorical variables, and normalizing numerical values to facilitate practical feature engineering [31]. It is pertinent to clarify that “features” and “descriptors” can be used interchangeably in AI materials design and development methods [31,241]. Descriptors in the context of materials design for CECs are representations of material properties that can serve as inputs for AI methods. On the other hand, features can be considered a subcategory of descriptors. For example, certain AI methods like deep learning often extract features from frequency values or raw pixels when images are used as inputs [34]. Therefore, it is essential to focus on effective feature engineering to optimize the representation and applicability of CEC materials data for AI methods. This involves selecting and engineering relevant features that capture the essential characteristics of the materials and align them with the goals of the AI methods. By refining the features, the materials data can be better utilized in AI models, leading to improved predictions, optimizations, and the discovery of material-property relationships in CECs. [242]. Feature selection involves creating new features from raw data by transforming existing features or using domain knowledge to enhance the performance of relevant AI methods for CECs [240,242]. It can help reduce the dimensionality and complexity of energy materials data [240] Feature selection typically involves four stages, as proposed by Muller [240]: pre-feature selection, in-depth feature selection, subset evaluation, and result validation (Fig. 8).

a **The pre-feature selection** is the first stage of feature selection, and it involves screening the features and reducing the dimensionality of the data using methods such as clustering, principal component analysis, or correlation analysis. This can aid in extracting the essential features that capture the variance of CEC structural and compositional data or use correlation analysis to identify features highly correlated with data from electrochemical process data [240].

b **The in-depth feature selection** stage involves applying the filter, embedded, or wrapper methods to select the optimal subset of features from the pre-selected features. The filter method is based on the correlation coefficient between the features and the target variable, while the wrapper method is based on the LASSO (least absolute shrinkage and selection operator) regression technique [242]. The in-depth feature selection process aims to find the smallest subset of features that achieves the best performance in terms of prediction accuracy and model complexity [240]. One popular approach for feature selection uses SHapley Additive exPlanations (SHAP) [243, 244], which assigns each feature a SHAP value reflecting its marginal contribution to a model’s output. SHAP values have desirable properties like consistency and missingness handling, making them suitable for explaining complex ML models [243,245]. SHAP values

Table 5
Comparison of descriptors for AI-enabled CECs materials discovery.

Descriptor type	Definition	Pros	Cons	Examples	Relevance for CECs
Controllable [108, 209,210]	Descriptors that can be chosen before synthesizing a material or preparing a mixture	(1) Allow directed design and optimization (2) Directly influence CEC performance and stability	(1) Cannot fully describe a material	(1) Composition (elements, stoichiometry) (2) External conditions (T, P)	Affect intrinsic properties like conductivity, stability, compatibility
Uncontrollable [209,217–219]	Descriptors that depend on actual synthesis or processing	(1) Capture complexity of materials (2) Reflect effects of fabrication on CECs	(1) Hard to manipulate and optimize (2) May introduce defects in CECs	(1) Crystal structure (2) Grain size (3) Defects	Affect transport and reaction properties by influencing charge carrier and gas migration.
Elemental [225, 228,229]	Descriptors of chemical composition	(1) Straightforward and general (2) Easy to obtain	- Do not reflect structure or interactions	(1) Atomic number (2) Electronegativity	Affect valence state and surface structure crucial for catalytic activity.
Structural [233–235]	Descriptors of geometric arrangement of atoms/ molecules	(1) Capture complexity of materials (2) Reflect crystallography effects on CECs	(1) Hard to obtain (2) May require complex modeling.	(1) Bond length (2) Coordination number	Affect phase stability, conductivity, oxygen vacancy concentration.
Numerical [230–232]	Descriptors with continuous values	(1) Precise and quantitative (2) Capture variation with conditions	(1) Require more data and computation (2) May introduce data noise	(1) Band gap (2) Density of states	Affect electronic structure, transport properties, kinetics of CECs
Categorical [233–235]	Descriptors with discrete values	(1) Require less data and computation (2) Capture classification of properties	(1) Less precise and quantitative (2) May introduce ambiguity	(1) Space group (2) Oxidation state	Affect symmetry, phase transitions, charge balance of CECs

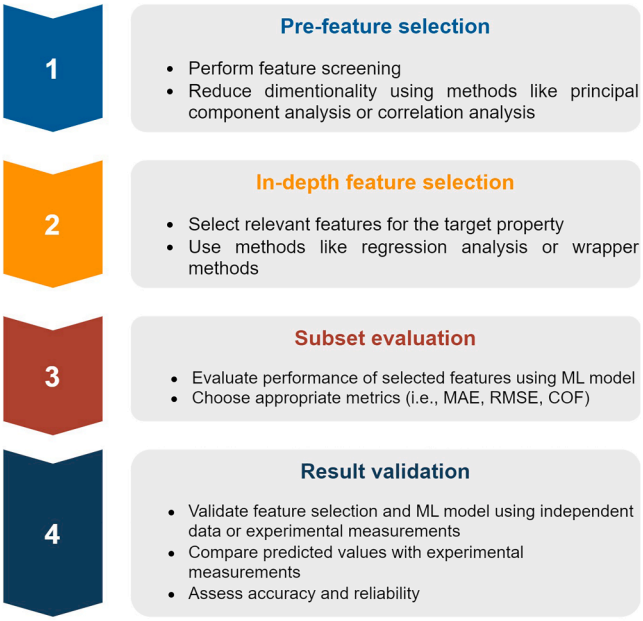

Fig. 8. Stages of feature selection.

can be used to rank features by importance, as those with higher average SHAP values have more impact on predictions [246]. SHAP-based selection has shown success in materials science, identifying key descriptors for properties like band gaps [246] and crystal structures [247]. For CECs, it could reveal influential descriptors for ionic conductivity, catalytic activity, and stability. SHAP-based selection has benefits like model agnosticism, interpretability, and robustness [246]. It can reduce computational costs for CEC models by removing irrelevant features. While not the only option, SHAP-based selection ispromisingfor enhancing AI-driven CEC materials discovery. SHAP values can be used to rank features by importance, as those with higher average SHAP values have more impact on predictions [246]. This allows SHAP-based selection of the most relevant features for a given model.

c **The subset evaluation step** involves evaluating the performance of the selected features using an appropriate AI-learning model and a suitable metric such as mean absolute error (MAE), root means squared error (RMSE), or the coefficient of determination (COF). The evaluation should use cross-validation or a separate test set to avoid overfitting. Cross-validation can evaluate how well selected features and the AI model can predict target property for different operating conditions [240].

d **Result validation:** This involves validating the feature selection results and the AI learning model using independent data or experimental measurements. The validation should be able to confirm that the selected features and the model can accurately predict the target property for new CEC materials or new operating conditions. For example, experimental measurements from literature can be used or from in-house experiments to compare with predicted values to assess their accuracy and reliability [240].

4. AI methods relevant to materials design and optimization for CECs

Artificial intelligence (AI) is a specialized field of computer science that endeavors to design and develop machines or systems capable of performing tasks that conventionally necessitate human cognitive abilities, such as learning, reasoning, and decision-making [23]. AI is a versatile technology that can be effectively applied to various domains of materials science, encompassing materials modeling, simulation, characterization, synthesis, and optimization [27]. AI methods can be divided into two main categories: learning and optimization. Learning methods can learn from data and make predictions or decisions based on the learned patterns or rules [248,249]. Optimization methods find the best solution or configuration for a problem or objective function. Both learning and optimization methods can be used for materials design and optimization for CECs, depending on the nature and goal of the problem [29,37].

Many AI methods are relevant for materials design and screening for CECs, including machine learning (ML), deep learning (DL), and optimization methods such as Bayesian Optimization (BO), Monte Carlo simulation (MCS), Genetic Algorithm (GA), and Particle Swarm Optimization (PSO), as simplified in Fig. 9 [27,30,32,34,196,250–264]. Each AI method has advantages and limitations, and their performance and applicability depend on different material aspects and tasks. This section provides an overview of the primary AI techniques that have been utilized in material design, which are also pertinent to optimizing CECs. We also summarized some guidelines and best practices for selecting and using appropriate AI methods for material development in CECs.

4.1. Learning methods

AI learning approaches, namely ML and DL, can learn from complex datasets and use the knowledge to make informed predictions and decisions [36,248,265–267]. This section will extensively discuss these two learning methods as relevant techniques for advancing material development for CECs. These AI learning methods employ statistical modeling and algorithms to help machines identify underlying patterns and rules from large volumes of data. As machines continuously learn from experience, their performance improves, and the accuracy of their predictions gradually increases [24,26,27,268].

4.1.1. Machine learning (ML)

ML is an AI learning method that allows systems to learn from data and make predictions or decisions based on the learned patterns or rules [264]. This approach can use several algorithms, such as regression, classification, clustering, and dimensionality reduction, to perform various tasks [264,269,270]. The three primary ML types are supervised, unsupervised and reinforcement learning [271,272]. Supervised learning involves training a system to learn a mapping function from input to output data using labeled data (training data) [273,274]. The system can then use the learned function to predict the output for new input data (test data) [36]. In contrast, unsupervised learning trains a system to discover patterns or structures in input data without labels or guidance, which can cluster, classify, or generate new data [275]. Finally, reinforcement learning trains a system to learn an optimal policy or strategy for interacting with an environment based on feedback from its actions (rewards or penalties), allowing the system to maximize its cumulative reward over time [276]. Fig. 10 schematically summarizes the various ML algorithms in existence.

ML has diverse applications for CECs, ranging from predicting materials properties [196] to optimizing materials composition [32] and designing materials microstructures [277]. Moreover, ML can be combined with other computational methods, such as density functional theory (DFT), molecular dynamics (MD), and finite element method (FEM), to develop hybrid models that leverage the strengths of both approaches [24,32,35,36]. For instance, ML can generate surrogate models or interatomic potentials that reduce DFT or MD simulations' computational cost and complexity [278,279]. Furthermore, ML can generate reduced-order models or surrogate models that can approximate the solutions of FEM simulations. In Table 6, we summarize the advantages and limitations of ML, and in Fig. 11, we present a flowchart of the guidelines and best practices for selecting and applying ML methods in CECs. The flowchart comprises three main steps: (i) selecting a suitable ML technique based on the task's nature and objective, (ii) choosing an ML algorithm that is most appropriate for the data's

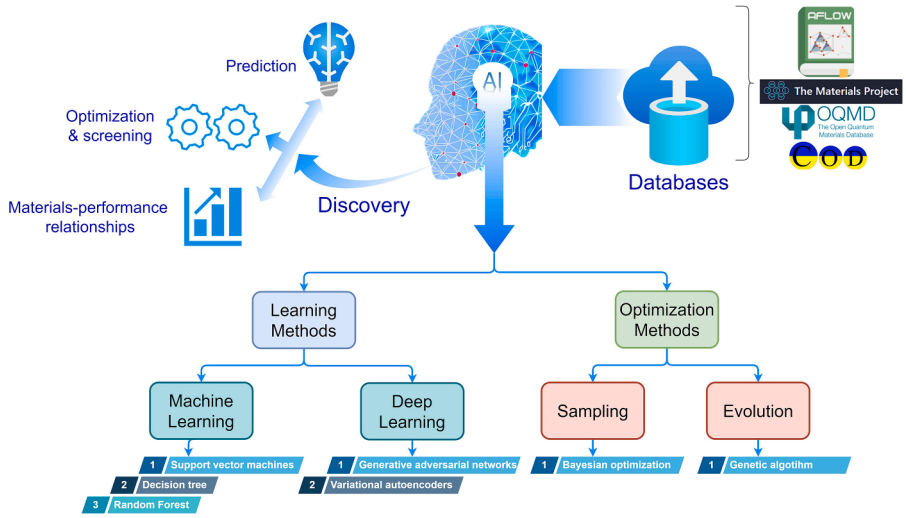

Fig. 9. Schematic illustrating the application of relevant AI methods in designing and optimizing materials for CECs.

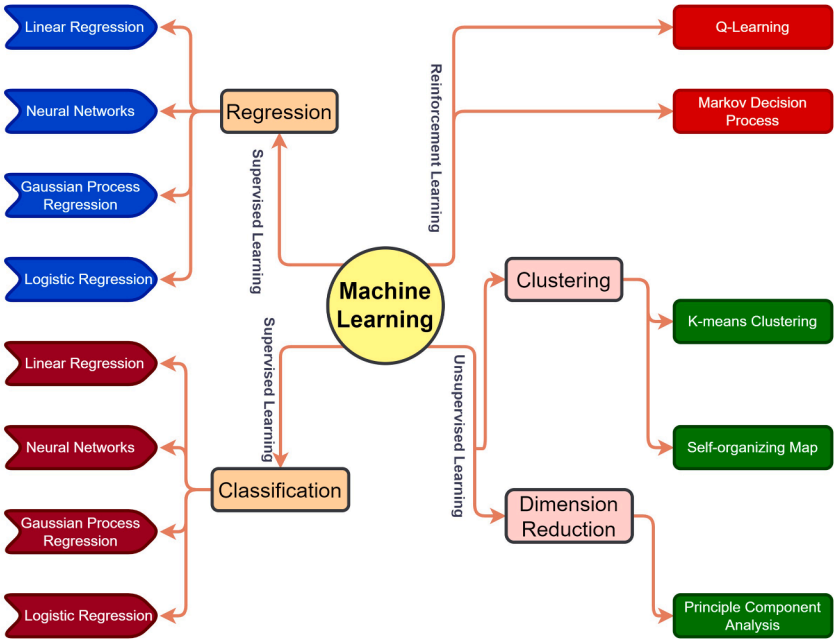

Fig. 10. Schematic illustrating various ML algorithms. Adapted from Elsevier [241] Copyright 2021.

characteristics and the problem's complexity, and (iii) systematically selecting appropriate hyperparameters when training the ML models. Each step includes further sub-steps that provide additional details and considerations for selecting and applying ML methods to material development in CECs [280,281].

While the studies shown in Fig. 12 are not directly focused on CEC materials, they illustrate general principles for how ML can be applied in inorganic materials discovery. For instance, Fig. 12**a** demonstrates how the chemical similarity of different elements, quantified by their Mendeleev number, can be correlated to the number of new compounds formed by combining those elements in an A-B-O system [296]. This provides insights into utilizing elemental properties and ML predictions to guide the exploration of new material compositions.

Similarly, Fig. 12**b** shows how the g_{ab} correlation metric captures ionic radii differences between common ICSD cations [297]. While not specific to CEC electrolytes or electrodes, such descriptors of elemental properties and structural features could also inform ML models for predicting promising compositions and structures when designing novel materials for CECs. The concepts are generally applicable, but care must be taken to use descriptors and training data relevant to the target CEC materials to produce valid predictions.

4.1.2. Deep learning (DL)

DL is a branch of AI learning methods that focuses on creating deep neural networks (DNNs) comprising multiple layers of neurons capable of learning complex and abstract features from data [34,249]. DNNs can be considered universal function approximators that can model any nonlinear relationship between input and output with enough neurons and layers [298]. Additionally, DNNs are hierarchical feature extractors that can learn different levels of abstraction from data, such as edges, shapes, and objects.

DL can be applied to various material aspects and tasks related to CECs, such as generating materials structures, designing materials properties, and optimizing materials performance [34,249,262]. DL methods, such as generative adversarial networks (GANs), variational autoencoders (VAEs), and graph-neural networks (GNNs), have been

Table 6
Summary and comparison of AI methods relevant to materials design and optimization for CECs.

AI method	Type	Main features	Advantages	Limitations
Machine learning (ML)	Data-driven (Learning method)	Learning from data and making predictions or decisions based on learned patterns or rules [198,269,281]	(1) Handling large and complex data sets (2) revealing hidden patterns or correlations in data (3) learning from existing data and extrapolating to new data (4) adapting to changing data or environments [198,269,281]	(1)Requiring sufficient amount of high-quality and representative data (2) suffering from overfitting or underfitting problems (3) lacking interpretability or explainability [281,282,283]
Deep learning (DL)	Data-driven (Learning method)	Creating deep neural networks that can learn complex and abstract features from data [249,251]	(1) Handling complex and high-dimensional data sets(2) learning high-level and abstract features from data(3) learning end-to-end mappings from input to output(4) adapting to changing data or environments [34,262,284]	(1)Requiring vast amounts of high-quality and representative data(2) suffering from overfitting or underfitting problems(3) lacking interpretability or explainability [282,283]
Genetic algorithms (GAs)	Evolutionary (Optimization method)	Creating evolutionary models that can explore and optimize the materials design space using fitness functions or surrogate models [285,286,287]	(1) Handling discrete and combinatorial optimization problems(2) exploring a large and diverse design space(3) discovering novel and optimal solutions(4) adapting to changing data or environments [285,286,287]	(1) Requiring a large number of evaluations or simulations(2) suffering from premature convergence or stagnation problems(3) lacking interpretability or explainability [282,283]
Bayesian optimization (BO)	Probabilistic (Optimization method)	Creating sequential models that can select and evaluate the most promising materials candidates using acquisition functions or surrogate models [288,289,290]	(1) Handling noisy and expensive optimization problems(2) exploiting the trade-off between exploration and exploitation(3) incorporating prior knowledge or beliefs(4) updating its model or parameters based on new observations or feedback [288,289,290]	(1) Requiring a suitable probabilistic model or surrogate model(2) suffering from the curse of dimensionality or scalability problems(3) lacking interpretability or explainability [282,283]
Neural networks (NNs)	Data-driven (Learning method)	A computational model that consists of multiple layers of interconnected nodes (neurons) that can learn from data and perform complex tasks [251,257,291]	(1) Can approximate any nonlinear function [184] (2) Can handle high-dimensional and heterogeneous data(3) Can adapt to changing data and environments [251,257,291]	(1) Require large amounts of data and computational resources (2) Suffer from overfitting and lack of interpretability (3) Sensitive to the choice of hyperparameters and network architecture [251,257,291]
Gaussian regression (GR)	Probabilistic (Learning method)	A statistical method that models the relationship between a dependent variable and one or more independent variables using a Gaussian process prior [290,292,293]	(1) Can provide uncertainty estimates along with predictions (2) Can incorporate prior knowledge and domain expertise (3) Can handle nonlinear and nonstationary data [290,292,293]	(1) Require high computational cost for large datasets (2) Sensitive to the choice of kernel function and hyperparameters (3) Prone to numerical instability and ill-conditioning [290,292,293]
Support vector machines (SVM)	Data-driven (Learning method)	Creating models that can find the optimal decision boundary between classes using kernel functions or surrogate models [271,294]	(1) Effective in high dimensional spaces (2) Kernel flexibility to handle linear and non-linear problems (3) Fast prediction using support vectors (4) Both classification and regression skills [260,295]	(1) Advanced settings and parameter tuning required (2) Suitable for small datasets (3) Costly computation and scaling issues (4) Feature vectors required (5) Low interpretability and overfitting risk [260,295]

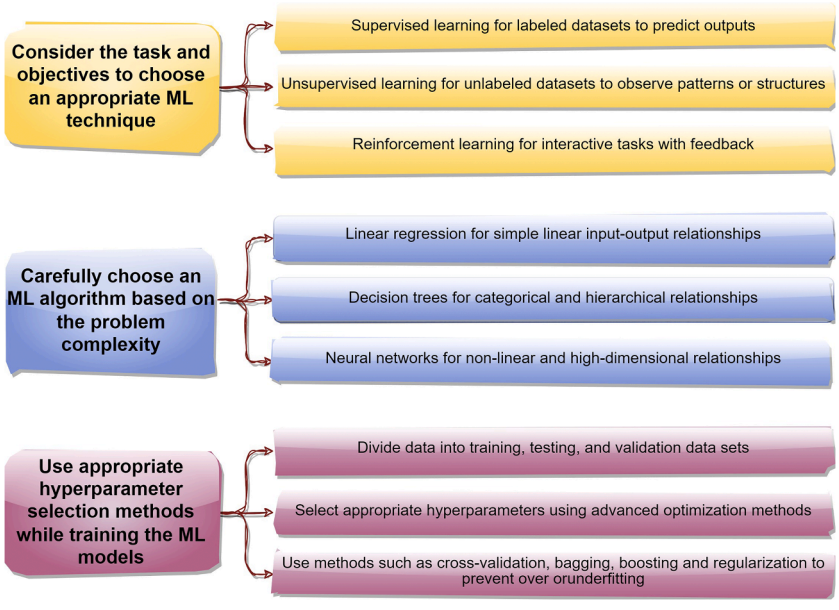

Fig. 11. Guidelines and best practices for selecting and applying ML methods for CECs.

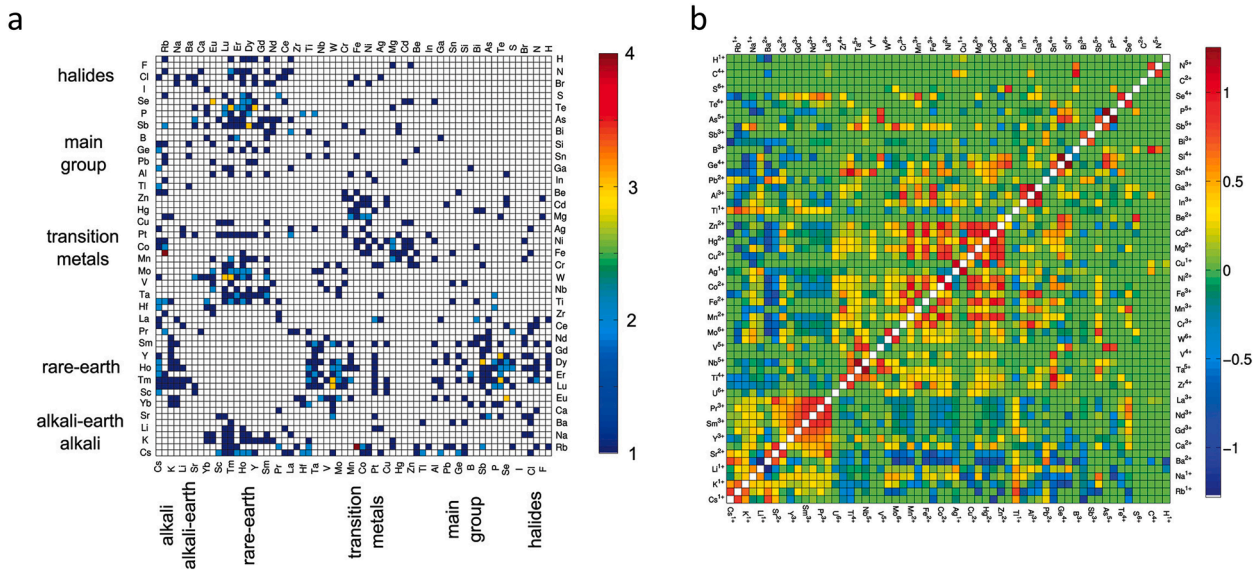

Fig. 12. Examples of ML application in materials development (a) New compounds by $A-B-O$ system and Mendeleev number. The plot displays the number of new compounds discovered for each pair of A and B elements. The elements are ordered by their Mendeleev number along the x-axis and y-axis Copyright 2010, American Chemical Society [296]. (b) Logarithmic plot of g_{ab} correlation pair for 60 most common cations in ICSD sorted based on Mendeleev number. Copyright 2011, American Chemical Society [297].

employed to create sturdy models for designing and optimizing CECs [254,262,298,284]. GANs can generate realistic and innovative materials structures by building generative models from random noise [32]. VAEs can encode and decode materials structures into latent spaces to create generative models, making interpolation and manipulation easier [299,300]. Fig. 13 **(a,b)** depict the application of VAE models for analyzing the martensitic microstructure of alloys from SEM images. The model outputs the concentrations of the alloy components and compresses the images into a low-dimensional latent space, which captures the essential features of the microstructure [301]. Graph-based models that directly access the structural representation of molecules and materials can be created using GNNs [302]. The advantages and limitations of DL are summarized in Table 6.

Fig. 14 presents a flowchart outlining guidelines and best practices for the selection and implementation of DL methods in CECs. The flowchart is composed of three primary steps that involve selecting a suitable DL method based on the task's nature and objectives, selecting an appropriate DL model architecture based on the data's characteristics and problem complexity, and using relevant hyperparameters and optimization methods during DL model training and testing. Each step contains sub-steps that provide further details and considerations for applying DL methods in CEC material development. These guidelines emphasize the importance of carefully considering the problem, data type, and task complexity when selecting and utilizing DL methods in CEC research [303,304].

Hwang et al. [34] proposed a neural network model capable of segmenting and analyzing the microstructure of SOFC anodes with different phases. The approach employed a convolution technique to capture fine details and boundaries of the phases. As shown in Fig. 15, their model was successful in accurately identifying and segmenting the different phases present in the anodes.

In addition to the material science applications covered in this review, DL methods like GANs are also gaining traction in other engineering fields [249,305]. For example, recent work has employed GANs to generate optimized multiphase microstructures for direct internal reforming SOFCs [306]. Other studies have applied GANs to produce

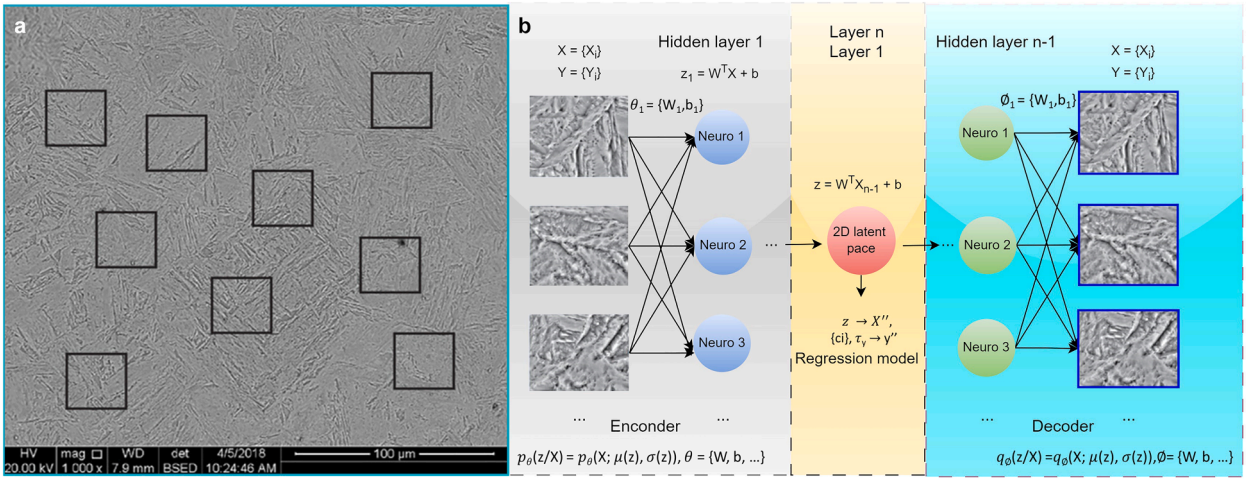

Fig. 13. (a,b) Sub-images of martensitic microstructure from SEM image and ML model (VAE) with encoder, decoder, and regression sub-models. The model outputs alloy concentrations and compresses images into latent space. Copyright 2021, Wiley [301].

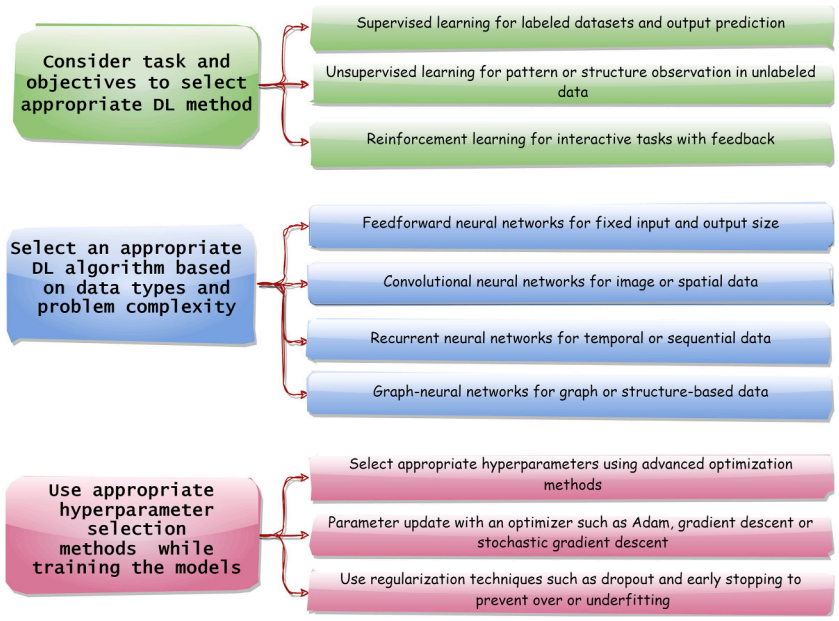

Fig. 14. Guidelines for selecting and using DL methods for CECs.

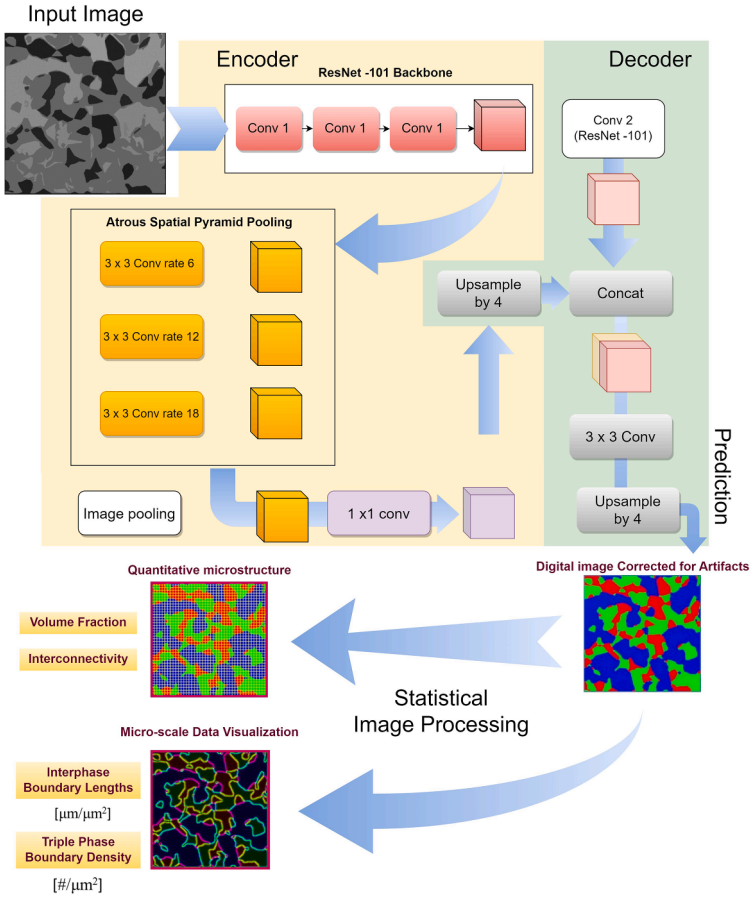

Fig. 15. A deep learning-based approach for applying semantic segmentation to the quantitative microstructure analysis of multiphase SOFC anode composites. (The neural network architecture that uses atrous convolution is shown in the dotted boxes.) Copyright 2021, Reproduced with permission from Elsevier [34].

optimized fin configurations for micro heat pipe cooling systems [307]. These applications demonstrate the versatility of DL techniques in solving complex design and optimization problems across disciplines.

4.2. Optimization methods

Optimization methods are a type of AI technique that can discover the optimal solution or configuration for a specific problem or objective

function. These methods use various approaches, such as search, sampling, or evolution, to explore the solution space and evaluate the quality of the solutions. Optimization methods are versatile and can optimize materials composition, microstructure, performance, synthesis, processing, and testing conditions for CECs. Among the various optimization algorithms used in AI-driven CECs research [265,288,289,308], Genetic Algorithm (GA) and Bayesian Optimization (BO) are the most widely adopted. Consequently, this section focuses on these two algorithms.

4.2.1. Genetic algorithms (GAs)

Inspired by the process of natural evolution, GAs are a class of AI-based optimization methods that use selection, mutation, crossover, and survival of the fittest to explore and optimize the materials design space. By using a fitness function as a learning algorithm, they can aid in the discovery of optimized solutions [295]. The existing body of literature [290,295,309,310] suggests that GAs have been used in various aspects of CECs, including material microstructure design, optimization of material composition, and material structure generation [290,295,309,310]. Furthermore, GAs can also be integrated with other learning and optimization methods, such as neural networks (NNs) and Bayesian optimization (BO), to create hybrid models for more effective optimization [290,310]. Surrogate models or fitness functions can be created using neural networks (NNs), which can aid in reducing the computational cost and complexity of GAs [310]. Global optimizers such as GAs can be used in conjunction with BO to select and evaluate the most promising materials candidates using sequential models [290,309]. Table 6 summarizes the advantages and limitations of GAs. Johnston was one of the pioneers in applying GAs in material development and reviewed the geometry optimization of clusters and nanoparticles through potential energy functions [311]. In his work, he talked about the fundamental ideas and principles behind GAs and how these could be modified to navigate the complicated potential energy surfaces of clusters and nanoparticles. Additionally, he showcased his GA program, which he created to deal with various potential energy functions and cluster representations [311]. He exhibited the adaptability and efficacy of his program by utilizing it to explore numerous instances of model clusters and nanoparticles, such as Morse clusters, ionic MgO clusters, and bimetallic "nanoalloy" clusters [311]. GA has shown promise in material development, as reported by recent studies [285,308]. Oz et al. [285] used GA to optimize the parameters of a kinetic model for the ORR of cathode materials SOFCs. They used AC impedance spectroscopy (ACIS) to measure the electrochemical performance of two cathode materials, $Ba_{0.5}Sr_{0.5}Fe_{0.91}Al_{0.09}O_{3-\delta}$ and $Ba_{0.5}Sr_{0.5}Fe_{0.8}Cu_{0.2}O_{3-\delta}$, with different electrolytes, $La_{0.8}Sr_{0.2}Ga_{0.8}Mg_{0.2}O_{3-\delta}$ and $Ba_{0.5}Sr_{0.5}Ce_{0.6}Zr_{0.2}Gd_{0.1}Y_{0.1}O_{3-\delta}$. Impedance spectroscopy genetic programming (ISGP), a technique that combines GA with ACIS, was then used to find the distribution function of relaxation times (DFRT) that best fits the experimental data. The DFRT model describes the ORR mechanism by decomposing it into several polarization subprocesses with different time constants and resistances. The GA was used to find the optimal values of these parameters that minimize the error between the DFRT model and the experimental data. They applied this approach to compare the ORR mechanisms of the two cathode materials and identify each system's rate-limiting steps [285]. Fig. 16 presents a flowchart that provides best practices for selecting and using genetic algorithms (GAs) to solve complex optimization problems in material design and optimization for CECs. The chart comprises four main steps: (i) selecting the appropriate GA type based on how the design variables are represented, (ii) selecting an appropriate GA algorithm that fits the

Fig. 16. Simplified Chart illustrating the guidelines and best practices for selecting and using GAs for CECs.

problem's characteristics and complexity, (iii) selecting an appropriate GA model architecture based on the problem's type and size, and (iv) choosing the right hyperparameters and optimization methods for running the GA models. These guidelines can help researchers and practitioners use GAs effectively [286,308,311].

4.2.2. *Bayesian optimization (BO)*

BO is an AI-based optimization method that relies on Bayesian inference and sequential decision-making. Its applications in CECs are diverse, ranging from optimizing materials composition to designing materials properties and generating materials structures [288,289,290]. BO can also be combined with other AI methods, such as GAs and NNs, to create hybrid models, leveraging the strength of multiple techniques [288,290]. For instance, GAs can serve as global optimizers exploring a large and diverse design space using BO as a local optimizer, while NNs can create surrogate models or fitness functions that reduce the computational cost and complexity of BO [288,290]. The advantages and limitations of BO are summarized in Table 6.

Liang et al. [82] provided an example of how BO can be used in material development. They used BO to benchmark the performance of different surrogate models and acquisition functions across multiple experimental material science domains. They compared BO to random sampling and grid search methods and found that Gaussian Process (GP) with anisotropic kernels and RF were the most robust and effective surrogate models for BO. They also reported that BO can significantly improve the materials discovery process compared to other methods.

Hou et al. [312] extensively reviewed how BO can be used to determine physical parameters of physics models, design experimental synthesis conditions, discover functional materials with targeted properties, and optimize atomic structures. They explained the fundamental methodologies associated with BO, such as surrogate models, acquisition functions, and hyperparameter optimization.

Like other AI methods described in this study, a flowchart outlining the guidelines and best practices for selecting and utilizing BO methods for CECs is provided in Fig. 17. The flowchart consists of four main steps: selecting an appropriate type of BO method based on the nature and objective of the problem, choosing a suitable BO algorithm based on the characteristics and complexity of the problem, selecting an appropriate BO model architecture based on the type and size of the problem, and selecting suitable hyperparameters and optimization methods when running BO models.

While many AI models for materials discovery act as black boxes without inherent interpretability [251,266,267], some recent works have explored more transparent AI techniques in the context of CECs [35,224,268]. Explainable AI methods attempt to make complex models more understandable by extracting meaningful insights about the relationships learned by the model. For example, Weng et al. [268] used symbolic regression, a type of genetic programming, to discover simple analytical expressions linking perovskite composition to catalytic activity. The generated equations provided direct insight into how the underlying descriptors influence the target property. In another study, Zhai et al. [35] introduced a physical descriptor called ionic Lewis acid strength and used machine learning to demonstrate its correlation with oxygen reduction activity. This provided an interpretable link between a material's electronic structure and its catalytic performance. Jacobs et al. [224] identified the oxygen p-band center as a useful descriptor for rationalizing trends in the surface exchange kinetics of perovskite cathodes. The p-band model gave a clear theoretical basis for how this electronic structure characteristic controls the material's activity.

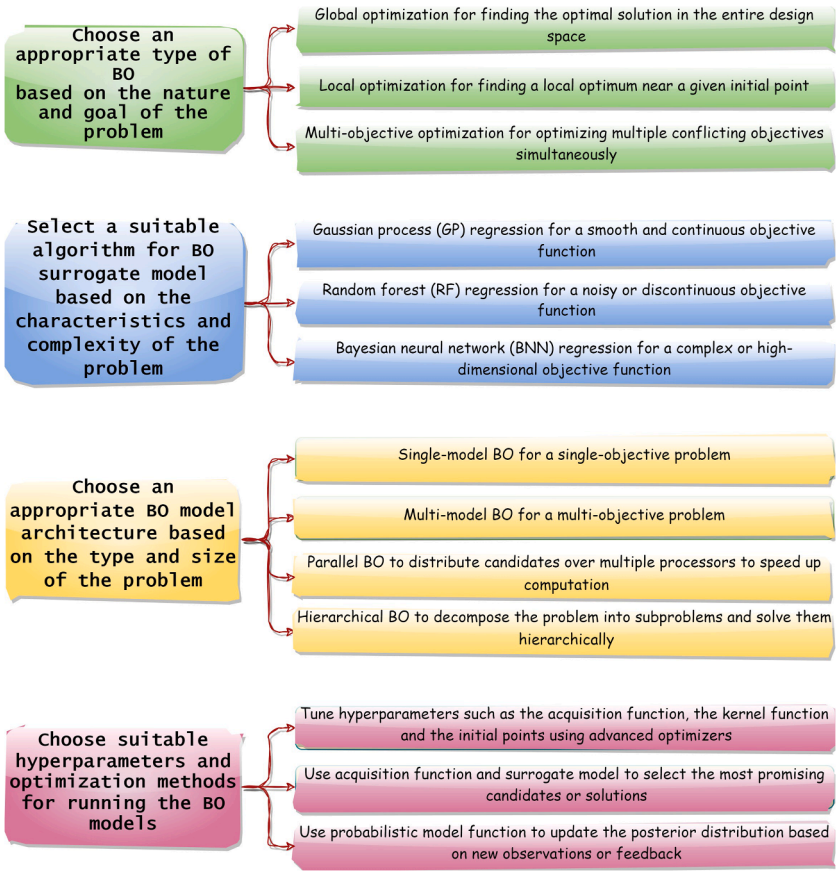

Fig. 17. Simplified chart outlining the guidelines and best practices for selecting and applying BO in materials development for CECs.

5. Case studies of AI-predicted and synthesized materials for CECs

5.1. AI-learning method-based approaches

Several researchers have employed AI-learning methods comprising ML and DL techniques to expedite the development of materials for CECs. These approaches leverage AI learning algorithms to predict material properties, accelerate screening processes, and guide material synthesis for enhanced performance. The following case studies exemplify the effectiveness of these AI-driven methods in materials design for CECs:

Wang et al. [36] used ML models to accelerate the development of efficient mixed protonic–electronic conducting oxides as the air electrodes for protonic ceramic cells (PCCs), as illustrated in Fig. 18. They predicted the hydrated proton concentration (HPC) of over 3000 new oxides and screened the most promising candidates. They then synthesized and tested one of the candidates, $La_{0.7}Ca_{0.3}Co_{0.8}Ni_{0.2}O_{3-\delta}$ (LCCN7382) and found that it showed high performance (719 mW cm^{-2} at 650 °C in fuel cell mode) and stability as an air electrode, demonstrating the efficacy of AI-ML-driven method for material design.

Fig. 18 provides a schematic illustration of the machine learning workflow used by Wang et al. [36] to accelerate the development of efficient mixed protonic-electronic conducting oxide cathodes for PCCs. The key steps include:

1 Compiling a database of 3000+ ABO_3 perovskite oxides along with their DFT-calculated HPC values as a target property.
2 Using this dataset to train a RF-ML model to predict HPC.
3 Screening the ML-predicted HPC values to identify the most promising candidates.
4 Validating the ML predictions by experimentally synthesizing and testing the cathode material LCCN7382, which demonstrated high performance.

The novelty of this approach lies in utilizing high-throughput DFT data coupled with ML predictions to rapidly navigate the materials space and discover enhanced protonic-electronic conducting oxides. The experimental validation proves the efficacy of the ML-driven methodology for accelerating the development of novel CEC cathode materials [36].

Zhai et al. [35] devised a machine-learning-based approach to expedite the exploration of efficient oxygen reduction electrodes for ceramic fuel cells. The methodology entailed gathering data on the ORR performance of various perovskite oxides, selecting nine ionic descriptors as material characteristics, and utilizing machine learning to establish connections between these descriptors and ORR activity. The authors introduced the ionic Lewis acid strength (ISA) as an effective physical descriptor to enhance the ORR activity of perovskite oxides. The experimental validation of this approach led to the successful synthesis and characterization of four oxides exhibiting superior activity metrics. Notably, among the tested oxides, $Sr_{0.9}Cs_{0.1}Co_{0.9}Nb_{0.1}O_3$ (SCCN) demonstrated the highest performance with an ASR of approximately 0.019 Ω cm^2 and a peak power density (PPD) of around 2050 mW cm^{-2} at 650 °C. The manipulation of A-site and B-site ISAs in perovskite oxides resulted in significant improvements in surface exchange kinetics. Theoretical calculations revealed that this enhanced activity primarily originated from the redistribution of electron pairs induced by the polarization distribution of ISAs at A and B sites, leading to a substantial reduction in oxygen vacancy formation energy and migration barrier.

Fig. 19 outlines the ML workflow developed by Zhai et al. [35] to rapidly explore and identify efficient oxygen reduction electrode materials for CFCs. The key steps are:

1 Compiling a dataset of perovskite oxides with their experimentally measured ORR activities.
2 Extracting nine composition-based ionic descriptors (features) for each material.
3 Using regression models like ANN and RF to correlate the ionic descriptors to the ORR activity.
4 Introducing a new physical descriptor called ionic Lewis acid strength (ISA) that strongly predicts ORR activity.
5 Validating the approach by experimentally synthesizing and characterizing four oxides with optimized ISA, which demonstrated enhanced performance.

The novelty of this methodology is using ML models to reveal the ISA as an influential descriptor for ORR activity. This provides new physical insights to guide the design of improved electrode materials. The

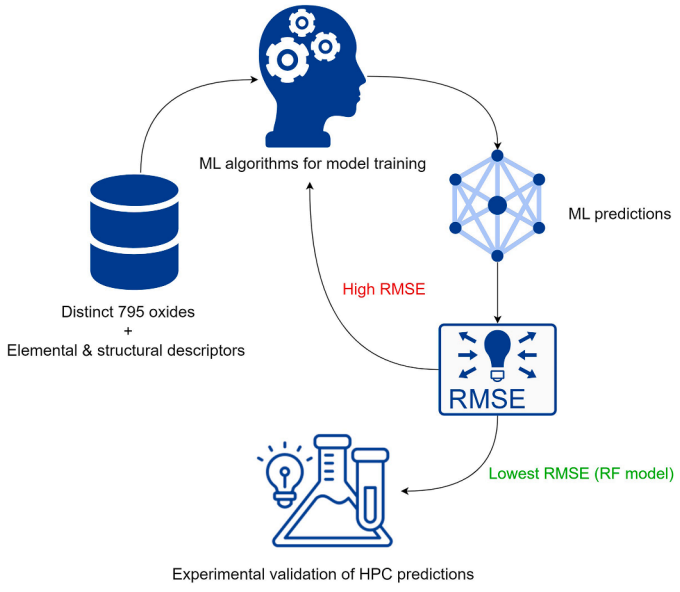

Fig. 18. (a) A schematic illustration of the machine-learning-accelerated development of efficient mixed protonic–electronic conducting oxides as the air electrodes for protonic ceramic cells.

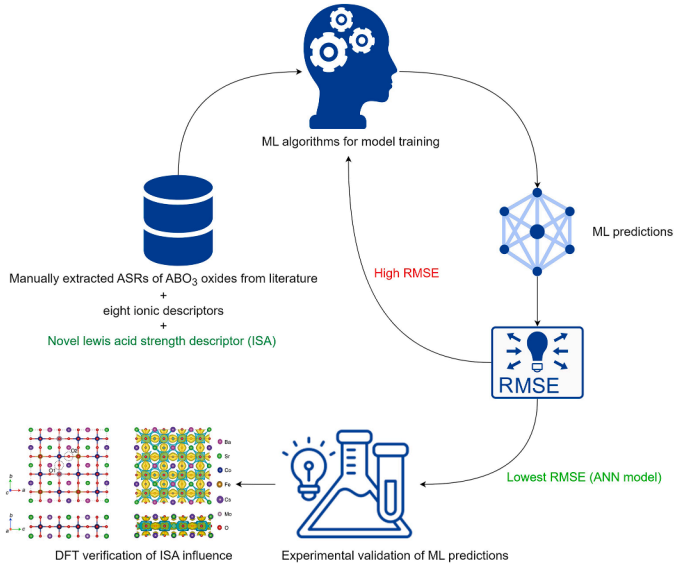

Fig. 19. A schematic illustration of the machine-learning-driven approach to predict efficient oxygen reduction electrodes for ceramic fuel cells, where ionic Lewis acid strength (ISA) is introduced as a physical descriptor for the oxygen reduction reaction (ORR) activity of perovskite oxides [35].

experimental validation highlights the power of combining data-driven ML techniques with targeted synthesis and testing.

Yang et al. [313] used ML to assist in predicting long-term performance degradation on SOFC cathodes induced by chromium poisoning. They used electrochemical impedance spectroscopy data to train a neural network model and validated it with experimental results. They predicted the performance degradation of cathode materials based on $SrFeO_3$ with different dopants, i.e., $SrFe_{0.75}M_{0.25}O_{3-\delta}$ (M = Co, Fe, Mn, Nb, and Ni), and found that the predicted data matched well with the experimental results; hence they concluded that ML approach could provide useful insights into the degradation mechanism of Cr-induced cathode material degradation.

Toyoura et al. [314] proposed an ML-based selective sampling procedure for identifying the low-energy region in a potential energy surface (PES) of a proton in a proton-conducting oxide, barium zirconate ($BaZrO_3$). They used a Gaussian process (GP) model to construct a statistical PES model and to select grid points in the configuration space that are most likely to have low potential energies. They also estimated the threshold of the low-energy region and the number of unsampled low-energy points and stopped when the sampling was sufficient. They demonstrated the efficiency and accuracy of the procedure by comparing it with other sampling methods, such as random sampling and preliminary PES sampling. They showed that the procedure could successfully identify the low-energy region characterizing the proton conduction mechanism in $BaZrO_3$, which involved rotational and hopping paths of protons around oxygen ions. This work could be considered a good case study for applying AI methods (ML) to develop materials for CECs. It demonstrated how their approach could accelerate and enrich the discovery cycle of materials by exploiting data, simulation, and automation.

Hwang et al. [284] proposed a novel method of integrating semantic segmentation-assisted DL to quantitative multi-phased microstructural analysis in composite materials, using cathode composite materials of SOFCs as a case study. They used a focused ion beam (FIB) to extract 3D images of the cathode layers, which were then processed by image-based stereological characterization to obtain size distributions and interconnectivity of the three phases: $Ce_{0.9}Gd_{0.1}O_{2-\delta}$ (GDC), $La_{0.6}Sr_{0.4}CoO_{3-\delta}$ (LSC), and pores, as illustrated in Fig. 20 **(a,b).** They then applied a CNN-based DL algorithm named DeepLabV3+ to segment the images and extract features that capture the contrast and boundaries of the phases. They finally demonstrated the accuracy, efficiency, and applicability of the DL approach by comparing it with manual segmentation and showing its ability to analyze the 9.5 μm × 9.5 μm × 2.4 μm volume of each sample. Hwang et al. [34] also explored the suitability of semantic segmentation for quantifying the microstructure of Ni, YSZ, and pores in the anode of SOFCs, which are essential for SOFC performance and efficiency, as depicted in Fig. 20 **(c,d)**. They used a FIB-SEM system to obtain high-quality image data of the anode composites and applied DeepLabV3+, a semantic DL segmentation algorithm, to extract quantitative parameters such as the interconnectivity, volume fraction, interphase boundaries, and triple phase boundaries. They found that the semantic segmentation-assisted DL approach effectively characterized the microstructure of the anode composites and that the intersection over union (IoU) of pixels was used to measure the accuracy.

Zheng et al. [315] developed a novel porous heterostructured cathode material $Nd_{0.8}Sr_{1.2}CoO_{4\pm\delta}/Nd_{0.5}Sr_{0.5}CoO_{3-\delta}$ ($NSC_{214/113}$) for intermediate temperature SOFCs that showed enhanced ORR kinetics with a high PPD of 1.10 W cm^{-2} at 800 °C. They utilized AI learning methods

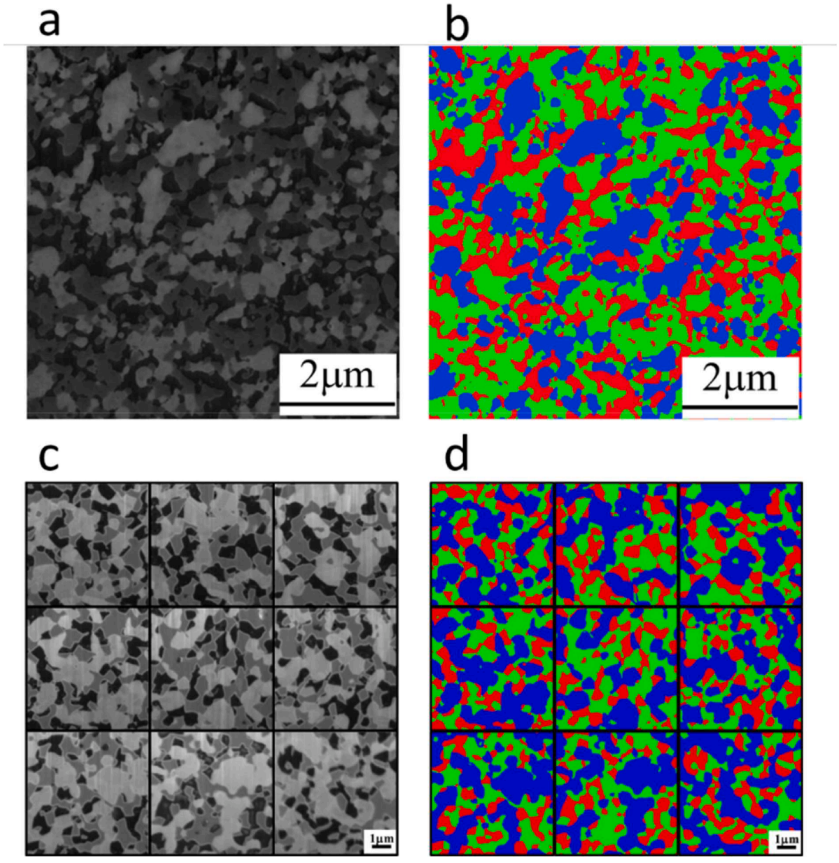

Fig. 20. Stereological analysis of the phase images to obtain microstructural parameters: (a) original electron microscopy image (light gray: GDC, dark gray: LSC, and black: pore), (b) image inferred by deep learning with semantic segmentation (blue: GDC, green: LSC & red: pore). Copyright 2020, Elsevier [284]. The distribution of Ni and YSZ phases in the anode composites obtained by deep learning segmentation (blue: Ni, green: YSZ & red: pores) (c) original electron microscopy image (d) ground truth images. Copyright 2021, Elsevier [34].

such as adaptive neuro-fuzzy inference system (ANFIS) and ANN to screen and optimize the cathode materials based on their thermal expansion coefficient (TEC) and microstructure. They found that the formation of heterojunction between NSC_{214} and NSC_{113} can lead to a narrowed energy bandgap and a decrease of the Co oxidation state, which further induces better conductivity, more available electrons, and oxygen vacancies to enhance the ORR.

Zhang et al. [280] reviewed a machine learning-facilitated multi-scale imaging approach for energy materials. They introduced the concept of ML imaging, which uses ML models to assist or replace human intervention in image acquisition, processing, analysis, and visualization. DL models, such as CNNs, GANs, and deep reinforcement learning (DRL) techniques, addressed different challenges in the multi-scale imaging of energy materials. They then expounded on applying the ML imaging approach to several case studies, such as X-ray tomography of lithium-ion batteries, electron microscopy of perovskite solar cells, and scanning probe microscopy of 2D materials. They demonstrated that ML imaging could improve image quality, resolution, speed, and interpretation and enable new imaging modalities and functionalities. The limitations and prospects of ML imaging for energy materials research were highlighted in the study.

Hsu et al. [316] used a large-scale, experimentally captured 3D microstructure data set of SOFC electrodes to train a GAN. They then used the GAN to generate 3D microstructures that are visually, statistically, and topologically realistic, with similar properties to the original microstructure. They also compared their results with another generation algorithm called DREAM.3D. They found that the GAN-generated microstructures matched the electrochemical performance of the original better than DREAM.3D. Their study demonstrates that GAN can capture and represent the essence of complex microstructures in a compact and manipulatable form. Wang et al. [265] developed a data-driven powder-to-power framework (see Fig. 21) based on numerical simulation, ML, and multi-objective optimization to predict and optimize the performance and durability of heterogeneous electrodes for CECs. They used a discrete element method to simulate the particle packing of NiO, YSZ, and pore former powders, a phase-field method to track the morphology evolution of Ni-based electrodes from sintering to reduction and long-term operation, and a lattice Boltzmann method to evaluate the electrochemical performance of the electrodes. They used an support vector machines (SVM) regression algorithm to construct a surrogate model that can quickly predict the electrode overpotentials under different fabrication parameters. They used a global sensitivity analysis to assess the importance of each parameter on the electrode performance and a multi-objective GA to find the optimal electrode microstructure and operating conditions that minimize the degradation rate and maximize the efficiency. They validated their framework by comparing the predicted and experimental polarization curves of Ni-YSZ electrodes with different compositions. They showed that their framework reduced the degradation rate of Ni-based electrodes from 2.132 % to 0.703 % kh^{-1} with a required maximum operation time of over 50, 000 h. This study demonstrates the potential of data-driven methods for designing and optimizing CECs with high performance and durability.

These diverse case studies demonstrate that AI-learning methods are powerful tools for accelerating materials discovery and optimization in CECs. These methods enable researchers to efficiently explore vast material spaces, predict material properties, and identify promising candidates for synthesis and testing. Integrating AI-driven methods with experimental validation showcases their potential to drive advancements in CEC technology and facilitate the development of high-performance materials for sustainable energy conversion and storage.

5.2. AI-optimization method-based approaches

In addition to AI-learning methods, AI-optimization methods have also been employed to enhance the characterization and performance evaluation of materials for CECs. These approaches utilize advanced algorithms to optimize experimental parameters and image analysis techniques. The following case study showcases the application of AI-optimization methods in the study of SOFC materials:

Meffert et al. [317] employed an innovative approach to optimize SEM imaging parameters for studying SOFC materials. Using Monte Carlo simulations (MCS), they investigated the influence of various secondary and backscattered electron (BSE) detectors and detection geometry on the image intensities. To prepare the SOFC samples, the researchers followed a deterministic technique involving screen printing and co-sintering on a substrate, followed by resin infiltration. They performed FIB-SEM tomography experiments using a state-of-the-art instrument and applied 3D segmentation and mesh generation methods to reconstruct the 3D structure of all functional SOFC layers. The study successfully demonstrated the ability of the proposed method to distinguish different materials and achieve highly accurate 3D reconstructions of SOFCs with exceptional resolution.

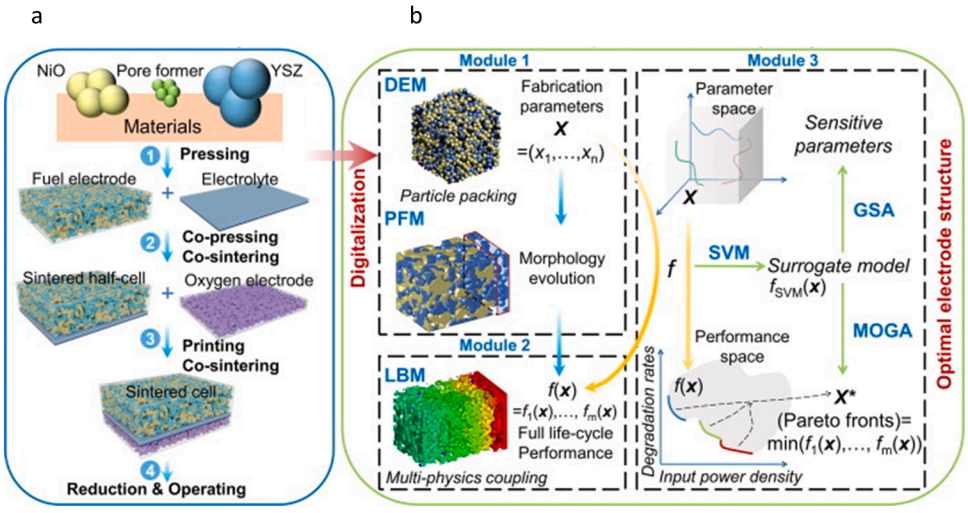

Fig. 21. (a) The steps of the electrode's full life cycle from powder compaction to long-term operation. (b) The workflow of the data-driven powder-to-power framework, which consists of three sub-modules: the electrode morphology tracking module (Module 1), the electrode performance evaluation module (Module 2), and the data-driven optimization module (Module 3). Module 1 digitalizes the evolution of the full life-cycle electrode morphology from powder pressing to long-term operation. Module 2 calculates the electrochemical performance based on the electrode morphology, and Module 3 performs the multi-objective optimization using a data-driven surrogate model.

Xing et al. [318] devised a novel approach to enhance the performance of SOFC by employing a multi-fidelity surrogate modeling technique. This method utilized spatially distributed outputs and BO. By incorporating a feature engineering step and a Gaussian process (GP) approximation into the multi-fidelity stochastic collocation method, Xing et al. [318] eliminated the necessity of low-fidelity simulations during the inference stage. The results indicated that their approach outperformed existing multi-fidelity methods, mainly when dealing with a limited number of high-fidelity training points, while efficiently managing high-dimensional outputs. Also, the authors showcased the flexibility of their approach in selecting various optimization objectives, including minimum, maximum, or average output values. Moreover, their method enabled the incorporation of nonlinear constraints and the consideration of multiple objectives.

Hence, using AI-optimization methods for materials characterization and analysis, researchers can fine-tune experimental parameters, optimize imaging techniques, and obtain more accurate and reliable data. These advancements enhance the understanding of material properties and facilitate the design and optimization of materials for CECs.

This section has provided a comprehensive overview of case studies from existing literature that showcase the application of AI in advancing the three focused material aspects of CECs. These case studies exemplify the potential and opportunities that AI-driven methods offer in materials design and optimization for CECs. Table 7 provides a concise overview of the case studies discussed in this section, enabling readers to grasp the diverse applications of AI in different material aspects of CECs and the valuable insights obtained through these studies. The table summarizes the main features and outcomes of all the case studies, including the

Table 7
Summary of selected case studies of AI-predicted and synthesized materials for CECs.

Case study	Material	AI model	Data source	Method	Findings & insights
Zhai et al. [35]	Electrode	ANN, RF, SVM etc.	Database, Experimental data and DFT calculations	Screening and validation (Learning)	Ionic Lewis acid strength is an effective descriptor for the oxygen reduction reaction activity of perovskite oxides
Wang et al. [36]	Electrode	RF	Database and DFT calculations	Screening and validation (Learning)	Hydrated proton concentration is an effective descriptor for the oxygen evolution reaction activity of mixed protonic–electronic conducting oxides. LCCN7382 as a promising candidate for air electrode.
Yang et al. [313]	Electrode	NN	Experimental data	Electrochemical impedance spectroscopy (EIS) (Learning)	Chromium (Cr) poisoning is one of the main sources for the performance degradation of solid oxide fuel cells (SOFCs) during long-term operation. A neural network model is constructed to predict the performance degradation of SOFC cathodes based on EIS data. The predicted data at 156 h match the experimental results well. The effect of dopant elements on the resistance to Cr poisoning is studied. $SrFe_{0.75}M_{0.25}O_{3-\delta}$ (M = Co, Fe, Mn, Mo, Nb, and Ni) are chosen as model systems. $SrFe_{0.75}Co_{0.25}O_{3-\delta}$ shows the best ASR performance.
Toyoura et al. [314]	Electrolyte	GP	Database and DFT calculations	Selective sampling procedure for identifying the low-energy region in a potential energy surface (Learning)	The proposed procedure can efficiently identify the low-energy region characterizing the proton conduction in the host crystal lattice and that the descriptors used for the statistical PES model greatly influence the performance.
Hwang et al. [284]	Electrode	DeepLabV3+ CNN	FIB-based SEM images of GDC/LSC composite	Semantic segmentation with atrous convolution and ASPP module (Learning)	Semantic segmentation can accurately and efficiently extract microstructural features such as phase fractions, size distributions, interconnectivities, and triple-phase boundaries. Semantic segmentation can be generalized to other multi-phase mixtures and reduce analysis time and human error.
Hwang et al. [34]	Electrode	DeepLabV3+ CNN	FIB-SEM images	Semantic segmentation and stereology (Learning)	Semantic segmentation can automatically detect and quantify microstructural parameters of multiphase composites, such as interconnectivity, volume fraction, interphase boundary, and triple phase boundary, which are crucial for optimizing SOFC performance.
Zheng et al. [315]	Electrode	ANFIS and ANN	Experimental measurements and literature data	Modeling and optimization (Learning)	Thermal expansion coefficient and microstructure of the heterostructured cathode material can be predicted by ANFIS and ANN models, respectively. The heterointerface between NSC_{214} and NSC_{113} creates favorable energy bandgaps and oxygen vacancies for oxygen reduction reaction.
Hsu et al. [316]	Electrode	GAN	3D microstructure data set	Learning and generating 3D microstructures (Learning)	Generated microstructures are visually, statistically, and topologically realistic, and closely match the electrochemical performance of the original; demonstrated the potential of generative machine learning model to capture and represent the essence of complex microstructures in a compact form.
Wang et al. [265]	Electrode	SVM, GSA, GA	Numerical simulation and database	Screening and optimization (Learning & Optimization)	Data-driven powder-to-power framework can digitalize the full life cycle of heterogeneous electrodes and optimize their performance and durability. Ion-conducting phase volume fraction is a key parameter to suppress Ni coarsening and migration.
Meffert et al. [214]	Electrode and Electrolyte	MCS	Material properties and SEM images	Simulation and validation (Optimization)	Simultaneous use of different SE and BSE detectors to achieve high contrast for all functional SOFC layers.
Xing et al. [318]	Electrode and Electrolyte	Multi-fidelity surrogate modeling with BO	Physics-based high and low fidelity models of SOFC	Sampling refinement and data fusion (Optimization)	Highly accurate predictions of multiple spatially distributed quantities at up to 250,000 locations

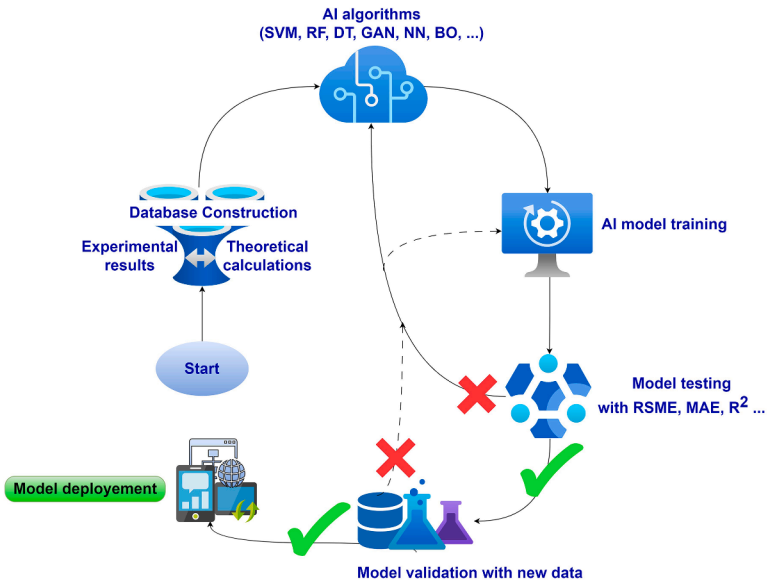

Fig. 22. Framework for applying AI methods for material discovery in CECs.

materials aspect, the AI model, the data source, the method, and the finding and insights.

Fig. 22 shows a framework proposed in this study for materials discovery for CECs based on the different case studies explored. AI-based models for material discovery for CECs typically begin with creating a comprehensive database [319]. This data can be acquired through various means, including leveraging open-source databases, AFLOWLIB, materials project, crystallography open database, conducting experimental investigations, and performing theoretical calculations [199,201,202,204]. Once the necessary dataset is gathered, pre-processing techniques like feature engineering and selection can be applied. Selecting a subset of features that can effectively predict the desired outcomes becomes crucial, as it helps enhance the model's accuracy and efficiency [240,242].

The exclusion of feature engineering/selection could cause overfitting and unnecessarily increase the model's computational complexity. Subsequently, an AI algorithm will be selected based on the objective of the model to be developed. The guidelines for choosing AI algorithms have been highlighted in Section 4.1 of the study. The next phase is model training and evaluation, where the selected AI algorithm is trained on the pre-processed dataset. During this phase, the model learns the patterns and relationships between the input features and the target variable. After training, the model's performance is evaluated on testing data using appropriate metrics to assess its effectiveness in predicting the desired outcomes. It is proposed that the developed model be validated using another set of data apart from the training and testing data to confirm its accuracy further.

After verifying and validating the effectiveness of the developed model in predicting the desired outcomes, the model can be deployed in the form of a web or mobile application to facilitate material discovery for CECs. The application will allow researchers and stakeholders to input specific criteria and obtain recommendations for potential materials based on the AI model's predictions. However, it is essential to note that deploying the model in a production environment also comes with its own set of challenges. The model's performance and robustness must be monitored and evaluated to ensure reliability. Regular updates and improvements may be required to incorporate new data, address emerging trends, and enhance the model's accuracy.

Furthermore, user feedback and engagement are essential for refining and optimizing the model's performance. Gathering user input and incorporating it into the model's development cycle can help tailor the recommendations better to meet the specific needs and preferences of the users.

6. Implications and contributions of the AI approach for CEC technologies

The AI approach for CECs has several implications and contributions for advancing the CEC technology, such as:

i Reducing the trial-and-error experiments by employing data analysis and ML to find optimal material designs and synthesis conditions [33,196].
ii Exploring the vast materials space using AI to generate novel and diverse candidates for ion-selective membranes (ISMs) based on atomic features and experimental data [31].
iii Discovering novel and optimal materials using DL and reinforcement learning to predict critical properties of materials and reveal how changes in certain principal parameters affect the overall behavior of materials [33].
iv Enhancing the understanding of the materials-performance relationships by using AI to assimilate trends and patterns within the design parameter space and identify key factors that influence the performance of CECs [33,196].

The AI approach can complement and integrate with other computational and experimental techniques for materials design and optimization for CECs, such as:

i Density functional theory (DFT), molecular dynamics (MD), high-throughput screening (HTS), and combinatorial synthesis (CS) by using AI as a bridge between the experimental data and computational chemistry to develop models that can use experimental data and atomic properties [31].
ii Knowledge representation frameworks, planning methods, causal inference methods, and algorithmic abstractions of AI-enabled human-machine, AI-enabled human-human, and machine-machine collaborations in science by using AI to address the bottlenecks of the scientific process, such as generating hypotheses, designing, prioritizing and executing experiments, integrating data, models, and simulations, drawing inferences and constructing explanations, reconciling scientific arguments, and communicating across disciplines [33,196].

7. Limitations of the AI approach for CECs

As with any cutting-edge technology, applying AI in CECs brings forth a range of possibilities and opportunities. However, it is crucial to acknowledge that the AI approach has limitations. In this section, we shed light on the challenges that warrant careful consideration in harnessing the full potential of AI for CECs.

i **Data quality and availability:** The performance and reliability of AI models depend on the quality and quantity of the data used for training and testing. However, the specific data for certain material aspects of CECs may be scarce, noisy, incomplete, or inconsistent, which can affect the accuracy and generalizability of the AI models [35,154,282].

ii **Model interpretability and generalizability:** The AI models for a specific aspect of CECs may be complex, nonlinear, and high-dimensional, making them difficult to interpret and explain. Moreover, the AI models may not generalize well to new or unseen data or scenarios, especially when there are changes in the material composition, microstructure morphology, and operating conditions. This can be due to overfitting or underfitting of the models. Another reason that might affect the generalizability is the scarcity of data. With limited data, training accurate and reliable models can be challenging, leading to potential inaccuracies or errors in the models' predictions. This can be particularly problematic in cases where the data are unrepresentative or biased, leading to inaccurate or incomplete models that may not accurately capture the full range of scenarios or outcomes [282].

iii **Computational power:** Developing complex AI models requires significant computational power and resources. Training and testing AI models can be computationally expensive, time-consuming, and resource-intensive for large numerical datasets or high-dimensional feature spaces. This can limit the scalability and practicality of AI approaches for materials discovery in CECs, especially in cases where large amounts of data need to be processed [25,29,282].

iv **Materials synthesis and characterization:** The AI models for CECs may provide promising candidates for novel and optimal materials, but they still need to be synthesized and characterized experimentally to validate their predictions. However, materials synthesis and characterization may be costly, time-consuming, or challenging, especially for complex or novel materials [25,29,282].

v **Dedicated CEC database:** Another main limitation of applying AI in CEC research and development is the absence of a specialized database that can store, share, and analyze data on various aspects of CEC materials and systems. Currently, no database is dedicated explicitly to CECs, showing the materials' ASRs, stability, or degradation rates. Hence, it is crucial to address this limitation to advance materials development for CECs [154].

vi **Limited AI algorithms:** The extensive literature review conducted in this study shows that previous studies have only focused on applying some ML and DL algorithms to CECs research problem. Advanced algorithms such as transformer-based models, TabNet, reinforcement learning techniques and transfer learning techniques are yet to be fully explored.

8. Recommendations and future direction for the application of AI approach for CECs materials design and development

The limitations of the AI-driven methods highlighted in the previous section can be mitigated by improving or extending the models, such as:

i **Data quality and management:** ML and DL models are as accurate as the data used for their development. The quality, quantity, diversity, and accessibility of the data used for training and testing the AI models must be ensured. Proper data preprocessing techniques, such as normalization, standardization, feature extraction, and dimensionality reduction, should be used to improve the performance of the AI models. To improve the robustness and generalization capability of the AI models, it is essential to use data augmentation techniques, such as rotation, scaling, and cropping, using suitable data annotation techniques, such as manual labeling, semi-supervised learning, and weakly supervised learning can help reduce the burden of supervision and enhance the interpretability of the AI models [33,196].

ii **Exploring new data sources and descriptors:** Future research can explore new data sources and descriptors that can enrich the information and representation of materials for CECs. For example, image data from microscopy or spectroscopy, text data (ASRs, PPDs, and stability) from literature or patents, and graph data from molecular structures or networks can improve the models [220,320,321].

iii **Creating dedicated CEC database:** Dedicated CEC database can be established by employing suitable material descriptors that account for the unique features and challenges of CECs, such as the electrochemical reactions, the stability and compatibility of materials, and the fabrication and integration of cells. Some possible steps to expedite the creation of this database include collecting and organizing data from existing literature, experiments, and simulations on CECs materials and systems; developing standardized methods and metrics for data generation, validation, and annotation; creating a user-friendly interface and platform for data access, sharing, and analysis; collaborating with researchers and stakeholders from different disciplines and sectors to enrich and update the database; and applying AI methods to mine and model the data for material discovery, design, optimization, and characterization.

iv **Exploring advanced algorithms:** While previous CECs research has utilized some ML and DL models, there remains significant potential to apply more advanced AI algorithms that have shown promise in other domains. Some techniques that could be beneficial include, transformer-based models, TabNet, and reinforcement and transfer learning-based models. Transformer-based models are neural networks that use attention mechanisms to capture long-range dependencies and contextual information from sequential data. They have been widely used for natural language processing and computer vision tasks, but they can also be applied to CECs data that have temporal or spatial dimensions. For example, transformer-based models can be used to model the dynamic behavior of CECs under different operating conditions or to analyze the spatial distribution of electrochemical phenomena in CECs . TabNet is a novel neural network architecture based on attention mechanism that is used for tabular data [322]. Tabular data are common in CECs research, such as sensor data and experimental measurements. TabNet could be well-suited for handling these types of data, as it can learn complex relationships from CECs data tables and provide interpretable feature attributions. TabNet has shown high performance with tabular data in other applications, such as finance and healthcare. Reinforcement learning (RL) methods like deep Q-learning have demonstrated success in applications like games and robotics [323]. For CECs, RL could be used to optimize control policies and material configurations to maximize performance over time. The sequential nature of RL matches well with the evolving states in CECs. For example, RL can be used to find the optimal charging strategy for a battery or the optimal operating parameters for a fuel cell [324,325]. Regarding transfer learning, given the limited labeled data in CECs research, transfer learning provides a way to leverage knowledge from related domains. Pretraining models on data-rich battery or fuel cell datasets before fine-tuning on CECs data could improve performance. Multi-task learning across related electrochemical systems is another promising transfer learning direction [326].

v **Incorporating more features and functionalities:** The AI models for CECs material development can be improved by incorporating more features and functionalities to enhance their performance and applicability. For example, multi-scale modeling can capture the interactions between different scales of materials; multi-objective optimization can find trade-offs between different performance criteria; active learning can select the most informative data points to update the models [283].

vi **Model validation:** Several evaluation metrics can be used to validate the model on a new set of data [327,328]. These metrics include the root mean square error (RMSE), mean absolute error (MAE), mean absolute percentage error (MAPE), root mean square percentage error (RMSPE), relative absolute error (RAE), relative root mean square error (RRSE), and root mean square logarithmic error (RMSLE). Further, Cross-validation techniques such as k-fold and leave-one-out cross-validation can be applied to avoid overfitting and underfitting the AI models. Comparison techniques, such as Bayesian model selection, Akaike information criterion (AIC), and Bayesian information criterion (BIC), can be explored to identify the best AI model among different alternatives [33,196].

vii **Materials synthesis:** AI models can be used to guide the synthesis of novel and optimal materials for CECs by providing suggestions on material composition and synthesis conditions. The feedback loops between AI models and experimental synthesis can be effectively explored to update and improve the AI models based on new data. To establish trade-offs between different performance criteria of CECs, multi-objective optimization techniques, such as Pareto optimality and GA, can be employed [33,196].

viii **Performance evaluation:** AI models can be used to predict the performance of CECs under different operating conditions, such as temperature, pressure, and humidity. In addition to feature importance frameworks, sensitivity analysis techniques such as Sobol indices and the Morris method can be used to identify the most influential parameters on the performance of CECs. Uncertainty quantification techniques such as Monte Carlo and Bayesian inference can be used to estimate the confidence intervals of the performance predictions [33,196].

ix **Developing hybrid approaches:** The AI models for CECs can be integrated with other computational and experimental techniques to form hybrid approaches that can complement each other's strengths and weaknesses. For example, DFT, Molecular Dynamics (MD), and High Throughput Screening (HTS), among others, can provide data or insights for the AI models, and the AI models can provide suggestions or feedback for the computational or experimental techniques [283].

x **Leveraging domain knowledge and human expertise:** The AI models for CECs can be enhanced by leveraging domain knowledge and human expertise that can provide guidance and constraints for the models. For example, knowledge representation frameworks can encode domain knowledge into symbolic or graphical forms; planning methods can generate sequences of actions to achieve goals; and causal inference methods can infer causal relationships from observational or experimental data [283].

xi **Fostering interdisciplinary and cross-sectoral partnerships:** Interdisciplinary and cross-sectoral partnerships are crucial for advancing research and addressing complex challenges. By bringing together experts from different fields and sectors, such partnerships can foster collaboration and communication, leading to more innovative and impactful solutions. In the context of CECs research, such partnerships can help bridge the gap between materials science and AI, enabling the development of more advanced AI models for CECs material development. Material scientists can provide their expertise in material synthesis and characterization, while computer scientists and engineers can contribute their expertise in AI and computational modeling. Chemists, Physicists, and Biologists can also provide valuable insights into the chemical and physical properties of CECs and their potential impact on the environment and human health [28,283].

In addition, partnerships between academia, industry, government, and NGOs can help ensure the research is relevant, impactful, and responsive to societal needs. Industry partners can provide resources and expertise in scaling up and commercializing CECs, while governments and NGOs can help shape policies and regulations that promote the safe and sustainable use of CECs. [282,283].

9. Conclusions

We have comprehensively surveyed state-of-the-art AI applications for designing materials and optimizing CECs. We have covered various material aspects and AI methods relevant to CECs and presented some representative case studies of AI-predicted and synthesized materials for CECs. We have underscored the main implications and contributions of the AI approach for advancing the CEC technology, such as reducing experimental trial-and-error, exploring vast materials spaces, discovering novel and optimal materials, and enhancing the understanding of materials-performance relationships. We have also discussed the AI approach's main limitations and future directions for CECs, such as addressing data and model challenges, improving and extending AI models and methods, and integrating with other computational and experimental techniques.

This article is significant as it offers a comprehensive and systematic overview of the current state-of-the-art and prospects of AI in materials design for CECs. It provides a critical analysis of the strengths and weaknesses of the AI approach for CECs and offers practical guidance and suggestions for researchers and practitioners in this field. This article can serve as a valuable reference and source of inspiration for future research and development in this emerging and promising area.

It is essential to acknowledge and address the limitations and challenges present in this article. For example, not all AI methods or material aspects relevant to material development for CECs are covered, and there is no quantitative or comparative analysis of the effectiveness of different AI methods or material candidates. Ethical issues arising from using AI in materials design for CECs are also not fully explored because we are unaware of that. Future work can extend or complement this article by exploring additional AI methods or material aspects, conducting more rigorous experiments or evaluations, and addressing salient ethical concerns that may have arisen.

Declaration of Competing Interest

The authors declare that they have no known competing financial interests or personal relationships that could have appeared to influence the work reported in this paper.

Acknowledgment

M. NI appreciates the grant (Project Number: N_PolyU552/20) from the Research Grants Council, University Grants Committee, Hong Kong SAR.

References

[1] Cozzi L, Gould T, Bouckart S, Crow D, Kim T-Y, McGlade C, et al. In: World Energy Outlook 2020. 2050; 2020. p. 1–461.
[2] Ritchie, Hannah, Roser M. Fossil fuels; our world in data. Our World in Data; 2018.

[3] Yang G, Su C, Shi H, Zhu Y, Song Y, Zhou W, et al. Toward reducing the operation temperature of solid oxide fuel cells: our past 15 years of efforts in cathode development. Energy Fuels 2020;34:15169–94. https://doi.org/10.1021/acs.energyfuels.0c01887.

[4] Duan C, Huang J, Sullivan N, O'Hayre R. Proton-conducting oxides for energy conversion and storage. Appl Phys Rev 2020;7:011314. https://doi.org/10.1063/1.5135319.

[5] Duan C, Kee R, Zhu H, Sullivan N, Zhu L, Bian L, et al. Highly efficient reversible protonic ceramic electrochemical cells for power generation and fuel production. Nat Energy 2019;4:230–40. https://doi.org/10.1038/s41560-019-0333-2.

[6] Shim JH. Ceramics breakthrough. Nat Energy 2018;3:168–9. https://doi.org/10.1038/s41560-018-0110-7.

[7] Bian W, Wu W, Wang B, Tang W, Zhou M, Jin C, et al. Revitalizing interface in protonic ceramic cells by acid etch. Nature 2022;604:479. https://doi.org/10.1038/s41586-022-04457-y.

[8] Shao Z, Haile SM. A high-performance cathode for the next generation of solid-oxide fuel cells. Nature 2004;431:170–3. https://doi.org/10.1038/nature02863.

[9] Zhang Y, Chen B, Guan D, Xu M, Ran R, Ni M, et al. Thermal-expansion offset for high-performance fuel cell cathodes. Nature 2021;591:246–51. https://doi.org/10.1038/s41586-021-03264-1.

[10] Duan C. Selective CO2 electrohydrogenation. Nat Catal 2021;4:264–5. https://doi.org/10.1038/s41929-021-00600-6.

[11] Yang L, Wang S, Blinn K, Liu M, Liu Z, Cheng Z, et al. Enhanced sulfur and coking tolerance of a mixed ion conductor for SOFCs: baZr 0.1 Ce 0.7 Y 0.2– x Yb x O 3–δ. Science (1979) 2009;326:126–9. https://doi.org/10.1126/science.1174811.

[12] Bello IT, Zhai S, He Q, Cheng C, Dai Y, Chen B, et al. Materials development and prospective for protonic ceramic fuel cells. Int J Energy Res 2021:1–29. https://doi.org/10.1002/er.7371.

[13] Zhang W, Hu YH. Progress in proton-conducting oxides as electrolytes for low-temperature solid oxide fuel cells: from materials to devices. Energy Sci Eng 2021. https://doi.org/10.1002/ese3.886. n/a.

[14] Lu N, Zhang Z, Wang Y, Li H-B, Qiao S, Zhao B, et al. Enhanced low-temperature proton conductivity in hydrogen-intercalated brownmillerite oxide. Nat Energy 2022;7:1208–16. https://doi.org/10.1038/s41560-022-01166-8.

[15] Duan C, Kee RJ, Zhu H, Karakaya C, Chen Y, Ricote S, et al. Highly durable, coking and sulfur tolerant, fuel-flexible protonic ceramic fuel cells. Nature 2018;557:217–22. https://doi.org/10.1038/s41586-018-0082-6.

[16] Li Z., Peng M., Zhao Y., Li J., Sun Y. cobalt-based perovskite air electrodes for 2021:20299–308. https://doi.org/10.1039/d1nr06845h.

[17] Zhang Y, Chen K, Xia C, Jiang SP, Ni M. A model for the delamination kinetics of La0.8Sr0.2MnO3 oxygen electrodes of solid oxide electrolysis cells. Int J Hydrogen Energy 2012;37:13914–20. https://doi.org/10.1016/j.ijhydene.2012.07.062.

[18] Wang Z, Wang Y, Wang J, Song Y, Robson MJ, Seong A, et al. Rational design of perovskite ferrites as high-performance proton-conducting fuel cell cathodes. Nat Catal 2022;5:777–87. https://doi.org/10.1038/s41929-022-00829-9.

[19] Medvedev D. Trends in research and development of protonic ceramic electrolysis cells. Int J Hydrogen Energy 2019;44:26711–40. https://doi.org/10.1016/j.ijhydene.2019.08.130.

[20] Kumar V, Kaur M, Kaur G, Arya SK, Pickrell G. Stacking designs and sealing principles for IT-solid oxide fuel cell. INC; 2019. https://doi.org/10.1016/B978-0-12-817445-6.00011-9.

[21] Lin CK, Huang LH, Chiang LK, Chyou YP. Thermal stress analysis of planar solid oxide fuel cell stacks: effects of sealing design. J Power Sources 2009;192:515–24. https://doi.org/10.1016/j.jpowsour.2009.03.010.

[22] Tsvetkov D, Tsvetkova N, Ivanov I, Malyshkin D, Sereda V, Zuev A. PrBaCo 2 O 6−δ -Ce 0.8 Sm 0.2 O 1.9 composite cathodes for intermediate-temperature solid oxide fuel cells: stability and cation interdiffusion. Energies (Basel) 2019;12. https://doi.org/10.3390/en12030417.

[23] Copeland, B.J.. "artificial intelligence". Encyclopedia Britannica, 8 Nov. 2023, https://www.britannica.com/technology/artificial-intelligence. Accessed 10 November 2023.

[24] Juan Y, Dai Y, Yang Y, Zhang J. Accelerating materials discovery using machine learning. J Mater Sci Technol 2021;79:178–90. https://doi.org/10.1016/J.JMST.2020.12.010.

[25] Li Z, Wang S, Xin H. Toward artificial intelligence in catalysis. Nat Catal 2018;1:641–2. https://doi.org/10.1038/S41929-018-0150-1.

[26] Tabor DP, Roch LM, Saikin SK, Kreisbeck C, Sheberla D, Montoya JH, et al. Accelerating the discovery of materials for clean energy in the era of smart automation. Nat Rev Mater 2018;3:5–20. https://doi.org/10.1038/S41578-018-0005-Z.

[27] Pyzer-Knapp EO, Pitera JW, Staar PWJ, Takeda S, Laino T, Sanders DP, et al. Accelerating materials discovery using artificial intelligence, high performance computing and robotics. Npj Comput Mater 2022;8:1–9. https://doi.org/10.1038/s41524-022-00765-z. 2022 8:1.

[28] Maleki R, Asadnia M, Razmjou A. Artificial intelligence-based material discovery for clean energy future. Adv Intell Syst 2022;4:2200073. https://doi.org/10.1002/aisy.202200073.

[29] Sadiku MNO, Suman GK, Musa SM. Artificial intelligence in materials science. Int J Adv Sci Res Eng 2021;07:77–81. https://doi.org/10.31695/IJASRE.2021.34057.

[30] Stanev V, Choudhary K, Kusne AG, Paglione J, Takeuchi I. Artificial intelligence for search and discovery of quantum materials. Commun Mater 2021;2:105. https://doi.org/10.1038/s43246-021-00209-z.

[31] Maleki R, Shams SM, Chellehbari YM, Rezvantalab S, Jahromi AM, Asadnia M, et al. Materials discovery of ion-selective membranes using artificial intelligence. Commun Chem 2022;5:132. https://doi.org/10.1038/s42004-022-00744-x.

[32] Guo K, Yang Z, Yu CH, Buehler MJ. Artificial intelligence and machine learning in design of mechanical materials. Mater Horiz 2021;8:1153–72. https://doi.org/10.1039/D0MH01451F.

[33] Choi JB, Nguyen PCH, Sen O, Udaykumar HS, Baek S. Artificial intelligence approaches for energetic materials by design: state of the art, challenges, and future directions. Propell Explos Pyrotech 2023;48. https://doi.org/10.1002/prep.202200276.

[34] Hwang H, Ahn J, Lee H, Oh J, Kim J, Ahn JP, et al. Deep learning-assisted microstructural analysis of Ni/YSZ anode composites for solid oxide fuel cells. Mater Charact 2021;172:110906. https://doi.org/10.1016/J.MATCHAR.2021.110906.

[35] Zhai S, Xie H, Cui P, Guan D, Wang J, Zhao S, et al. A combined ionic Lewis-acid descriptor and machine-learning approach to prediction of efficient oxygen reduction electrodes for ceramic fuel cells. Nat Energy 2022:1–10. https://doi.org/10.1038/s41560-022-01098-3.

[36] Wang N, Yuan B, Tang C, Du L, Zhu R, Aoki Y, et al. Machine-learning-accelerated development of efficient mixed protonic–electronic conducting oxides as the air electrodes for protonic ceramic cells. Adv Mater 2022;34:2203446. https://doi.org/10.1002/adma.202203446.

[37] Gomes CP, Selman B, Gregoire JM. Artificial intelligence for materials discovery. MRS Bull 2019;44:538–44. https://doi.org/10.1557/MRS.2019.158/FIGURES/1.

[38] Xu Q, Guo Z, Xia L, He Q, Li Z, Temitope I, et al. A comprehensive review of solid oxide fuel cells operating on various promising alternative fuels. Energy Convers Manag 2022;253:115175. https://doi.org/10.1016/j.enconman.2021.115175.

[39] Bello IT, Song Y, Yu N, Li Z, Zhao S, Maradesa A, et al. Evaluation of the electrocatalytic performance of a novel nanocomposite cathode material for ceramic fuel cells. J Power Sources 2023;560:232722. https://doi.org/10.1016/J.JPOWSOUR.2023.232722.

[40] Bello IT, Yu N, Song Y, Wang J, Chan T, Zhao S, et al. Electrokinetic insights into the triple ionic and electronic conductivity of a novel nanocomposite functional material for protonic ceramic fuel cells. Small 2022;18:2203207. https://doi.org/10.1002/smll.202203207.

[41] Thabet K, Le Gal La Salle A, Quarez E, Joubert O. Protonic-based ceramics for fuel cells and electrolyzers. INC; 2020. https://doi.org/10.1016/b978-0-12-818285-7.00004-6.

[42] Iwahara H. Oxide-ionic and protonic conductors based on perovskite-type oxides and their possible applications. Solid State Ion 1992;52:99–104. https://doi.org/10.1016/0167-2738(92)90095-7.

[43] Kim JH, Cassidy M, Irvine JTS, Bae J. Advanced electrochemical properties of Ln Ba0.5 Sr0.5 CO2 O5+δ (Ln=Pr, Sm, and Gd) as cathode materials for IT-SOFC. J Electrochem Soc 2009;156:B682–9. https://doi.org/10.1149/1.3110989.

[44] Zhang W, Yu B, Xu J. Investigation of single SOEC with BSCF anode and SDC barrier layer. Int J Hydrogen Energy 2012;37:837–42. https://doi.org/10.1016/j.ijhydene.2011.04.049.

[45] Zhang X, O'Brien JE, O'Brien RC, Hartvigsen JJ, Tao G, Housley GK. Improved durability of SOEC stacks for high temperature electrolysis. Int J Hydrogen Energy 2013;38:20–8. https://doi.org/10.1016/j.ijhydene.2012.09.176.

[46] Kusnezoff M, Trofimenko N, M•ller M, Michaelis A. Influence of electrode design and contacting layers on performance of electrolyte supported SOFC/SOEC single cells. Materials (Basel) 2016;9. https://doi.org/10.3390/ma9110906.

[47] Eveloy V. Anode fuel and steam recycling for internal methane reforming SOFCs: analysis of carbon deposition. J Fuel Cell Sci Technol 2011;8:1–8. https://doi.org/10.1115/1.4002230.

[48] Hassan D, Janes S, Clasen R. Proton-conducting ceramics as electrode/electrolyte materials for SOFC's—Part I: preparation, mechanical and thermal properties of sintered bodies. J Eur Ceram Soc 2003;23:221–8. https://doi.org/10.1016/S0955-2219(02)00173-5.

[49] Bello IT, Yu N, Zhai S, Song Y, Zhao S, Cheng C, et al. Effect of engineered lattice contraction and expansion on the performance and CO2 tolerance of Ba0.5Sr0.5Co0.7Fe0.3O3-δ functional material for intermediate temperature solid oxide fuel cells. Ceram Int 2022;48:21457–68. https://doi.org/10.1016/j.ceramint.2022.04.110.

[50] Swierczek K, Zheng K, Klimkowicz A. Optimization of transport properties of a-site ordered LnBa1-xSrxCo2-yFeyO5+ perovskite-type cathode materials. ECS Trans 2013;57:1993–2001. https://doi.org/10.1149/05701.1993ecst.

[51] Jin F, Liu J, Niu B, Ta L, Li R, Wang Y, et al. Evaluation and performance optimization of double-perovskite LaSrCoTiO5+δ cathode for intermediate-temperature solid-oxide fuel cells. Int J Hydrogen Energy 2016;41:21439–49. https://doi.org/10.1016/j.ijhydene.2016.08.059.

[52] Wei K, Li N, Wu Y, Song W, Wang X, Guo L, et al. Characterization and optimization of highly active and Ba-deficient BaCo0.4Fe0.4Zr0.1Y0.1O3-δ-based cathode materials for protonic ceramics fuel cells. Ceram Int 2019;45:18583–91. https://doi.org/10.1016/j.ceramint.2019.06.081.

[53] Park S, Choi S, Shin J, Kim G. Tradeoff optimization of electrochemical performance and thermal expansion for Co-based cathode material for intermediate-temperature solid oxide fuel cells. Electrochim Acta 2014;125:683–90. https://doi.org/10.1016/j.electacta.2014.01.112.

[54] Jun A, Kim J, Shin J, Kim G. Optimization of Sr content in layered SmBa 1-xSr xCo 2O 5+δ perovskite cathodes for intermediate-temperature solid oxide fuel cells. Int J Hydrogen Energy 2012;37:18381–8. https://doi.org/10.1016/j.ijhydene.2012.09.048.

[55] Yu X, Long W, Jin F, He T. Cobalt-free perovskite cathode materials SrFe1-xTi xO3-δ and performance optimization for intermediate-temperature solid oxide

fuel cells. Electrochim Acta 2014;123:426–34. https://doi.org/10.1016/j.electacta.2014.01.020.
[56] Gwon O, Yoo S, Shin J, Kim G. Optimization of La1-xSrxCoO3-δ perovskite cathodes for intermediate temperature solid oxide fuel cells through the analysis of crystal structure and electrical properties. Int J Hydrogen Energy 2014;39:20806–11. https://doi.org/10.1016/j.ijhydene.2014.07.137.
[57] Li Z, Wang C, Bello IT, Guo M, Yu N, Zhu M, et al. Direct ammonia protonic ceramic fuel cell: a modelling study based on elementary reaction kinetics. J Power Sources 2023;556:232505. https://doi.org/10.1016/J.JPOWSOUR.2022.232505.
[58] Li Z, He Q, Wang C, Yu N, Bello IT, Guo M, et al. Protonic ceramic fuel cells for power-ethylene cogeneration: a modelling study on structural parameters. Energy 2023;264:126193. https://doi.org/10.1016/J.ENERGY.2022.126193.
[59] Li Z, He Q, Wang C, Xu Q, Guo M, Bello IT, et al. Ethylene and power cogeneration from proton ceramic fuel cells (PCFC): a thermo-electrochemical modelling study. J Power Sources 2022;536:231503. https://doi.org/10.1016/J.JPOWSOUR.2022.231503.
[60] Campana R., Larrea A., Kilner J.A., Orera V.M. Performance and aging of microtubular YSZ-based solid oxide regenerative fuel cells 2011:116–23. https://doi.org/10.1002/fuce.201000069.
[61] Norby T, Hartmanová M. Electrical conductivity and ionic transport number of YSZ and Cr-doped YSZ single crystals at 200-1000°C. Solid State Ion 1993;67:57–64. https://doi.org/10.1016/0167-2738(93)90309-Q.
[62] Zhan Z, Wen T-L, Tu H, Lu Z-Y. AC Impedance Investigation of Samarium-Doped Ceria. J Electrochem Soc 2001;148:A427. https://doi.org/10.1149/1.1359198/XML.
[63] Zhang X, Robertson M, Deċes-Petit C, Qu W, Kesler O, Maric R, et al. Internal shorting and fuel loss of a low temperature solid oxide fuel cell with SDC electrolyte. J Power Sources 2007;164:668–77. https://doi.org/10.1016/J.JPOWSOUR.2006.10.087.
[64] Pine TS, Lu X, Do A-TV, Mumm DR, Brouwer J. Operation of an LSGMC electrolyte-supported SOFC with composite ceramic anode and cathode. Electrochem Solid-State Lett 2007;10:B183–5. https://doi.org/10.1149/1.2769100.
[65] Aguadero A, Alonso JA, Escudero MJ, Daza L. Evaluation of the La2Ni1−xCuxO4+δ system as SOFC cathode material with 8YSZ and LSGM as electrolytes. Solid State Ion 2008;179:393–400. https://doi.org/10.1016/j.ssi.2008.01.099.
[66] Shang M, Tong J, O'Hayre R. A promising cathode for intermediate temperature protonic ceramic fuel cells: baCo0.4Fe0.4Zr0.2O3−δ. RSC Adv 2013;3:15769. https://doi.org/10.1039/c3ra41828f.
[67] Zohourian R, Merkle R, Maier J. Proton uptake into the protonic cathode material BaCo0.4Fe0.4Zr0.2O3-δ and comparison to protonic electrolyte materials. Solid State Ion 2017;299:64–9. https://doi.org/10.1016/j.ssi.2016.09.012.
[68] Hong T, Lu W, Ren K, Liu T. The two-fold diffusion process for proton uptake reaction in BCFZY e-/H+/O2- triple conductor measured by electrical conductivity relaxation. Ionics (Kiel) 2020;26:5293–7. https://doi.org/10.1007/s11581-020-03757-5.
[69] Kuai X, Yang G, Chen Y, Sun H, Dai J, Song Y, et al. Boosting the activity of BaCo0.4Fe0.4Zr0.1Y0.1O3−δ perovskite for oxygen reduction reactions at low-to-intermediate temperatures through tuning b-site cation deficiency. Adv Energy Mater 2019;9:0–10. https://doi.org/10.1002/aenm.201902384.
[70] Magnone E. A systematic literature review on BSCF-based cathodes for solid oxide fuel cell applications. J Fuel Cell Sci Technol 2010;7. https://doi.org/10.1115/1.4001323.
[71] Tsai T, Barnett SA. Effect of LSM-YSZ cathode on thin-electrolyte solid oxide fuel cell performance. Solid State Ion 1997;93:207–17. https://doi.org/10.1016/S0167-2738(96)00524-3.
[72] Bausá N, Escolástico S, Serra JM. Direct CO2 conversion to syngas in a BaCe0.2Zr0.7Y0.1O3- δ-based proton-conducting electrolysis cell. J CO_2 Utiliz 2019;34:231–8. https://doi.org/10.1016/j.jcou.2019.05.037.
[73] Zhang S-L, Chen K, Zhang A-P, Li C-X, Li C-J. Effect of Fe doping on the performance of suspension plasma-sprayed PrBa0.5Sr0.5Co2−xFexO5+δ cathodes for intermediate-temperature solid oxide fuel cells. Ceram Int 2017;43:11648–55. https://doi.org/10.1016/j.ceramint.2017.05.348.
[74] Park S, Choi S, Shin J, Kim G. A collaborative study of sintering and composite effects for a PrBa 0.5Sr0.5Co1.5Fe0.5O 5+δ IT-SOFC cathode. RSC Adv 2014;4:1775–81. https://doi.org/10.1039/c3ra45296d.
[75] Nguyen NTQ, Yoon HH. Preparation and evaluation of BaZr0.1Ce0.7Y0.1Yb0.1O3 − δ (BZCYYb) electrolyte and BZCYYb-based solid oxide fuel cells. J Power Sources 2013;231:213. https://doi.org/10.1016/j.jpowsour.2013.01.011.
[76] Zhu H, Ricote S, Duan C, O'Hayre RP, Kee RJ. Defect chemistry and transport within dense BaCe 0.7 Zr 0.1 Y 0.1 Yb 0.1 O 3 − δ (BCZYYb) proton-conducting membranes. J Electrochem Soc 2018;165:F845–53. https://doi.org/10.1149/2.1091810jes.
[77] Ricote S, Bonanos N, Rørvik PM, Haavik C. Microstructure and performance of La 0.58Sr 0.4Co 0.2Fe 0.8O 3-δ cathodes deposited on BaCe 0.2Zr 0.7Y 0.1O 3-δ by infiltration and spray pyrolysis. J Power Sources 2012;209:172–9. https://doi.org/10.1016/j.jpowsour.2012.02.090.
[78] Hou J, Zhu Z, Qian J, Liu W. A new cobalt-free proton-blocking composite cathode La2NiO 4+δ-LaNi0.6Fe0.4O3-δ for BaZr0.1Ce0.7Y0.2O3-δ-based solid oxide fuel cells. J Power Sources 2014;264:67–75. https://doi.org/10.1016/j.jpowsour.2014.04.089.
[79] Ding H, Wu W, Jiang C, Ding Y, Bian W, Hu B, et al. Self-sustainable protonic ceramic electrochemical cells using a triple conducting electrode for hydrogen and power production. Nat Commun 2020;11:1–11. https://doi.org/10.1038/s41467-020-15677-z. 2020 11:1.
[80] Ji H Il, Lee JH, Son JW, Yoon KJ, Yang S, Kim BK. Protonic ceramic electrolysis cells for fuel production: a brief review. J Korean Ceram Soc 2020;57:480–94. https://doi.org/10.1007/s43207-020-00059-4.
[81] Fu C, Sun K, Zhang N, Chen X, Zhou D. Electrochemical characteristics of LSCF-SDC composite cathode for intermediate temperature SOFC. Electrochim Acta 2007;52:4589–94. https://doi.org/10.1016/j.electacta.2007.01.001.
[82] Xi X, Kondo A, Kozawa T, Naito M. LSCF-GDC composite particles for solid oxide fuel cells cathodes prepared by facile mechanical method. Adv Powder Technol 2016;27:646–51. https://doi.org/10.1016/j.apt.2016.02.022.
[83] Plonczak P, Gazda M, Kusz B, Jasinski P. Fabrication of solid oxide fuel cell supported on specially performed ferrite-based perovskite cathode. J Power Sources 2008;181:1–7. https://doi.org/10.1016/j.jpowsour.2007.12.019.
[84] Chen X, Tao Z, Hou G, Xu N, Zhang Q. La0.7Sr0.3FeO3-δ composite cathode enhanced by Sm0.5Sr0.5CoO3-δ impregnation for proton conducting SOFCs. Electrochim Acta 2015;165:142–8. https://doi.org/10.1016/j.electacta.2015.02.237.
[85] Kim J, Sengodan S, Kwon G, Ding D, Shin J, Liu M, et al. Triple-conducting layered perovskites as cathode materials for proton-conducting solid oxide fuel cells. ChemSusChem 2014;7:2811–5. https://doi.org/10.1002/cssc.201402351.
[86] Xu Y, Xu X, Bi L. A high-entropy spinel ceramic oxide as the cathode for proton-conducting solid oxide fuel cells. J Adv Ceram 2022;11:794–804. https://doi.org/10.1007/s40145-022-0573-7.
[87] Bi L, Fabbri E, Traversa E. Novel Ba0.5Sr0.5(Co0.8Fe0.2)1 − xTixO3 − δ (x = 0, 0.05, and 0.1) cathode materials for proton-conducting solid oxide fuel cells. Solid State Ion 2012;214:1–5. https://doi.org/10.1016/J.SSI.2012.02.049.
[88] Zhuang S, Han N, Zou Q, Zhang S, Song F. Insight into steam permeation through perovskite membrane via transient modeling. Membranes (Basel) 2020;10:1–15. https://doi.org/10.3390/membranes10080164.
[89] Zunic M, Chevallier L, Deganello F, D'Epifanio A, Licoccia S, Di Bartolomeo E, et al. Electrophoretic deposition of dense BaCe0.9Y0.1O3−x electrolyte thick-films on Ni-based anodes for intermediate temperature solid oxide fuel cells. J Power Sources 2009;190:417–22. https://doi.org/10.1016/j.jpowsour.2009.01.046.
[90] Chevallier L, Zunic M, Esposito V, Di Bartolomeo E, Traversa E. A wet-chemical route for the preparation of Ni–BaCe0.9Y0.1O3−δ cermet anodes for IT-SOFCs. Solid State Ion 2009;180:715–20. https://doi.org/10.1016/j.ssi.2009.03.005.
[91] Fu YP, Subardi A, Hsieh MY, Chang WK. Electrochemical properties of La0.5Sr0.5Co0.8M0.2O3-δ (M=Mn, Fe, Ni, Cu) perovskite cathodes for IT-SOFCs. J Am Ceram Soc 2016;99:1345–52. https://doi.org/10.1111/jace.14127.
[92] Fu YP, Wen SB, Lu CH. Preparation and characterization of samaria-doped ceria electrolyte materials for solid oxide fuel cells. J Am Ceram Soc 2008;91:127–31. https://doi.org/10.1111/J.1551-2916.2007.01923.X.
[93] Song B, Ruiz-Trejo E, Bertei A, Brandon NP. Quantification of the degradation of Ni-YSZ anodes upon redox cycling. J Power Sources 2018;374:61–8. https://doi.org/10.1016/j.jpowsour.2017.11.024.
[94] Herradon C, Le L, Meisel C, Huang J, Chmura C, Kim YD, et al. Proton-conducting ceramics for water electrolysis and hydrogen production at elevated pressure. Front Energy Res 2022;10:1–12. https://doi.org/10.3389/fenrg.2022.1020960.
[95] Lust E, Möller P, Kivi I, Nurk G, Kallip S, Nigu P, et al. Optimisation of the cathode composition for the intermediate temperature SOFC. Proc Electrochem Soc 2005:1607–16. https://doi.org/10.1149/200507.1607pv. PV 2005-07.
[96] Serra JM, Vert VB. Compositional improvement of Ln0.435Ba0.145Sr 0.4Fe0.8Co0.2O3-δ IT-SOFC cathodes performance by multiple lanthanide substitution. J Electrochem Soc 2010;157:B1349–57. https://doi.org/10.1149/1.3465646.
[97] Lust E, Möller P, Kivi I, Nurk G, Kallip S, Nigu P, et al. Optimization of the cathode composition for the intermediate-temperature SOFC. J Electrochem Soc 2005;152:A2306–8. https://doi.org/10.1149/1.2103727.
[98] Fang X, Zhu J, Lin Z. Effects of electrode composition and thickness on the mechanical performance of a solid oxide fuel cell. Energies (Basel) 2018;11. https://doi.org/10.3390/en11071735.
[99] Rioja-Monllor L, Bernuy-Lopez C, Fontaine ML, Grande T, Einarsrud MA. Compositional engineering of a La1-xBaxCoO3-δ-(1-a) BaZr0.9Y0.1O2.95 (a = 0.6, 0.7, 0.8 and x = 0.5, 0.6, 0.7) nanocomposite cathodes for protonic ceramic fuel cells. Materials (Basel) 2019;12:1–15. https://doi.org/10.3390/ma12203441.
[100] Mejía Gómez A, Sacanell J, Leyva AG, Lamas DG. Performance of La0.6Sr0.4Co1−yFeyO3 (y=0.2, 0.5 and 0.8) nanostructured cathodes for intermediate-temperature solid-oxide fuel cells: influence of microstructure and composition. Ceram Int 2016;42:3145–53. https://doi.org/10.1016/j.ceramint.2015.10.104.
[101] Bello IT, Zhai S, Zhao S, Li Z, Yu N, Ni M. Scientometric review of proton-conducting solid oxide fuel cells. Int J Hydrogen Energy 2021;46:37406–28. https://doi.org/10.1016/j.ijhydene.2021.09.061.
[102] Fabbri E, Pergolesi D, Licoccia S, Traversa E. Does the increase in Y-dopant concentration improve the proton conductivity of BaZr1-xYxO3-δ fuel cell electrolytes? Solid State Ion 2010;181:1043–51. https://doi.org/10.1016/j.ssi.2010.06.007.
[103] Tarutina LR, Vdovin GK, Lyagaeva JG, Medvedev DA. BaCe0.7−xZr0.2Y0.1FexO3−δ derived from proton-conducting electrolytes: a way of designing chemically compatible cathodes for solid oxide fuel cells. J Alloys Compd 2020;831. https://doi.org/10.1016/j.jallcom.2020.154895.
[104] Zhang H, Zhao F, Chen F, Xia C. with zirconia electrolytes. Solid State Ion 2011;192:591–4. https://doi.org/10.1016/j.ssi.2010.05.024.

[105] Sammells AF, Cook RL, White JH, Osborne JJ, MacDuff RC. Rational selection of advanced solid electrolytes for intermediate temperature fuel cells. Solid State Ion 1992;52:111–23. https://doi.org/10.1016/0167-2738(92)90097-9.

[106] Lee JG, Naden AB, Savaniu CD, Connor PA, Payne JL, Skelton J M, et al. Use of interplay between a-site non-stoichiometry and hydroxide doping to deliver novel proton-conducting perovskite oxides. Adv Energy Mater 2021;11:2101337. https://doi.org/10.1002/AENM.202101337.

[107] Liu Y, Huang H, Xue L, Sun J, Wang X, Xiong P, et al. Recent advances in the heteroatom doping of perovskite oxides for efficient electrocatalytic reactions. Nanoscale 2021;13:19840–56. https://doi.org/10.1039/D1NR05797A.

[108] Kasyanova AV, Zvonareva IA, Tarasova NA, Bi L, Medvedev DA, Shao Z. Electrolyte materials for protonic ceramic electrochemical cells: main limitations and potential solutions. Mater Rep Energy 2022;2:100158. https://doi.org/10.1016/J.MATRE.2022.100158.

[109] Higuchi T, Tsukamoto T, Yamaguchi S, Sata N, Hiramoto K, Ishigame M, et al. Protonic conduction in the single crystal of *Sc*-doped SrZrO3. Japan J Appl Phys Part 1 Regular Papers Short Notes Rev Papers 2002;41:6440–2. https://doi.org/10.1143/jjap.41.6440.

[110] Meng Y, Gao J, Zhao Z, Amoroso J, Tong J, Brinkman KS. Review: recent progress in low-temperature proton-conducting ceramics. J Mater Sci 2019;54:9291–312. https://doi.org/10.1007/s10853-019-03559-9.

[111] Cao J, Ji Y, Shao Z. Perovskites for protonic ceramic fuel cells: a review. Energy Environ Sci 2022;15:2200–32. https://doi.org/10.1039/D2EE00132B.

[112] Kim J, Sengodan S, Kwon G, Ding D, Shin J, Liu M, et al. Triple-conducting layered perovskites as cathode materials for proton-conducting solid oxide fuel cells. Chemsuschem Commun 2014:10. https://doi.org/10.1002/cssc.201402351. 1864564x.

[113] Xie X-B, Xiao J, Xu Q, Chen M, Chen D-C, Huang D-P, et al. Property evaluation of Sm1-xSrxFe0.7Cr0.3O3-δ perovskites as cathodes for intermediate temperature solid oxide fuel cells. Int J Energy Res 2019;43:2832–42. https://doi.org/10.1002/er.4377.

[114] Miruszewski T., Skubida W., Winiarz P., Wachowski S., Gazda M. Proton-electron hole interactions in Sr (Ti, Fe) O 3 − δ mixed-conducting perovskites proton-electron hole interactions in Sr (Ti, Fe) O 3 − δ mixed- conducting perovskites 2022. https://doi.org/10.1149/1945-7111/ac6e8f.

[115] Zhao H, Zheng Y, Yang C, Shen Y, Du Z, Świerczek K. Electrochemical performance of Pr1-xYxBaCo 2O5+δ layered perovskites as cathode materials for intermediate-temperature solid oxide fuel cells. Int J Hydrogen Energy 2013;38:16365–72. https://doi.org/10.1016/j.ijhydene.2013.10.003.

[116] Tucker MC. Progress in metal-supported solid oxide electrolysis cells: a review. Int J Hydrogen Energy 2020;45:24203–18. https://doi.org/10.1016/j.ijhydene.2020.06.300.

[117] Baharuddin NA, Muchtar A, Somalu MR. Short review on cobalt-free cathodes for solid oxide fuel cells. Int J Hydrogen Energy 2017;42:9149–55. https://doi.org/10.1016/j.ijhydene.2016.04.097.

[118] Junaida A, Aziz A, Akidah N, Rao M, Muchtar A. Review of composite cathodes for intermediate-temperature solid oxide fuel cell applications. Ceram Int 2020;46:23314–25. https://doi.org/10.1016/j.ceramint.2020.06.176.

[119] Ni M, Shao Z. Fuel cells that operate at 300° to 500°C. Science 2020;369:138LP–139. https://doi.org/10.1126/science.abc9136.

[120] Li M, Ni M, Su F, Xia C. Proton conducting intermediate-temperature solid oxide fuel cells using new perovskite type cathodes. J Power Sources 2014;260:197–204. https://doi.org/10.1016/J.JPOWSOUR.2014.03.013.

[121] Dong F, Ni M, He W, Chen Y, Yang G, Chen D. An ef fi cient electrocatalyst as cathode material for solid oxide fuel 2016. J Power Sources 2016;326:459–65. https://doi.org/10.1016/j.jpowsour.2016.07.023.

[122] Yu J, Ran R, Zhong Y, Zhou W, Ni M, Shao Z. Advances in porous perovskites: synthesis and electrocatalytic performance in fuel cells and metal–air batteries. Energy Environ Mater 2020;3:121–45. https://doi.org/10.1002/eem2.12064.

[123] Lei L, Zhang J, Yuan Z, Liu J, Ni M, Chen F. Progress report on proton conducting solid oxide electrolysis cells. Adv Funct Mater 2019;29:1–17. https://doi.org/10.1002/adfm.201903805.

[124] He W, Wu X, Yang G, Shi H, Dong F, Ni M. BaCo0.7Fe0.22Y0.08O3-δ as an active oxygen reduction electrocatalyst for low-temperature solid oxide fuel cells below 600 °c. ACS Energy Lett 2017;2:301–5. https://doi.org/10.1021/acsenergylett.6b00617.

[125] Yuan R, He W, Zhang C, Ni M, Leung MKH. Cobalt free SrFe0.95Nb0.05O3−δ cathode material for proton-conducting solid oxide fuel cells with BaZr0.1Ce0.7Y0.2O3−δ electrolyte. Mater Lett 2017;200:75–8. https://doi.org/10.1016/j.matlet.2017.04.103.

[126] Zhang Z, Zhu Y, Zhong Y, Zhou W, Shao Z. Anion doping: a new strategy for developing high-performance perovskite-type cathode materials of solid oxide fuel cells. Adv Energy Mater 2017;7. https://doi.org/10.1002/aenm.201700242.

[127] Sun C, Bian L, Qi J, Yu W, Li S, Hou Y, et al. Boosting CO2 directly electrolysis by electron doping in Sr2Fe1.5Mo0.5O6-δ double perovskite cathode. J Power Sources 2022;521:1–7. https://doi.org/10.1016/j.jpowsour.2022.230984.

[128] Ueno K, Hatada N, Han D, Uda T. Thermodynamic maximum of y doping level in barium zirconate in co-sintering with NiO. J Mater Chem A Mater 2019;7:7232–41. https://doi.org/10.1039/c8ta12245h.

[129] Unger LS, Ruhl R, Meffert M, Niedrig C, Menesklou W, Wagner SF, et al. Yttrium doping of Ba0.5Sr0.5Co0.8Fe0.2O3-δ part II: influence on oxygen transport and phase stability. J Eur Ceram Soc 2018;38:2388–95. https://doi.org/10.1016/j.jeurceramsoc.2017.12.042.

[130] Rioja-Monllor L, Bernuy-Lopez C, Fontaine M-L, Grande T, Einarsrud M-A. Processing of high performance composite cathodes for protonic ceramic fuel cells by exsolution. J Mater Chem A Mater 2019;7:8609–19. https://doi.org/10.1039/C8TA10950H.

[131] Rioja-Monllor L, Bernuy-Lopez C, Fontaine ML, Grande T, Einarsrud MA. Processing of high performance composite cathodes for protonic ceramic fuel cells by exsolution. J Mater Chem A Mater 2019;7:8609–19. https://doi.org/10.1039/c8ta10950h.

[132] Lv H, Lin L, Zhang X, Li R, Song Y, Matsumoto H, et al. Promoting exsolution of RuFe alloy nanoparticles on Sr2Fe1.4Ru0.1Mo0.5O6−δ via repeated redox manipulations for CO2 electrolysis. Nat Commun 2021;12. https://doi.org/10.1038/s41467-021-26001-8.

[133] Rioja-Monllor L, Ricote S, Bernuy-Lopez C, Grande T, O'Hayre R, Einarsrud M-A, et al. High-performance La0.5Ba0.5Co1/3Mn1/3Fe1/3O3−δ-BaZr1−zYzO3−δ cathode composites via an exsolution mechanism for protonic ceramic fuel cells. Inorganics (Basel) 2018;6:83. https://doi.org/10.3390/inorganics6030083.

[134] Rioja-Monllor L, Ricote S, Bernuy-Lopez C, Grande T, O'Hayre R, Einarsrud M-A. High-performance La0.5Ba0.5Co1/3Mn1/3Fe1/3O3−δ-BaZr1−zYzO3−δ cathode composites via an exsolution mechanism for protonic ceramic fuel cells. Inorganics (Basel) 2018;6:83. https://doi.org/10.3390/inorganics6030083.

[135] Jiang Z, Xia C, Chen F. Nano-structured composite cathodes for intermediate-temperature solid oxide fuel cells via an infiltration/impregnation technique. Electrochim Acta 2010;55:3595–605. https://doi.org/10.1016/j.electacta.2010.02.019.

[136] Vohs B.J.M., Gorte R.J. High-performance SOFC cathodes prepared by infiltration 2009:943–56. https://doi.org/10.1002/adma.200802428.

[137] Ding D, Li X, Lai SY, Gerdes K, Liu M. Enhancing SOFC cathode performance by surface modification through infiltration. Energy Environ Sci 2014;7:552–75. https://doi.org/10.1039/c3ee42926a.

[138] Ricote S, Bonanos N, Rørvik PM, Haavik C. Microstructure and performance of La0.58Sr0.4Co0.2Fe0.8O3−δ cathodes deposited on BaCe0.2Zr0.7Y0.1O3−δ by infiltration and spray pyrolysis. J Power Sources 2012;209:172–9. https://doi.org/10.1016/J.JPOWSOUR.2012.02.090.

[139] Guesnet L, Geffroy P-M, Flura A, Nicollet C, Grenier J-C, Vulliet J, et al. Shaping of ceria-based SOC Cells: development of a combined tape-casting and infiltration route. ECS Trans 2019;91:291–9. https://doi.org/10.1149/09101.0291ecst.

[140] Lv H, Zhou Y, Zhang X, Song Y, Liu Q, Wang G, et al. Infiltration of Ce0.8Gd0.2O1.9 nanoparticles on Sr2Fe1.5Mo0.5O6-Δ cathode for CO2 electroreduction in solid oxide electrolysis cell. J Energy Chem 2019;35:71–8. https://doi.org/10.1016/j.jechem.2018.11.002.

[141] Choi S, Yoo S, Shin J-Y, Kim G. High performance SOFC cathode prepared by infiltration of La n+11NinO3n1 (n 1, 2, and 3) in porous YSZ. J Electrochem Soc 2011;158:B995–9. https://doi.org/10.1149/1.3598170.

[142] Gao J, Meng Y, Lee S, Tong J, Brinkman KS. Effect of infiltration of barium carbonate nanoparticles on the electrochemical performance of La0.6Sr0.4Co0.2Fe0.8O3−δ cathodes for protonic ceramic fuel cells. JOM 2019;71:90–5. https://doi.org/10.1007/s11837-018-3098-3.

[143] Jafari M, Salamati H, Zhiani M, Shahsavari E. Enhancement of an IT-SOFC cathode by introducing YSZ: electrical and electrochemical properties of La 0.6 Ca 0.4 Fe 0.8 Ni 0.2 O 3-Δ -YSZ composites. Int J Hydrogen Energy 2019;44:1953–66. https://doi.org/10.1016/j.ijhydene.2018.10.151.

[144] Sun W., Soc J.E. Proton-blocking composite cathode for proton-conducting solid oxide fuel cell proton-blocking composite cathode for proton-conducting 2011. https://doi.org/10.1149/2.076111jes.

[145] Chen X, Tao Z, Hou G, Xu N, Zhang Q. La0.7Sr0.3FeO3−δ composite cathode enhanced by Sm0.5Sr0.5CoO3−δ impregnation for proton conducting SOFCs. Electrochim Acta 2015;165:142–8. https://doi.org/10.1016/J.ELECTACTA.2015.02.237.

[146] Duan C, Hook D, Chen Y, Tong J, O'Hayre R. Zr and Y co-doped perovskite as a stable, high performance cathode for solid oxide fuel cells operating below 500°C. Energy Environ Sci 2017;10:176–82. https://doi.org/10.1039/c6ee01915c.

[147] Duan C, Tong J, Shang M, Nikodemski S, Sanders M, Ricote S, et al. Readily processed protonic ceramic fuel cells with high performance at low temperatures. Science 2015;349:1321–6. https://doi.org/10.1126/science.aab3987.

[148] Kwon O, Joo S, Choi S, Sengodan S, Kim G. Review on exsolution and its driving forces in perovskites. J Phys Energy 2020;2:032001. https://doi.org/10.1088/2515-7655/AB8C1F.

[149] Kim YH, Jeong H, Won B-R, Myung J-H, Kim YH, Jeong H, et al. Exsolution modeling and control to improve the catalytic activity of nanostructured electrodes. Adv Mater 2023;35:2208984. https://doi.org/10.1002/ADMA.202208984.

[150] Fabbri E, Pergolesi D, Traversa E. Materials challenges toward proton-conducting oxide fuel cells: a critical review. Chem Soc Rev 2010;39:4355–69. https://doi.org/10.1039/b902343g.

[151] Sun C, Hui R, Roller J. Cathode materials for solid oxide fuel cells: a review. J Solid State Electrochem 2010;14:1125–44. https://doi.org/10.1007/s10008-009-0932-0.

[152] Nechache A, Hody S. Alternative and innovative solid oxide electrolysis cell materials: a short review. Renew Sustain Energy Rev 2021;149. https://doi.org/10.1016/j.rser.2021.111322.

[153] Chiara A, Giannici F, Pipitone C, Longo A, Aliotta C, Gambino M, et al. Solid-solid interfaces in protonic ceramic devices: a critical review. ACS Appl Mater Interfaces 2020;12:55537–53. https://doi.org/10.1021/acsami.0c13092.

[154] Bello IT, Guan D, Yu N, Li Z, Song Y, Chen X, et al. Revolutionizing material design for protonic ceramic fuel cells: Bridging the limitations of conventional experimental screening and machine learning methods. Chem Eng J 2023;477:147098. https://doi.org/10.1016/J.CEJ.2023.147098.

[155] Koo B, Kim K, Kim JK, Kwon H, Han JW, Jung WC. Sr segregation in perovskite oxides: why it happens and how it exists. Joule 2018;2:1476–99. https://doi.org/10.1016/j.joule.2018.07.016.

[156] Hauch A, Jensen H, Bilde-sørensen JB. Silica segregation in the Ni / YSZ electrode. J Electrochem Soc 2007. https://doi.org/10.1149/1.2733861.

[157] Zhao L, Drennan J, Kong C, Amarasinghe S, Jiang SP. Insight into surface segregation and chromium deposition on La 0.6Sr0.4Co0.2Fe0.8O 3-δ cathodes of solid oxide fuel cells. J Mater Chem A Mater 2014;2:11114–23. https://doi.org/10.1039/c4ta01426j.

[158] Knibbe R., Soc J.E., Knibbe R., Traulsen L., Hauch A., Ebbesen S.D., et al. Solid oxide electrolysis cells : degradation at high current densities solid oxide electrolysis cells : degradation at high current densities 2010. https://doi.org/10.1149/1.3447752.

[159] Chen K., Ping S., Electrochem J.J., Soc F. Review — materials degradation of solid oxide electrolysis cells Kongfa Chen and San Ping Jiang z review — materials degradation of solid oxide electrolysis cells 2016. https://doi.org/10.1149/2.0101611jes.

[160] Guo R, Han D, Chen W, Dai L, Ji K, Xiong Q, et al. Degradation mechanisms of perovskite solar cells under vacuum and one atmosphere of nitrogen. Nat Energy 2021;6. https://doi.org/10.1038/s41560-021-00912-8.

[161] Wang Y, Li W, Ma L, Li W, Liu X. Degradation of solid oxide electrolysis cells: phenomena, mechanisms, and emerging mitigation strategies—a review. J Mater Sci Technol 2020;55:35–55. https://doi.org/10.1016/j.jmst.2019.07.026.

[162] Moçoteguy P, Brisse A. A review and comprehensive analysis of degradation mechanisms of solid oxide electrolysis cells. Int J Hydrogen Energy 2013;38:15887–902. https://doi.org/10.1016/j.ijhydene.2013.09.045.

[163] Ren R, Wang Z, Xu C, Sun W, Rooney DW, Sun K. Tuning the defects of the triple conducting oxide. J Mater Chem A 2019;7:18365–72. https://doi.org/10.1039/c9ta04335g.

[164] Catlow CRA. Defect processes and migration mechanisms in solid state ionics. Solid State Ion 1992;12:219–31. https://doi.org/10.1016/b978-0-444-89354-3.50033-7.

[165] Yamazaki Y, Yang CK, Haile SM. Unraveling the defect chemistry and proton uptake of yttrium-doped barium zirconate. Scr Mater 2011;65:102–7. https://doi.org/10.1016/j.scriptamat.2010.12.034.

[166] Guan D, Zhang K, Zhou W, Shao Z. Utilizing the charge-transfer model to design promising electrocatalysts. Curr Opin Electrochem 2021;30. https://doi.org/10.1016/J.COELEC.2021.100805.

[167] Adler SB. Limitations of charge-transfer models for mixed-conducting oxygen electrodes. Solid State Ion 2000;135:603–12. https://doi.org/10.1016/S0167-2738(00)00423-9.

[168] Maier J. Ionic conduction in space charge regions. Progr Solid State Chem 1995;23:171–263. https://doi.org/10.1016/0079-6786(95)00004-E.

[169] Yoon S, Noh T, Kim W, Choi J, Lee H. Structural parameters and oxygen ion conductivity of Y2O3–ZrO2 and MgO–ZrO2 at high temperature. Ceram Int 2013;39:9247–51. https://doi.org/10.1016/J.CERAMINT.2013.05.032.

[170] Knauth P. Solid State Proton Conductors. Wiley; 2012. doi.org/10.1002/9781119962502.

[171] Wachsman ED, Lee KT. Lowering the temperature of solid oxide fuel cells. Science 2011;334:935–9. https://doi.org/10.1126/science.1204090.

[172] Tolchard JR, Grande T. Chemical compatibility of candidate oxide cathodes for BaZrO3 electrolytes. Solid State Ion 2007;178:593–9. https://doi.org/10.1016/j.ssi.2007.01.018.

[173] Tarutin AP, Lyagaeva JG, Medvedev DA, Bi L, Yaremchenko AA. Recent advances in layered Ln2NiO4+δ nickelates: fundamentals and prospects of their applications in protonic ceramic fuel and electrolysis cells. J Mater Chem A Mater 2021;9:154–95. https://doi.org/10.1039/D0TA08132A.

[174] Gushee BE, Katz L, Ward R. The preparation of a barium cobalt oxide and other phases with similar structures. J Am Chem Soc 1957;79:5601–3. https://doi.org/10.1021/ja01578a004.

[175] Shao-horn Y. Kinetics of oxygen surface exchange on Epitaxial Ruddlesden − popper phases and correlations to first-principles descriptors. J Phys Chem Lett 2016;7:244–9. https://doi.org/10.1021/acs.jpclett.5b02423.

[176] Berger C, Bucher E, Merkle R, Nader C, Lammer J, Grogger W, et al. Influence of Y-substitution on phase composition and proton uptake of self-generated Ba(Ce, Fe)O $_{3-\delta}$–Ba(Fe,Ce)O $_{3-\delta}$ composites. J Mater Chem A Mater 2022;10:2474–82. https://doi.org/10.1039/D1TA07208K.

[177] Zhao L, Zhang X, He B, Liu B, Xia C. Micro-tubular solid oxide fuel cells with graded anodes fabricated with a phase inversion method. J Power Sources 2011;196:962–7. https://doi.org/10.1016/j.jpowsour.2010.08.074.

[178] Mineev AM, Zvonareva IA, Medvedev DA, Shao Z. Maintaining pronounced proton transportation of solid oxides prepared with a sintering additive. J Mater Chem A Mater 2021;9:14553–65. https://doi.org/10.1039/d1ta03399a.

[179] Li F, Xu Y, Zhao D, Jiang L, Wu Q, Shen H, et al. Structural, transport, thermal, and electrochemical properties of (La1−xSrx)2CoO4±δ cathode in solid-oxide fuel cells. J Appl Electrochem 2021. https://doi.org/10.1007/s10800-020-01514-0.

[180] De Souza RA, Kilner JA. Oxygen transport in La1−xSrxMn1−yCoyO3±δ perovskites. Solid State Ion 1999;126:153–61. https://doi.org/10.1016/s0167-2738(99)00228-3.

[181] Norby T, Larring Y. Concentration and transport of protons in oxides. Curr Opin Solid State Mater Sci 1997;2:593–9. https://doi.org/10.1016/S1359-0286(97)80051-4.

[182] Nikitin SS, Markov AA, Leonidov IA, Patrakeev MV. Impact of cerium content on ion and electron transport in Sr $_{1-x}$ Ce $_{x}$ FeO $_{3-\delta}$. J Phys Chem C 2021;125:17546–55. https://doi.org/10.1021/acs.jpcc.1c05144.

[183] Sasaki K, Wurth J-P, Gschwend R, Gödickemeier M, Gauckler LJ. Microstructure-property relations of solid oxide fuel cell cathodes and current collectors: cathodic polarization and ohmic resistance. J Electrochem Soc 1996;143:530–43. https://doi.org/10.1149/1.1836476.

[184] Bello IT, Zhai S, He Q, Xu Q, Ni M. Scientometric review of advancements in the development of high-performance cathode for low and intermediate temperature solid oxide fuel cells: three decades in retrospect. Int J Hydrogen Energy 2021;46:26518–36. https://doi.org/10.1016/j.ijhydene.2021.05.134.

[185] Liu X, Martin CL, Bouvard D, Di Iorio S, Laurencin J, Delette G. Strength of highly porous ceramic electrodes. J Am Ceram Soc 2011;94:3500–8. https://doi.org/10.1111/j.1551-2916.2011.04669.x.

[186] Zhao F, Liu Q, Wang S, Chen F. Infiltrated multiscale porous cathode for proton-conducting solid oxide fuel cells. J Power Sources 2011;196:8544–8. https://doi.org/10.1016/j.jpowsour.2011.06.029.

[187] Ricote S, Bonanos N, Manerbino A, Sullivan NP, Coors WG. Effects of the fabrication process on the grain-boundary resistance in BaZr0.9Y0.1O3-δ. J Mater Chem A Mater 2014;2:16107–15. https://doi.org/10.1039/c4ta02848a.

[188] Pergolesi D, Fabbri E, D'epifanio A, Di Bartolomeo E, Tebano A, Sanna S, et al. High proton conduction in grain-boundary-free yttrium-doped barium zirconate films grown by pulsed laser deposition. Nat Mater 2010. https://doi.org/10.1038/NMAT2837.

[189] Zvonareva I, Fu X-Z, Medvedev D, Shao Z. Electrochemistry and energy conversion features of protonic ceramic cells with mixed ionic-electronic electrolytes †. Energy Environ Sci 2022;15:439. https://doi.org/10.1039/d1ee03109k.

[190] Holzer L, Iwanschitz B, Hocker T, Münch B, Prestat M, Wiedenmann D. Microstructure degradation of cermet anodes for solid oxide fuel cells : quantification of nickel grain growth in dry and in humid atmospheres. J Power Sources 2011;196:1279–94. https://doi.org/10.1016/j.jpowsour.2010.08.017.

[191] Ce B, Proton YYO, Electrolyte C, Vahidmohammadi A, Cheng Z, Soc JE, et al. Fundamentals of synthesis, sintering issues, and chemical stability of fundamentals of synthesis, sintering issues, and chemical electrolyte for SOFCs. J Electrochem Soc 2015;162:F803. https://doi.org/10.1149/2.0021508jes.

[192] Costa R, Grünbaum N, Berger M-H, Dessemond L, Thorel A. On the use of NiO as sintering additive for BaCe0,9Y0,1O3−α. Solid State Ion 2009;180:891–5. https://doi.org/10.1016/j.ssi.2009.02.018.

[193] Nikodemski S, Tong J, O'Hayre R. Solid-state reactive sintering mechanism for proton conducting ceramics. Solid State Ion 2013;253:201–10. https://doi.org/10.1016/j.ssi.2013.09.025.

[194] Kim S, Joh DW, Lee DY, Lee J, Kim HS, Khan MZ, et al. Microstructure tailoring of solid oxide electrolysis cell air electrode to boost performance and long-term durability. Chem Eng J 2021;410:128318. https://doi.org/10.1016/J.CEJ.2020.128318.

[195] Basbus JF, Arce MD, Prado FD, Caneiro A, Mogni LV. A high temperature study on thermodynamic, thermal expansion and electrical properties of BaCe0.4Zr0.4Y0.2O3−δ proton conductor. J Power Sources 2016;329:262–7. https://doi.org/10.1016/j.jpowsour.2016.08.083.

[196] Huang JS, Liew JX, Ademiloye AS, Liew KM. Artificial intelligence in materials modeling and design. Arch Comput Methods Eng 2021;28:3399–413. https://doi.org/10.1007/s11831-020-09506-1.

[197] Nosengo N. The material code. Nature 2016;533:22–5. https://doi.org/10.1038/533022A.

[198] Schmidt J, Marques MRG, Botti S, Marques MAL. Recent advances and applications of machine learning in solid-state materials science. Npj Comput Mater 2019;5:1–36. https://doi.org/10.1038/s41524-019-0221-0. 2019 5:1.

[199] Jain A, Ong SP, Hautier G, Chen W, Richards WD, Dacek S, et al. Commentary: the materials project: a materials genome approach to accelerating materials innovation. APL Mater 2013;1:11002. https://doi.org/10.1063/1.4812323/119685/COMMENTARY-THE-MATERIALS-PROJECT-A-MATERIALS.

[200] Materials project - home n.d. https://materialsproject.org/#search/materials (accessed June 4, 2023).

[201] Aflow - Automatic FLOW for Materials Discovery n.d. https://www.aflowlib.org/(accessed June 4, 2023).

[202] Saal JE, Kirklin S, Aykol M, Meredig B, Wolverton C. Materials design and discovery with high-throughput density functional theory: the open quantum materials database (OQMD). JOM 2013;65:1501–9. https://doi.org/10.1007/S11837-013-0755-4/FIGURES/1.

[203] OQMD | The open quantum materials database n.d. https://oqmd.org/materials/ (accessed June 5, 2023).

[204] Vaitkus A, Merkys A, Grazulis S. Validation of the crystallography open database using the crystallographic information framework. J Appl Crystallogr 2021;54:661–72. https://doi.org/10.1107/S1600576720016532/YR5065SUP1.PDF.

[205] Gražulis S, Merkys A, Vaitkus A, Okulič-Kazarinas M. Computing stoichiometric molecular composition from crystal structures. J Appl Crystallogr 2015;48:85–91. https://doi.org/10.1107/S1600576714025904/KK5188SUP1.ZIP.

[206] Gražulis S, Chateigner D, Downs RT, Yokochi AFT, Quirós M, Lutterotti L, et al. Crystallography Open Database – an open-access collection of crystal structures. J Appl Crystallogr 2009;42:726–9. https://doi.org/10.1107/S0021889809016690.

[207] Stoeckert CJ, Parkinson H. The MGED ontology: a framework for describing functional genomics experiments. Comp Funct Genom 2003;4:127–32. https://doi.org/10.1002/cfg.234.

[208] Wang B, Zhang F. Main descriptors to correlate structures with the performances of electrocatalysts. Angewandte Chemie 2022;134. https://doi.org/10.1002/ange.202111026.

[209] Andersen KB, Charlas B, Stamate E, Hansen KK. Permeability, strength and electrochemical studies on ceramic multilayers for solid-state electrochemical cells. Heliyon 2017;3:371. https://doi.org/10.1016/j.heliyon.2017.e00371.

[210] Choi S, Davenport TC, Haile SM. Protonic ceramic electrochemical cells for hydrogen production and electricity generation: exceptional reversibility, stability, and demonstrated faradaic efficiency. Energy Environ Sci 2019;12: 206–15. https://doi.org/10.1039/C8EE02865F.

[211] Goodall REA, Lee AA. Predicting materials properties without crystal structure: deep representation learning from stoichiometry. Nat Commun 2020;11:1–9. https://doi.org/10.1038/s41467-020-19964-7. 2020 11:1.

[212] Song J, Zhu S, Ning D, Bouwmeester HJM. Defect chemistry and transport properties of perovskite-type oxides La1−xCaxFeO3−δ. J Mater Chem A Mater 2021;9:974–89. https://doi.org/10.1039/D0TA07508F.

[213] Minervini L, Zacate MO, Grimes RW. Defect cluster formation in M2O3-doped CeO2. Solid State Ion 1999;116:339–49. https://doi.org/10.1016/S0167-2738(98)00359-2.

[214] Shmueli U. Materials Today. Kidlington England, 2007;10(11):53. doi:10.1016/s1369-7021(07)70280-8.

[215] Fossdal A, Menon M, Wærnhus I, Wiik K, Einarsrud M-A, Grande T. Crystal structure and thermal expansion of La1−xSrxFeO3−δ materials. J Am Ceram Soc 2004;87:1952–8. https://doi.org/10.1111/j.1151-2916.2004.tb06346.x.

[216] Popoola A, Ghosh PS, Kingsland M, Kashikar R, DeTellem D, Xu Y, et al. First-principles property assessment of hybrid formate perovskites. J Chem Phys 2023;159(7). https://doi.org/10.1063/5.0159526.

[217] Chen D, Shao Z. Surface exchange and bulk diffusion properties of. Int J Hydrogen Energy 2011;36:6948–56. https://doi.org/10.1016/j.ijhydene.2011.02.087.

[218] Chroneos A, Parfitt D, Vovk RV, Goulatis IL. Optimizing oxygen diffusion in cathode materials for solid oxide fuel cells. Modern Phys Lett B 2012;26. https://doi.org/10.1142/S0217984912501965.

[219] Itoh T, Imai H. Oxide ion diffusion mechanism related to Co and Fe ions in (Ba0.5Sr0.5)(Co0.8Fe0.2)O3−δ using in-situ X–ray absorption spectroscopy. Physica B Condens Matter 2018;532:54–8. https://doi.org/10.1016/j.physb.2017.05.023.

[220] Lee YL, Kleis J, Rossmeisl J, Yang SH, Morgan D. Prediction of solid oxide fuel cell cathode activity with first-principles descriptors. Energy Environ Sci 2011;4: 3966–70. https://doi.org/10.1039/C1EE02032C.

[221] Suntivich J, Gasteiger HA, Yabuuchi N, Nakanishi H, Goodenough JB, Shao-Horn Y. Design principles for oxygen-reduction activity on perovskite oxide catalysts for fuel cells and metal–air batteries. Nat Chem 2011;3:546–50. https://doi.org/10.1038/nchem.1069. 2011 3:7.

[222] Calle-Vallejo F, Díaz-Morales OA, Kolb MJ, Koper MTM. Why is bulk thermochemistry a good descriptor for the electrocatalytic activity of transition metal oxides? ACS Catal 2015;5:869–73. https://doi.org/10.1021/CS5016657/ASSET/IMAGES/LARGE/CS-2014-016657_0005.JPEG.

[223] Hong WT, Stoerzinger KA, Lee YL, Giordano L, Grimaud A, Johnson AM, et al. Charge-transfer-energy-dependent oxygen evolution reaction mechanisms for perovskite oxides. Energy Environ Sci 2017;10:2190–200. https://doi.org/10.1039/C7EE02052J.

[224] Jacobs R, Mayeshiba T, Booske J, Morgan D. Material discovery and design principles for stable, high activity perovskite cathodes for solid oxide fuel cells. Adv Energy Mater 2018;8:1702708. https://doi.org/10.1002/AENM.201702708.

[225] Guan D, Zhou J, Huang YC, Dong CL, Wang JQ, Zhou W, et al. Screening highly active perovskites for hydrogen-evolving reaction via unifying ionic electronegativity descriptor. Nat Commun 2019;10:1–8. https://doi.org/10.1038/s41467-019-11847-w. 2019 10:1.

[226] Calle-Vallejo F, Inoglu NG, Su HY, Martínez JI, Man IC, Koper MTM, et al. Number of outer electrons as descriptor for adsorption processes on transition metals and their oxides. Chem Sci 2013;4:1245–9. https://doi.org/10.1039/C2SC21601A.

[227] Stoerzinger KA, Risch M, Han B, Shao-Horn Y. Recent insights into manganese oxides in catalyzing oxygen reduction kinetics. ACS Catal 2015;5:6021–31. https://doi.org/10.1021/ACSCATAL.5B01444/ASSET/IMAGES/LARGE/CS-2015-014448_0007.JPEG.

[228] Brown ID, Skowron A. Electronegativity and Lewis acid strength. J Am Chem Soc 1990;112:3401–3. https://doi.org/10.1021/ja00165a023.

[229] Li K, Xue D. Estimation of electronegativity values of elements in different valence states. J Phys Chem A 2006;110:11332–7. https://doi.org/10.1021/jp062886k.

[230] Hu E, Jiang Z, Fan L, Singh M, Wang F, Raza R, et al. Junction and energy band on novel semiconductor-based fuel cells. IScience 2021;24:102191. https://doi.org/10.1016/j.isci.2021.102191.

[231] Hu E, Jiang Z, Fan L, Singh M, Wang F, Raza R, et al. iScience ll Junction and energy band on novel semiconductor- based fuel cells. IScience 2021;24:102191. https://doi.org/10.1016/j.isci.2021.102191.

[232] Meng XY, Liu DY, Qin GW. Band engineering of multicomponent semiconductors: a general theoretical model on the anion group. Energy Environ Sci 2018;11: 692–701. https://doi.org/10.1039/c7ee03503a.

[233] Heras-Juaristi G, Amador U, Fuentes RO, Chinelatto AL, Romero De Paz J, Ritter C, et al. Thermal evolution of structures and conductivity of Pr-substituted BaZr0.7Ce0.2Y0.1O3-:δ: potential cathode components for protonic ceramic fuel cells. J Mater Chem A Mater 2018;6:5324–34. https://doi.org/10.1039/c7ta09570h.

[234] Azad AK, Setsoafia DDY, Ming LC, Petra I. Synthesis and characterization of high density and low temperature sintered proton conductor BaCe0.5Zr0.35In0.1Zn0.05O3-δ. Adv Mat Res 2015;1098:104–9. https://doi.org/10.4028/www.scientific.net/AMR.1098.104.

[235] Pagnier T, Charrier-Cougoulic I, Ritter C, Lucazeau G. Neutron diffraction study of BaCexZr1-xO3. EPJ Appl Phys 2000;9:1–9. https://doi.org/10.1051/epjap:2000192.

[236] Jung J Il, Park S, Kim MG, Cho J. Tunable internal and surface structures of the bifunctional oxygen perovskite catalysts. Adv Energy Mater 2015;5:1–7. https://doi.org/10.1002/aenm.201501560.

[237] Hou J, Qian J, Bi L, Gong Z, Peng R, Liu W. The effect of oxygen transfer mechanism on the cathode performance based on proton-conducting solid oxide fuel cells. J Mater Chem A Mater 2015;3:2207–15. https://doi.org/10.1039/c4ta04397a.

[238] Vignesh D, Sonu BK, Rout E. Factors constituting proton trapping in BaCeO 3 and BaZrO 3 perovskite proton conductors in fuel cell technology: a review. Energy Fuels 2022;36:7219–44. https://doi.org/10.1021/acs.energyfuels.2c00650.

[239] Simböck J, Ghiasi M, Schönebaum S, Simon U, de Groot FMF, Palkovits R. Electronic parameters in cobalt-based perovskite-type oxides as descriptors for chemocatalytic reactions. Nat Commun 2020;11:1–10. https://doi.org/10.1038/s41467-020-14305-0.

[240] Müller IM. Feature selection for energy system modeling: identification of relevant time series information. Energy AI 2021;4:100057. https://doi.org/10.1016/J.EGYAI.2021.100057.

[241] Liu Y, Esan OC, Pan Z, An L. Machine learning for advanced energy materials. Energy AI 2021;3:100049. https://doi.org/10.1016/J.EGYAI.2021.100049.

[242] Mangal A, Holm EA. A comparative study of feature selection methods for stress hotspot classification in materials. Integr Mater Manuf Innov 2018;7:87–95. https://doi.org/10.1007/S40192-018-0109-8/FIGURES/1.

[243] Lundberg SM, Erion G, Chen H, DeGrave A, Prutkin JM, Nair B, et al. From local explanations to global understanding with explainable AI for trees. Nat Mach Intell 2020;2:56–67. https://doi.org/10.1038/s42256-019-0138-9. 2020 2:1.

[244] Lundberg SM, Allen PG, Lee S-I. A unified approach to interpreting model predictions. Adv Neural Inf Process Syst 2017;30.

[245] Lee YG, Oh JY, Kim D, Kim G. SHAP value-based feature importance analysis for short-term load forecasting. J Electr Eng Technol 2023;18:579–88. https://doi.org/10.1007/S42835-022-01161-9/METRICS.

[246] Marcilio WE, Eler DM. From explanations to feature selection: assessing SHAP values as feature selection mechanism. In: Proceedings - 2020 33rd SIBGRAPI Conference on Graphics, Patterns and Images, SIBGRAPI 2020; 2020. p. 340–7. https://doi.org/10.1109/SIBGRAPI51738.2020.00053.

[247] Schütt KT, Sauceda HE, Kindermans PJ, Tkatchenko A, Müller KR. SchNet - a deep learning architecture for molecules and materials. J Chem Phys 2018;148. https://doi.org/10.1063/1.5019779/962591.

[248] Golbabaei MH, Saeidi Varnoosfaderani M, Zare A, Salari H, Hemmati F, Abdoli H, et al. Performance analysis of anode-supported solid oxide fuel cells: a machine learning approach. Materials (Basel) 2022;15. https://doi.org/10.3390/ma15217760.

[249] Hai T, Dahan F, Dhahad HA, Almojil SF, Alidade A, sharma A, et al. Deep-learning optimization and environmental assessment of nanomaterial's boosted hydrogen and power generation system combined with SOFC. Int J Hydrogen Energy 2022. https://doi.org/10.1016/j.ijhydene.2022.11.332.

[250] Hirata A, Wada T, Obayashi I, Hiraoka Y. Structural changes during glass formation extracted by computational homology with machine learning. Commun Mater 2020;1:98. https://doi.org/10.1038/s43246-020-00100-3.

[251] Kuenneth C, Lalonde J, Marrone BL, Iverson CN, Ramprasad R, Pilania G. Bioplastic design using multitask deep neural networks. Commun Mater 2022;3: 96. https://doi.org/10.1038/s43246-022-00319-2.

[252] Mao KS, Gerczak TJ, Harp JM, McKinney CS, Lach TG, Karakoc O, et al. Identifying chemically similar multiphase nanoprecipitates in compositionally complex non-equilibrium oxides via machine learning. Commun Mater 2022;3: 21. https://doi.org/10.1038/s43246-022-00244-4.

[253] Morsali S, Qian D, Minary-Jolandan M. Designing bioinspired brick-and-mortar composites using machine learning and statistical learning. Commun Mater 2020; 1:12. https://doi.org/10.1038/s43246-020-0012-7.

[254] Sieverts M, Obata Y, Rosenberg JL, Woolley W, Parkinson DY, Barnard HS, et al. Unraveling the effect of collagen damage on bone fracture using in situ synchrotron microtomography with deep learning. Commun Mater 2022;3. https://doi.org/10.1038/s43246-022-00296-6.

[255] Li J, Zhang Y, Cao X, Zeng Q, Zhuang Y, Qian X, et al. Accelerated discovery of high-strength aluminum alloys by machine learning. Commun Mater 2020;1:73. https://doi.org/10.1038/s43246-020-00074-2.

[256] Moradi S, Kundu S, Rezazadeh M, Yeddu V, Voznyy O, Saidaminov MI. High-throughput exploration of halide perovskite compositionally-graded films and degradation mechanisms. Commun Mater 2022;3:13. https://doi.org/10.1038/s43246-022-00235-5.

[257] Reiser P, Neubert M, Eberhard A, Torresi L, Zhou C, Shao C, et al. Graph neural networks for materials science and chemistry. Commun Mater 2022;3:93. https://doi.org/10.1038/s43246-022-00315-6.

[258] Lee A, Sarker S, Saal JE, Ward L, Borg C, Mehta A, et al. Machine learned synthesizability predictions aided by density functional theory. Commun Mater 2022;3:73. https://doi.org/10.1038/s43246-022-00295-7.

[259] Fujinuma N, DeCost B, Hattrick-Simpers J, Lofland SE. Why big data and compute are not necessarily the path to big materials science. Commun Mater 2022;3:59. https://doi.org/10.1038/s43246-022-00283-x.

[260] Zhai X, Ding F, Zhao Z, Santomauro A, Luo F, Tong J. Predicting the formation of fractionally doped perovskite oxides by a function-confined machine learning method. Commun Mater 2022;3:42. https://doi.org/10.1038/s43246-022-00269-9.

[261] Martynec T, Karapanagiotis C, Klapp SHL, Kowarik S. Machine learning predictions of surface migration barriers in nucleation and non-equilibrium growth. Commun Mater 2021;2:90. https://doi.org/10.1038/s43246-021-00188-1.
[262] Davariashtiyani A, Kadkhodaie Z, Kadkhodaei S. Predicting synthesizability of crystalline materials via deep learning. Commun Mater 2021;2:115. https://doi.org/10.1038/s43246-021-00219-x.
[263] Hatakeyama-Sato K, Oyaizu K. Integrating multiple materials science projects in a single neural network. Commun Mater 2020;1. https://doi.org/10.1038/s43246-020-00052-8.
[264] Gu GH, Noh J, Kim I, Jung Y. Machine learning for renewable energy materials. J Mater Chem A Mater 2019;7:17096–117. https://doi.org/10.1039/C9TA02356A.
[265] Wang Y, Wu C, Zhao S, Guo Z, Han M, Zhao T, et al. Boosting the performance and durability of heterogeneous electrodes for solid oxide electrochemical cells utilizing a data-driven powder-to-power framework. Sci Bull 2023;68:516–27. https://doi.org/10.1016/j.scib.2023.02.019.
[266] Nair SS, Muddapu VR, Vigneswaran C, Balasubramani PP, Ramanathan DS, Mishra J, et al. A generalized reinforcement learning based deep neural network agent model for diverse cognitive constructs. Sci Rep 2023;13:1–12. https://doi.org/10.1038/s41598-023-32234-y. 2023 13:1.
[267] Ke H, Fu X, Zhang D, Li X, Xu F. Deep convolutional neural networks for SOFC core-shell recognition. In: Proceedings of the 13th IEEE Conference on Industrial Electronics and Applications, ICIEA 2018; 2018. p. 2721–4. https://doi.org/10.1109/ICIEA.2018.8398171.
[268] Weng B, Song Z, Zhu R, Yan Q, Sun Q, Grice CG, et al. Simple descriptor derived from symbolic regression accelerating the discovery of new perovskite catalysts. Nat Commun 2020;11:1–8. https://doi.org/10.1038/s41467-020-17263-9.
[269] Butler KT, Davies DW, Cartwright H, Isayev O, Walsh A. Machine learning for molecular and materials science. Nature 2018;559:547–55. https://doi.org/10.1038/S41586-018-0337-2.
[270] Sun W, Zheng Y, Yang K, Zhang Q, Shah AA, Wu Z, et al. Machine learning–assisted molecular design and efficiency prediction for high-performance organic photovoltaic materials. Sci Adv 2019;5. https://doi.org/10.1126/SCIADV.AAY4275/SUPPL_FILE/AAY4275_SM.PDF.
[271] machine learning - when to use random forest over SVM and vice versa? - Data science stack exchange n.d. https://datascience.stackexchange.com/questions/6838/when-to-use-random-forest-over-svm-and-vice-versa (accessed April 14, 2023).
[272] Taiwo R, Ben Seghier MEA, Zayed T. Toward sustainable water infrastructure: the state-of-the-art for modeling the failure probability of water pipes. Water Resour Res 2023;59. https://doi.org/10.1029/2022WR033256. e2022WR033256.
[273] Belyadi H., Haghighat A. Supervised learning. Machine learning guide for oil and gas using python 2021:169–295. https://doi.org/10.1016/B978-0-12-821929-4.00004-4.
[274] Taiwo R, Shaban IA, Zayed T. Development of sustainable water infrastructure: a proper understanding of water pipe failure. J Clean Prod 2023;398. https://doi.org/10.1016/J.JCLEPRO.2023.136653.
[275] Raschka, S. Model evaluation, model selection, and algorithm selection in machine learning 2018. Retrieved from http://arxiv.org/abs/1811.1280.
[276] Iwasaki Y, Sawada R, Saitoh E, Ishida M. Machine learning autonomous identification of magnetic alloys beyond the Slater-Pauling limit. Commun Mater 2021;2. https://doi.org/10.1038/s43246-021-00135-0.
[277] Schmidt J, Marques MRG, Botti S, Marques MAL. Recent advances and applications of machine learning in solid-state materials science. NPJ Comput Mater 2019;5. https://doi.org/10.1038/S41524-019-0221-0.
[278] Gao T, Shock CJ, Stevens MJ, Frischknecht AL, Nakamura I. Surrogate molecular dynamics simulation model for dielectric constants with ensemble neural networks. MRS Commun 2022;12:966–74. https://doi.org/10.1557/S43579-022-00283-5/FIGURES/3.
[279] Fedik N, Zubatyuk R, Kulichenko M, Lubbers N, Smith JS, Nebgen B, et al. Extending machine learning beyond interatomic potentials for predicting molecular properties. Nat Rev Chem 2022;6:653–72. https://doi.org/10.1038/s41570-022-00416-3. 2022 6:9.
[280] Zhang GX, Song Y, Zhao W, An H, Wang J. Machine learning-facilitated multiscale imaging for energy materials. Cell Rep Phys Sci 2022;3:101008. https://doi.org/10.1016/J.XCRP.2022.101008.
[281] Morgan D, Jacobs R. Opportunities and challenges for machine learning in materials science. Annu Rev Mater Res 2020;50:71–103. https://doi.org/10.1146/annurev-matsci-070218-010015.
[282] Hechler E, Oberhofer M, Schaeck T. Limitations of AI. Deploying AI in the enterprise. Berkeley, CA: Apress; 2020. p. 299–312. https://doi.org/10.1007/978-1-4842-6206-1_13.
[283] Amyot D., Bronson K., Eltis K., Fallavollita P. Future directions: artificial intelligence. 2019.
[284] Hwang H, Choi SM, Oh J, Bae SM, Lee JH, Ahn JP, et al. Integrated application of semantic segmentation-assisted deep learning to quantitative multi-phased microstructural analysis in composite materials: case study of cathode composite materials of solid oxide fuel cells. J Power Sources 2020;471:228458. https://doi.org/10.1016/j.jpowsour.2020.228458.
[285] Oz A, Singh K, Gelman D, Thangadurai V, Tsur Y. Understanding of oxygen reduction reaction on perovskite-type Ba0.5Sr0.5Fe0.91Al0.09O3-δ and Ba0.5Sr0.5Fe0.8Cu0.2O3-δ using AC impedance spectroscopy genetic programming. J Phys Chem C 2018;122:15097–107. https://doi.org/10.1021/acs.jpcc.8b03036.
[286] Genetic algorithms + neural networks = best of both worlds | by Suryansh S. | Towards data science n.d. https://towardsdatascience.com/gas-and-nns-6a41f1e8146d (accessed April 3, 2023).
[287] Li Y, Leong H. Kinematics control of redundant manipulators using a CMAC neural network combined with a genetic algorithm. Robotica 2004;22:611–21. https://doi.org/10.1017/S0263574704000414.
[288] Liang Q, Gongora AE, Ren Z, Tiihonen A, Liu Z, Sun S, et al. Benchmarking the performance of Bayesian optimization across multiple experimental materials science domains. NPJ Comput Mater 2021;7:188. https://doi.org/10.1038/S41524-021-00656-9.
[289] Ciucci F, Chen C. Analysis of electrochemical impedance spectroscopy data using the distribution of relaxation times: a Bayesian and hierarchical Bayesian approach. Electrochim Acta 2015;167:439–54. https://doi.org/10.1016/j.electacta.2015.03.123.
[290] Lei B, Kirk TQ, Bhattacharya A, Pati D, Qian X, Arroyave R, et al. Bayesian optimization with adaptive surrogate models for automated experimental design. Npj Comput Mater 2021;7:1–12. https://doi.org/10.1038/s41524-021-00662-x. 2021 7:1.
[291] Janet JP, Ramesh S, Duan C, Kulik HJ. Accurate multiobjective design in a space of millions of transition metal complexes with neural-network-driven efficient global optimization. ACS Cent Sci 2020. https://doi.org/10.1021/ACSCENTSCI.0C00026.
[292] Maradesa A, Py B, Quattrocchi E, Ciucci F. The probabilistic deconvolution of the distribution of relaxation times with finite Gaussian processes. Electrochim Acta 2022;413:140119. https://doi.org/10.1016/j.electacta.2022.140119.
[293] Seko A, Togo A, Tanaka I. Descriptors for machine learning of materials data. Nanoinformatics 2018:3–23. https://doi.org/10.1007/978-981-10-7617-6_1/FIGURES/10.
[294] Siemers FM, Bajorath J. Differences in learning characteristics between support vector machine and random forest models for compound classification revealed by Shapley value analysis. Sci Rep 2023;13:1–12. https://doi.org/10.1038/s41598-023-33215-x. 2023 13:1.
[295] Chen G, Zhang K, Xue X, Zhang L, Yao C, Wang J, et al. A radial basis function surrogate model assisted evolutionary algorithm for high-dimensional expensive optimization problems. Appl Soft Comput 2022;116:108353. https://doi.org/10.1016/J.ASOC.2021.108353.
[296] Hautier G, Fischer CC, Jain A, Mueller T, Ceder G. Finding natures missing ternary oxide compounds using machine learning and density functional theory. Chem Mater 2010;22:3762–7. https://doi.org/10.1021/CM100795D/SUPPL_FILE/CM100795D_SI_003.ZIP.
[297] Hautier G, Fischer C, Ehrlacher V, Jain A, Ceder G. Data mined ionic substitutions for the discovery of new compounds. Inorg Chem 2011;50:656–63. https://doi.org/10.1021/IC102031H/SUPPL_FILE/IC102031H_SI_001.TXT.
[298] Honda T, Muroga S, Nakajima H, Shimizu T, Kobashi K, Morita H, et al. Virtual experimentations by deep learning on tangible materials. Commun Mater 2021;2. https://doi.org/10.1038/s43246-021-00195-2.
[299] Kingma DP, Welling M. Auto-encoding variational Bayes. In: 2nd International Conference on Learning Representations, ICLR 2014 - Conference Track Proceedings; 2013.
[300] Lew AJ, Buehler MJ. Encoding and exploring latent design space of optimal material structures via a VAE-LSTM model. Forces Mech 2021;5:100054. https://doi.org/10.1016/J.FINMEC.2021.100054.
[301] Pei Z, Rozman KA, Doğan ÖN, Wen Y, Gao N, Holm EA, et al. Machine-learning microstructure for inverse material design. Adv Sci 2021;8. https://doi.org/10.1002/ADVS.202101207.
[302] Guo K, Buehler MJ. A semi-supervised approach to architected materials design using graph neural networks. Extreme Mech Lett 2020;41:101029. https://doi.org/10.1016/J.EML.2020.101029.
[303] Ma Q, Xu D. Deep learning shapes single-cell data analysis. Nat Rev Molec Cell Biol 2022;23:303–4. https://doi.org/10.1038/s41580-022-00466-x. 2022 23:5.
[304] Choudhary K, DeCost B, Chen C, Jain A, Tavazza F, Cohn R, et al. Recent advances and applications of deep learning methods in materials science. Npj Comput Mater 2022;8:1–26. https://doi.org/10.1038/s41524-022-00734-6. 2022 8:1.
[305] Niu Z, Zhao W, Wu B, Wang H, Lin WF, Pinfield VJ, et al. π Learning: a performance-informed framework for microstructural electrode design. Adv Energy Mater 2023;13:2300244. https://doi.org/10.1002/AENM.202300244.
[306] Wang Y, Wu C, Zhao S, Wang J, Zu B, Han M, et al. Coupling deep learning and multi-objective genetic algorithms to achieve high performance and durability of direct internal reforming solid oxide fuel cell. Appl Energy 2022;315:119046. https://doi.org/10.1016/J.APENERGY.2022.119046.
[307] Guo Z, Wang Y, Zhao S, Zhao T, Ni M. Modeling and optimization of micro heat pipe cooling battery thermal management system via deep learning and multi-objective genetic algorithms. Int J Heat Mass Transf 2023;207:124024. https://doi.org/10.1016/J.IJHEATMASSTRANSFER.2023.124024.
[308] Katoch S, Chauhan SS, Kumar V. A review on genetic algorithm: past, present, and future. Multimed Tools Appl 2021;80:8091–126. https://doi.org/10.1007/S11042-020-10139-6/FIGURES/8.
[309] Nyshadham C, Rupp M, Bekker B, Shapeev AV, Mueller T, Rosenbrock CW, et al. Machine-learned multi-system surrogate models for materials prediction. Npj Comput Mater 2019;5:1–6. https://doi.org/10.1038/s41524-019-0189-9. 2019 5:1.
[310] Jin Y, Branke J. Evolutionary optimization in uncertain environments - a survey. IEEE Trans Evolut Comput 2005;9:303–17. https://doi.org/10.1109/TEVC.2005.846356.
[311] Johnston RL. Evolving better nanoparticles: genetic algorithms for optimising cluster geometries. Dalton Trans 2003:4193. https://doi.org/10.1039/b305686d.

[312] Hou Z, Tsuda K. Bayesian optimization in materials science. Lecture Notes Phys 2020;968:413–26. https://doi.org/10.1007/978-3-030-40245-7_19/FIGURES/2.
[313] Yang K, Liu J, Wang Y, Shi X, Wang J, Lu Q, et al. Machine-learning-assisted prediction of long-term performance degradation on solid oxide fuel cell cathodes induced by chromium poisoning. J Mater Chem A Mater 2022;10:23683–90. https://doi.org/10.1039/D2TA03944C.
[314] Toyoura K, Hirano D, Seko A, Shiga M, Kuwabara A, Karasuyama M, et al. Machine-learning-based selective sampling procedure for identifying the low-energy region in a potential energy surface: A case study on proton conduction in oxides. Phys Rev B 2016;93:054112. https://doi.org/10.1103/PhysRevB.93.054112.
[315] Zheng Y, Zhao C, Wu T, Li Y, Zhang W, Zhu J, et al. Enhanced oxygen reduction kinetics by a porous heterostructured cathode for intermediate temperature solid oxide fuel cells. Energy AI 2020;2. https://doi.org/10.1016/j.egyai.2020.100027.
[316] Hsu T, Epting WK, Kim H, Abernathy HW, Hackett GA, Rollett AD, et al. Microstructure generation via generative adversarial network for heterogeneous, topologically complex 3D materials. JOM 2021;73:90–102. https://doi.org/10.1007/S11837-020-04484-Y/FIGURES/7.
[317] Meffert M, Wankmüller F, Störmer H, Weber A, Lupetin P, Ivers-Tiffée E, et al. Optimization of material contrast for efficient FIB-SEM tomography of solid oxide fuel cells. Fuel Cells 2020;20:580–91. https://doi.org/10.1002/FUCE.202000080.
[318] Xing WW, Shah AA, Dai G, Zhang Z, Guo T, Qiu H, et al. Multi-fidelity design optimization of solid oxide fuel cells using a Bayesian feature enhanced stochastic collocation. Int J Hydrogen Energy 2023. https://doi.org/10.1016/J.IJHYDENE.2023.04.012.
[319] Sha W, Guo Y, Yuan Q, Tang S, Zhang X, Lu S, et al. Artificial intelligence to power the future of materials science and engineering. Adv Intell Syst 2020;2:1900143. https://doi.org/10.1002/AISY.201900143.
[320] Wang B, Zhang F. Main descriptors to correlate structures with the performances of electrocatalysts. Angewandte 2022:202111026. https://doi.org/10.1002/ange.202111026.
[321] Lee YL, Lee D, Wang XR, Lee HN, Morgan D, Shao-Horn Y. Kinetics of oxygen surface exchange on epitaxial Ruddlesden–Popper phases and correlations to first-principles descriptors. J Phys Chem Lett 2016;7:244–9. https://doi.org/10.1021/acs.jpclett.5b02423.
[322] Arık S, Pfister T. TabNet: attentive interpretable tabular learning. In: 35th AAAI Conference on Artificial Intelligence, AAAI 2021. 8A; 2019. p. 6679–87. https://doi.org/10.1609/aaai.v35i8.16826.
[323] Liu J, Tian T, Liu Y, Hu S, Li M. iTabNet: an improved neural network for tabular data and its application to predict socioeconomic and environmental attributes. Neural Comput Appl 2023;35:11389–402. https://doi.org/10.1007/S00521-023-08304-7/METRICS.
[324] Park S, Pozzi A, Whitmeyer M, Perez H, Kandel A, Kim G, et al. A deep reinforcement learning framework for fast charging of Li-ion batteries. IEEE Trans Transp Electrif 2022;8:2770–84. https://doi.org/10.1109/TTE.2022.3140316.
[325] Li J, Li Y, Yu T. Distributed imitation-orientated deep reinforcement learning method for optimal PEMFC output voltage control. Front Energy Res 2021;9:741101. https://doi.org/10.3389/FENRG.2021.741101/BIBTEX.
[326] Taiwo R, Ben Seghier MEA, Zayed T. Predicting wall thickness loss in water pipes using machine learning techniques. Ce/Papers 2023;6:1087–92. https://doi.org/10.1002/CEPA.2075.
[327] Taiwo R, Hussein M, Zayed T. An integrated approach of simulation and regression analysis for assessing productivity in modular integrated construction projects. Buildings 2022;12. https://doi.org/10.3390/buildings12112018.
[328] Ben Seghier MEA, Keshtegar B, Tee KF, Zayed T, Abbassi R, Trung NT. Prediction of maximum pitting corrosion depth in oil and gas pipelines. Eng Fail Anal 2020;112:104505. https://doi.org/10.1016/j.engfailanal.2020.104505.